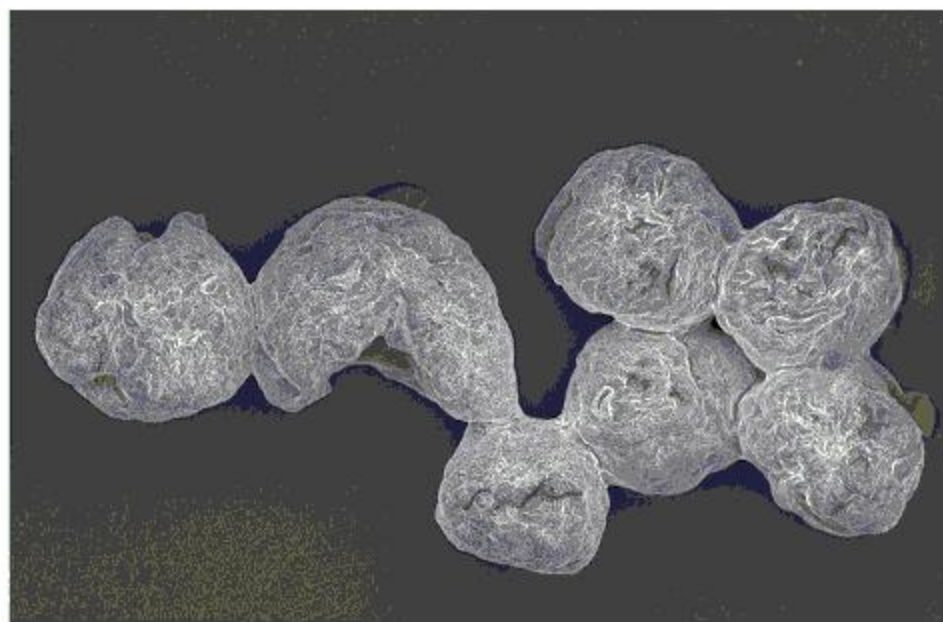Angelina Yoo

κ-Carrageenan Micropellets:
Production and Dissolution Behavior

Cuvillier Verlag Göttingen
Internationaler wissenschaftlicher Fachverlag

κ-Carrageenan Micropellets:
Production and Dissolution Behavior

INAUGURAL - DISSERTATION

zur

Erlangung des Doktorgrades der
Mathematisch-Naturwissenschaftlichen Fakultät der
Heinrich-Heine-Universität Düsseldorf

vorgelegt von

Angelina Yoo
aus Hamburg

Düsseldorf, Dezember 2008

Table of content

List of abbreviations

Abbreviation	meaning
Abs	absorption value
Amoxi	amoxicillin trihydrate
ANOVA	analysis of variance
API	active pharmaceutical ingredient
ar	aspect ratio
BCS	Biopharmaceutics Classification Scheme
ι-Carr	ι-carrageenan (iota)
κ-Carr	κ-carrageenan (kappa)
λ-Carr	λ-carrageenan (lambda)
CCC	central composite circumscribed design
CIAA	Confederation of the Food and Drink Industries in the EU
C13-03	tricalcium phosphate (Tri-Cafos$^{®}$ PF)
C53-06	tricalcium phosphate (TCP 30$^{®}$)
C92-14	dicalcium phosphate (Di-Cafos)
d_d	dimensionless diameter
d_{eq}	equivalent diameter
DAB	Deutsches Arzneibuch
DOE	design of experiments
DSC	differential scanning calorimetry
DST	dose sipping technology
FCC	Food chemicals codex
FDA	US Food and Drug Administration
FeSSIF	Fed State Simulating Intestinal Fluid
ffc	flowability function
f_2	similarity factor
GDA	Guideline daily amount
GIT	gastrointestinal tract
GL200	lactose monohydrate (GranuLac200$^{®}$)
GRAS	generally recognized as safe
GsF	griseofulvin
h	hours
HCl	hydrochloric acid
HCT	hydrochlorothiazide
HPLC	high performance liquid chromatography
ICP-OES	inductively coupled plasma optical emission spectrometry

ICZ	itraconazole
inl	inlet air pressure
IQR	interquartile range
IVIVC	in vitro in vivo correlation
L-HPC	low substituted hydroxypropylcellulose
loa	loading of the spheronizer
M	$mol \cdot l^{-1}$
mc	moisture content (of extrudates)
MCC	microcrystalline cellulose
MUDF	multiple unit dosage form
NaCl	sodium chloride
NaOH	sodium hydroxide
ndr	normalized drug release
p	p-value of statistic (lack of fit)
p.a.	pro analysis
Ph.Eur.	Pharmacopoeia Europaea
Q	single charge point
Q^2	Predictibility
REM	scanning electron microscopy
rpm	round per minute
R^2_{adj}	adjusted coefficient of determination
SD	standard deviation
spd	spheronization speed
SpL	spironolactone
SUDF	single unit dosage form
SUPAC-MR	scale-up and post-approval changes-modified release
temp	temperature of the spheronizer wall
ThP	theophylline monohydrate
tim	residence time
USP	United States Pharmacopoeia
$\overline{x}$	mean
x_{50}	median

1 Introduction

1.1 Multiple unit dosage forms

Peroral dosage forms for modified drug release are classified into single or multiple unit dosage forms. Pellets, powders and granules are considered to be multiple unit dosage forms (MUDFs). Compared to single unit dosage forms (SUDF, e.g. enteric-coated tablets), they consist of multiple particles or they disintegrate rapidly into particles after intake [Kleinebudde, 1997].

MUDFs have many advantages: 1. Due to the small size (< 2 mm) they are able to pass the pylorus continuously even under closed conditions of the sphincter and therefore, distribute evenly in the entire gastrointestinal tract (GIT) and show a gradual decrease in the amount present in the stomach. As a result, local irritation and side-effects are reduced and more consistent plasma levels are achieved [Bechgaard and Nielsen, 1978; Davis et al., 1986; Voigt, 2006b]. 2. Modified drug release is often achieved by coating. The risk of defects in coatings of SUDFs such as cracking causes intoxication due to 'dose dumping'. Coated MUDFs prevents the risk of 'dose dumping' due to the use of multiple particles. 3. MUDFs can be variously designed: One dosage form can be composed of pellets containing different (incompatible) active pharmaceutical ingredients (APIs) or particles with different dissolution behavior. Therefore the combination of different multiple particles may reduce the daily required number of drugs, which can improve patient compliance. Finally, pellets offer technological advantages such as good flowability, low friability, narrow particle size distribution and uniform packing [Reynolds, 1970; Rowe et al., 2005]. Therefore, MUDFs are the preferred dosage forms.

MUDFs also have disadvantages. The main disadvantage is the complex production process. Furthermore, MUDFs can be bigger in volume than tablets, which can affect patient compliance. However, overall MUDFs have increasingly gained importance over the years due to their distinctive advantages in both technological and pharmacological aspects.

1.2 Micropellets

1.2.1 Definition

Pharmaceutical pellets are isometric aggregates with smooth surfaces and narrow particle size distribution [Knop, 1991]. Nowadays, the mean pellet size ranges from 300 µm to 3 mm. According to Kleinebudde, microparticles are defined as aggregates < 500 µm [Kleinebudde, 1997]. However, there is no commonly accepted definition for micropellets in the literature. Due to the production technique the diameter of the orifices for wet extrusion/ spheronization was limited to ensure a reproducible and robust process. Therefore, in this thesis pellets up to 700 µm were considered as micropellets, whereby the closer to 500 µm the better.

Micropellets have the same advantages as regular pellets (~1 mm). Besides the shape, they also have low porosity and high mechanical stability. Due to the roundness and closed shape of the particles, the flowability of pellets is excellent. Micropellets show a number of additional favorable properties. The most important of which is the larger specific surface area, which results in faster dissolution rates.

Micropellets can be used in a number of dosage forms that may be beneficial for certain patient groups. Micropellets and regular pellets are usually processed into tablets or filled into capsules. Further investigations are underway to use micropellets as solid drops in a 'sprinkle capsule' [Kjellman et al., 1988; Carrigan et al., 1990] or in a 'dose sipping technology' (DST) [Tuleu, 2005; Breitkreutz and Boos, 2007; Krause and Breitkreutz, 2008]. These application forms are especially suitable for patients who have problems swallowing drug products and therefore refuse to take medicine at all (e.g. pediatric or elderly patients). Difficulties with administering drugs to children are a widespread problem, which needs improvement with regard to off-label use for example [Schirm et al., 2003; Kearns et al., 2003; Standing and Tuleu, 2005].

1.2.2 Sprinkle capsule

A sprinkle capsule is a hard gelatin, pull-apart capsule containing drug loaded pellets, which is designed to be administered either intact or opened to sprinkle on soft food. However, the co-administration of a solid meal must be handled with care [Pedersen and Mollerpetersen, 1984]. The presence of food can be beneficial in terms of patient compliance, especially in children, and those concerned by bad taste, nausea or vomiting.

1.2.3 Dose sipping technology

With dose sipping technology, the micropellets are filled into a plastic drinking straw. The straw consists of four components (Fig. 1): the drinking straw, the micropellets, the controller and the cap. The controller is located at the bottom of the system and acts like a filter. Therefore, it will transport the micropellets to the top with sipping. The cap on top of the straw, for hygienic safeguards and to keep the micropellets inside the straw, has to be removed before use.
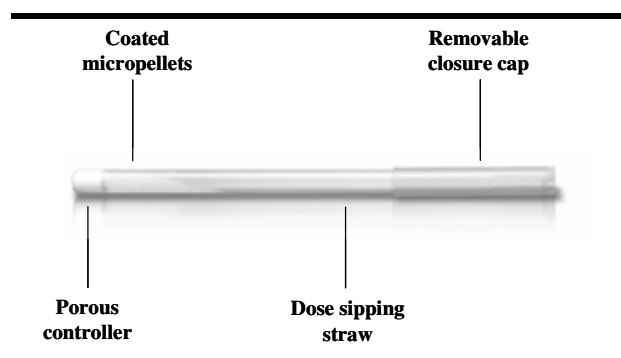
The DST is a flow-through system, which is dependent on the entering liquid. Therefore, carbonated drinks, teas and liquids with low viscosity are suitable, while juice with pulp and viscose liquids like milk shakes might block the system.

Fig. 1:   Dose sipping technology

2

The advantages of DST and sprinkle capsules are basically related to patient psychology. Patients may be reluctant to take their medication due to the size of a tablet; especially children who often refuse to take drugs and can spit them out easily. However, a straw is associated with drinking and therefore, related to a natural habit. They can be carried in the bag without peculiarities and used for almost every drink. During sipping, micropellets disperse in the liquid and enter the mouth easily. The small pellet size of the micropellets (combined with the concomitant intake of liquid) helps to pass the mouth almost unnoticed. Therefore, the drug is given to the patient without difficulties.

For example, Clarosip® (Grünenthal GmbH) was an antibiotic in a drinking straw. It contained clarithromycin as API and was available in 3 different dosages: 125 mg, 187.5 mg and 250 mg. The micropellets were enteric coated with a copolymer of methacrylic acid-ethyl acrylate (1:1).

1.3   Pelletization aids

1.3.1   Definition

To produce pellets by wet extrusion/ spheronization the formulation must contain a pelletization aid and meet specific rheological requirements for the process. During extrusion the wetted mass must show i) suitable flow characteristics, which allows a mass transport during the process; ii) self-lubricating properties without sticking to each other and; iii) sufficient rigidity to keep the shape of the extrudate.

For the spheronization process the moistened extrudates must show i) sufficient firmness; ii) enough brittleness to break into smaller pieces (cylinders) at the beginning of the spheronization process; iii) plasticity to convert the cylinders into pellets and; iv) that it is non-adhesive to remain in shape [Fielden et al., 1992].

Due to the various required properties, the range of materials suitable to act as pelletization aid in the extrusion/ spheronization process is limited.

1.3.2   Microcrystalline Cellulose

Microcrystalline cellulose (MCC) was the first excipient used as pelletization aid to produce pharmaceutical pellets successfully with a relatively low amount in the formulation. After its discovery for pharmaceutical pelletization by Reynolds [1970] and Conine and Hadley [1970], numerous investigations followed in which MCC showed its special role as a pelletization aid - during wet extrusion, MCC binds the moisture and therefore, the wetted mass becomes rigid to be extruded. At the same time in the spheronization process, the extrudates are still brittle to break into small cylinders and simultaneously plastic enough to convert into pellets. However the drawbacks of MCC, such as matrix dissolution and prolonged drug release [O'Connor and Schwartz, 1993; Zimm et al., 1995] led to further investigations. To try to overcome its drawbacks, MCC was combined with different excipients to improve the drug

release [Mesiha and Valles, 1993; Gazzaniga et al., 1998; Souto et al., 2005] or wetted with different extrusion liquids than pure water [Millili and Schwartz, 1990; Schroder and Kleinebudde, 1995; Boutell et al., 2002]. Alternative pelletization aids were also sought [Liew et al., 2005; Sergio et al., 2007; Charoenthai et al., 2007]. Bornhoft et al. [2005] introduced κ-carrageenan, which showed special capacities for pellet production and became a suitable pelletization aid, which was confirmed by subsequent investigations [Thommes and Kleinebudde, 2006a; b].

1.3.3 κ-Carrageenan

κ-Carrageenan belongs to a group of acid polysaccharides taken from the cell walls of red seaweeds, in particular of the *Gigartinales spp.* [Dawes et al., 1977; Amimi et al., 2001]. It is a natural ingredient and generally recognized as safe (GRAS-status). Some physiological effects of carrageenan have been reported. Wagner [1999] observed that it had effects on blood coagulation and defecation and Hänsel et al. [1999] suspected low-molecular carrageenan as a cause for ulceration in the GIT. Therefore, Rochas and Heyraud [1981] emphasized the avoidance of acid and enzymatic hydrolysis in the production.

As carrageenans are not absorbed after oral intake [Fiedler, 1996], they are mainly used in food applications (also known as E407, a food additive) [Bundesministerium für Gesundheit, 2006]. Thus, they serve as thickening, suspending or gelling agents [Voragen, 2001].
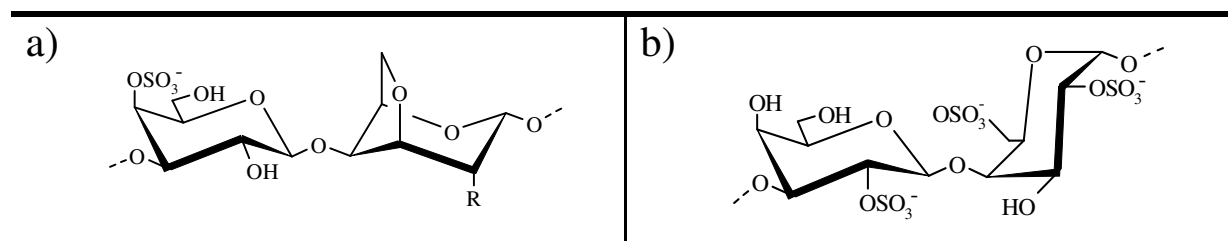
Fig. 2: **Ideal repeating dimer unit of different types of carrageenan a) κ-carrageenan or ι-carrageenan, b) λ-carrageenan**

The production of carrageenan involves several steps: hot extraction, clarification, evaporation, precipitation and drying. Through these processes, the commercially available types, ι-, κ- and λ-carrageenan, are obtained [FMC, 1993]. Due to the production process, the obtained carrageenans are not pure. They show impurities from one another [Rochas et al., 1989; Ridout et al., 1996]. The linear backbone of κ-carrageenan bases on the repetition of disaccharide sequences of sulfate esters of β-1,3-linked galactose and α-1,4-linked 3,6-anhydrogalactose, which are mainly charged with potassium, sodium, calcium, magnesium and ammonium as counter-ions. κ-Carrageenan differs from ι- and λ-carrageenan in the amount and location of the sulfate ester groups and the presence (or absence) of the 3,6-anhydrogalactose residue [Voragen, 2001; Stortz and Cerezo, 2003]. Fig. 2 contains the different structures of the carrageenans, where κ-carrageenan showed $R = OH$ and ι-carrageenan had $R = OSO_3^-$.

After the inclusion of carrageenan in the US Pharmacopoeia [USP 31 NF26, 2008] with its own monograph, it was used in numerous investigations in pharmaceutical technology. In particular κ-carrageenan was investigated in i) gels [Hoffman, 2002; Mangione et al., 2007]; ii) films [Park et al., 2001]; iii) tablets [Picker, 1999; Gupta et al., 2001; Rosario and Ghaly, 2002]; iv) capsules [Scherer RP, 2003; Tuleu et al., 2007]; v) inhalants [Yamada et al., 2005]; vi) pellets [Garcia and Ghaly, 2001; Sipahigil and Dortunc, 2001; Bornhoft et al., 2005]. It was also investigated with regard to the pronounced effects of ions and its interactions with APIs [Hugerth, 2001; Sipahigil and Dortunc, 2001; Naim et al., 2004].

2 Micropellets production techniques

2.1 Introduction

Several methods to produce micropellets are well-known such as extrusion/ spheronization; direct pelletization [Kristensen et al., 2000]; spray-drying [Eldem et al., 1991; Giunchedi and Conte, 1995]; spray-layering of solutions, suspensions or powders [Jones, 1989; Goodhart and Jan, 1989]; spray-congealing [Akiyama et al., 1993; Maschke et al., 2007] or different emulsification-solvent evaporation/ extraction or emulsion-congealing techniques [Kim et al., 1994; Hassan et al., 1995; Berchane et al., 2007]. Extrusion processes are classified into solvent-free extrusion (melt extrusion, solid-lipid extrusion) and wet extrusion. The latter is the commonly used technique in the pharmaceutical industry to produce pellets since the pioneering work of Reynolds [1970] and Conine and Hadley [1970]. The methods of extrusion have a number of advantages: i) the processes are robust; ii) they have good reproducibility; and iii) they enable the production of pellets with often high loading, high density and narrow size distribution. Thus, the methods are used for manufacturing multiple unit dosage forms by coating, tableting or encapsulation [Ghebre-Sellassie, 1989a].

2.2 Extrusion

Extrusion is a process of applying pressure to a mass until it flows through an orifice or a defined opening [Hicks and Freese, 1989]. There are several techniques for extrusion on the market, but screw extrusion is most commonly used in the pharmaceutical industry [Hicks and Freese, 1989; Baert et al., 1993a; Vervaet et al., 1995]. The screw extruder exists as a single or twin-screw extruder. The spinning direction of the twin-screw extruder can either be a 'co-rotate' or 'counter-rotate' [Mollan, 2003]. Co-rotation of the twin-screw is generally used for pharmaceutical production, due to the low energy input. Furthermore, a twin-screw extruder shows the advantage of a one-step extrusion combining blending, wetting, wet massing and extrusion in one apparatus. With one-step extrusion, several variables affect the pellet properties, which can be categorized into three groups: i) the equipment effects, e.g. type of extruder; ii) the process effects, settings of the process and; iii) the material effects, e.g. physical properties of the formulation [Erkoboni, 2003]. The interactions can be evaluated by measuring the power consumption or the torque during the process [Kleinebudde et al., 1994; Soh et al., 2006].

The production of micropellets using wet extrusion/ spheronization is challenging and scarcely reported in the literature. Previous studies with (axial) extrusion showed difficulties due to the effects of the moisture content on pellet properties, as well as the effects of the orifice size and formulation. With micropellets, the pressure on the screen increases due to the decrease in orifice size [Kanbe et al., 2007]. Micropellets have been successfully produced using L-HPC or glycerides with the addition of a surfactant [Dupont et al., 2002; Kanbe et al., 2007].

2.3 Spheronization

Compared to the extrusion process, spheronization is a discontinuous process in which the wetted extrudates are converted into spherical micropellets. Hence, spheronization is the essential step in the production, where collision of particles occurs due to the generated force of the spinning friction plate. Therefore, the extrudates must show a combination of cohesiveness, firmness and plasticity to go through the various states of forming [Erkoboni, 2003].

A spheronizer consists of a vertical hollow cylinder with an inner horizontal rotating disc (friction plate) [Hicks and Freese, 1989]. Spheronizers may vary in the friction plate diameter and its features as well as additional process variables. The surface texture of the friction plate can be designed with different grooves from which the 'cross-hatched' pattern is commonly used. Furthermore, differences in additional spheronizer process variables such as a double jacket wall or an inlet air pressure can also exist.

The mechanism of spheronization is complex and the process is affected by mechanical stress and by the temperature. Besides the requirements of the extrudates, the spheronization process is mainly dependent on three different factors: spheronization speed, residence time and loading [Hellen and Yliruusi, 1993; Wan et al., 1993; Hellen et al., 1993a; b]. Therefore, the mutual effects between the extrusion and spheronization process, especially with regard to the moisture content of the extrudates, have been investigated [Woodruff and Nuessle, 1972; Bains et al., 1991; Baert et al., 1993b].

2.4 Drying

The final step of the production is the drying process of the micropellets to remove the extrusion liquid in which the micropellets lose their plasticity. Although several methods exist, in general the fluidized bed method is preferred and commonly used [Erkoboni, 2003; Thommes et al., 2007]. In this work, no further investigations on drying were performed.

3 Dissolution behavior

3.1 Introduction

The dissolution rate of an API is often the rate-limiting step of the drug absorption. Therefore, dissolution tests provide important information about the biopharmaceutical quality of a dosage form to determine the release profiles. Several 'in-vitro' tests are described in the pharmacopoeias [Ph.Eur. 6, 2008; USP 31 NF26, 2008] containing different apparatus and various requirements for different dosage forms. Depending on the dosage form, the dissolution shows fast or modified drug release, whereby the latter is usually achieved through coating of the dosage form or embedment of the API in a matrix.

3.2 Matrix dissolution

3.2.1 Definition

There are a number of principles of classifying drug release from matrices: i) matrix is not degradable, while the API is fully dissolved; ii) matrix is not degradable, while the API is mostly suspended; iii) matrix is poreless or gets pores during dissolution; iv) matrix is gelling or v) matrix is eroding [Leuenberger, 2001]. The dissolution kinetic varies depending on the system. Different models are used and well known to describe the drug release with regard to defined conditions such as sink-conditions.

3.2.2 Diffusion-controlled dissolution

Two different mechanisms are known for diffusion-controlled drug release. The matrix is not degradable and the API is either fully dissolved or mostly suspended. In the latter case, the matrix is a diffusion barrier in which water penetrates during the dissolution process and the API dissolves. Thus, the drug release is only diffusion-controlled.

The Higuchi equation [Higuchi, 1961; 1963] describes the kinetic of the drug release, which assumes the existence of sink conditions and a decreasing gradient of concentration. A linear relationship between drug release and the square root of time demonstrates that a diffusional process occurs (Eq. 1):

$$Q = \sqrt{\frac{D\varepsilon}{\tau} * Cs * (2A - \varepsilon Cs) * t} = k_H * \sqrt{t} \qquad \text{Eq. (1)}$$

where Q is the cumulative amount of drug released after time per unit surface area of the matrix [mg·cm^{-2}], D is the diffusion coefficient of the drug in the permeating fluid [cm^2·min^{-1}], ε is the porosity factor of the matrix, τ is the tortuosity factor of the capillary system, A is the concentration of drug in the matrix [mg·cm^{-3}], Cs is the solubility of the API in the permeating fluid [mg·cm^{-3}], t is the time [min] and k_H is the system-dependent proportionality

constant (slope). Hence, a plot of the amount of drug release (Q) versus the square root of time predicts a linear relationship.

Changes in the dissolution kinetic are obtained when the total concentration is below the saturated concentration or the diffusion coefficient is changed due to matrix changes (Eq. 2):

$$D = \frac{R*T}{6*\pi*\eta*r*N}$$
Eq. (2)

where R is the gas constant [8.314 J·K^{-1}·mol^{-1}], T the absolute temperature, η the viscosity of the solvent, r the hydrodynamic radius of the dissolved molecules and N is Avogadro's number [6.0221*10^{23}].

Although the Higuchi equation was originally derived to describe drug release from a planar surface system, it is also an accepted method for multiparticulate pellet systems [O'Connor and Schwartz, 1989]. The evaluation by Korsmeyer and Peppas [Korsmeyer et al., 1983] considered the geometry dependence of the matrix system on drug release.

3.3   Evaluation by Korsmeyer and Peppas

An empirical equation was developed to determine the mechanism of drug release by means of the effects of structural characteristics of polymeric matrices [Korsmeyer and Peppas, 1981]. In general, the dissolution behavior from polymers was strictly limited to thin films. The drug release can be described by Fickian diffusion in which the first 60 % of the fractional release is characterized by the square root of time profile at any time. However, another drug release behavior, where the release rate is independent on the time, is characterized to be a zero-order kinetic. Therefore, Korsmeyer and Peppas postulated a double logarithmic plot of drug release as a function of time combining both drug release behaviors (Eq. 3):

$$\frac{M_t}{M_\infty} = kt^n$$
Eq. (3)

where M_t/M_∞ is the fraction of drug released at the time t, k is the apparent release rate constant with respect to the structural and geometric characteristics of the drug delivery system and n is the diffusional exponent which characterizes the transport mechanism of the drug.

The evaluation by Korsmeyer and Peppas considered the effects of the matrix geometry on the dissolution kinetic. It describes the intermediate range between Fickian diffusion and zero-order kinetics with respect to the shape. Thus, the exponent n and the kinetic constant k

strongly depend on the geometry of the matrix. The Fickian diffusion is generally defined by n = 0.5 and zero-order kinetic by n = 1. The release processes in between, $0.5 < n < 1$, is characterized as anomalous (non-Fickian) diffusion, where swelling, diffusion and erosion play an important role.

Tab. 1: Diffusional exponent and drug release mechanism of different geometry of the matrix

Diffusional exponent (n)			Drug release mechanism
Cylindrical sample	Spherical sample	Thin film	
0.45	0.43	0.5	Fickian diffusion
$0.45 < n < 0.89$	$0.43 < n < 0.85$	$0.5 < n < 1.0$	Anomalous (non-Fickian) diffusion
0.89	0.85	1.0	Zero order kinetic

Due to the composition of both drug release behaviors in one equation, some agreements remained like the validity for the first 60 % of the fractional release. In addition, [Ritger and Peppas, 1987a; b] concluded that the Fickian diffusion process, described by n = 0.5, was only acceptable for thin films. For spherical particles, the gradient was about 0.43 (Tab. 1).

4 Aims of this work

The primary aim of this work is to develop and characterize micropellets (500 µm to 700 µm diameter) based on κ-carrageenan by wet extrusion/ spheronization. As the conversion of extrudates to spherical pellets is the most challenging step, the main focus is the spheronization process and the comparison of two types of spheronizers.

The secondary aims are focussed on the effects of using κ-carrageenan as a pelletization aid on dissolution behavior, especially in terms of the ionic interactions. Different dissolution media including biorelevant media and different fillers are investigated. Further, different APIs and different ratios of API and pelletization aid are used to verify the impact of the ionic interactions on drug release. By doing so, conclusions about expected food interactions, which affect the bioavailability of the drug, may be drawn.

Finally, the potential interchangeability of the different types of κ-carrageenans as pelletization aid for wet extrusion/ spheronization are investigated with respect to the contained ions and the rheological behavior.

5 Results and Discussion

5.1 Optimization of spheronizer conditions

5.1.1 Introduction and objective

The primary objective of this part of the work was to determine the optimum process conditions for spheronizers to convert extrudates of 500 µm diameter into micropellets. The behavior of the formulations containing κ-carrageenan as a pelletization aid during spheronization was investigated. To date, pellets based on κ-carrageenan have been extruded using a die plate with 1 mm diameter orifices. The spheronization of extrudates with small diameter was previously found to be more difficult and the conditions for spheronization of 1 mm extrudates [Bornhoft et al., 2005] could not be easily adapted to obtain spherical micropellets. Therefore, different spheronization conditions are needed for pelletization of small extrudates. The spheronization was performed using a Schlueter spheronizer. The influences of spheronization speed, residence time, temperature of the spheronizer wall and loading on the responses aspect ratio, pellet size and yield, were studied with a central composite circumscribed design (CCC-design).

The secondary objective was to compare two spheronizers (RM 300, Schlueter, Neustadt/ Ruebenberge, Germany and S320, Nica System AB, Moelndal, Sweden) at two different spheronization speeds and variable moisture content of the extrudates with respect to the pellet properties and yield. A full factorial (mixed) design was used retrospectively for the evaluation of the results. While the Schlueter spheronizer was equipped with a cross-hatched friction plate of 300 mm diameter, the Nica spheronizer was equipped with a cross-hatched friction plate of 320 mm diameter and a lip around the friction plate [Hellen et al., 1993b]. The Schlueter spheronizer had a double jacket wall, which can be used to adjust a certain temperature. Both spheronizers allow bottom air stream through the gap between friction plate and spheronizer wall at a defined inlet air pressure.

At last, the additional spheronizer process variables such as temperature of the spheronizer wall and inlet air pressure were investigated with regard to the pellet properties and yield. A full factorial (mixed) design was used retrospectively to evaluate the results.

5.1.2 Production

For the extrusion process, the screen plate for the CCC-design had 87 dies and the screen plate for the other parts of the work had 92 dies. The orifices of both die plates had a diameter of 0.5 mm and a length of 2.5 mm. For formulations without API the extrusion took place under standard conditions (Chap. 8.2.1.2). The formulation containing spironolactone was extruded at a constant screw speed of 160 rpm. The powder feed rate was constant at 33 g·min^{-1}. The spheronizer conditions are described in each chapter.

5.1.3   Evaluation parameters

5.1.3.1   Introduction

To characterize the pelletization process and the micropellets systematically, parameters were selected such as moisture content of the extrudates as well as pellet size and shape to evaluate the conditions of wet extrusion/ spheronization. For the quantitative characterization the yield was used.

5.1.3.2   Moisture content

The quality of the micropellets is dependent on the formulation properties. Therefore, extrusion liquid was added to the dry powder which is responsible for the plastic-deformation of the wetted mass during the extrusion/ spheronization process. The amount of extrusion liquid plays an essential role [Schmidt and Kleinebudde, 1999] and must be adjusted to every formulation and process conditions. The moisture content (mc) is often used to describe the amount of water during extrusion (Chap. 8.2.2.1).

5.1.3.3   Shape

To determine the shape of a micropellet various techniques have been developed [Chapman et al., 1988; Lovgren and Lundberg, 1989] and also numerous parameters have been described [Hellen and Yliruusi, 1993]. However, Bouwman et al. [2005] describe the aspect ratio (ar) as a simple and common parameter to describe micropellet shape from wet extrusion/ spheronization (Chap. 8.2.2.3).

The ideal value of the aspect ratio is 1. The closer the value gets to 1, the more spherical the pellet shape. Aspect ratios below 1.1 are rated as good and above 1.2 are regarded as inappropriate [Kleinebudde, 1995].

5.1.3.4   Size and size distribution

The micropellet size is mainly determined by the diameter of the orifices in the die plate and ranges for wet extrusion/ spheronization generally between 500 µm and 2 mm. The size of the micropellets is dependent on the diameter of the extrudates. Due to elastic recovery of the swelling product as it leaves the dies, the diameter of the extrudates can slightly increase [Harrison et al., 1985]. In addition, the micropellet size is affected by the spheronization and the drying process. Therefore, agglomeration ('snow balling') during the spheronization process increases the micropellet sizes, while during the drying process shrinking may occur [Kleinebudde, 1994].

Besides the mean of the micropellet size, the size distribution can hardly be influenced and is therefore a good parameter to evaluate different formulations for wet extrusion/ spheronization. To compare the different size distribution function, the dimensionless diameter (d_d) is calculated (Chap. 8.2.2.3).

Thommes and Kleinebudde [2006a] characterized the size distribution by the fraction of the pellets in the interval of $0.9 < d_d < 1.1$, which is called the 10 %-interval. It is a measure for the width of the distribution and is independent from the median of micropellet size. Values between 50 % and 75 % are rated as good, while exceeding 75 % is assumed to be excellent.

5.1.3.5 Yield

The yield is the percentage by weight of the defined sieve fraction between 200 µm and 710 µm related to the total weight of the batch (Chap. 8.2.2.2). Independent from the adhesion to the spheronizer wall, the complete batch was dried and classified.

5.1.4 Design of Experiments - Quality of the Model

The quality of a model determines the quality of the results of the design of experiments (DOE). If the model describes the results only insufficient the effects obtained cannot be correlated to the varying factors. A DOE has been used to study the influences of factors and their combinations with regard to the responses. The chosen central composite circumscribed design (CCC-design) is a preferred design for optimization. It belongs to the group of response surface modeling designs (RSM-design) which allows the inclusion of quadratic effects in order to provide a more realistic model [Eriksson et al., 2000]. To investigate the experimental error, replicated center-point experiments are carried out. Usually, between three and five replicates are made.

The full factorial (mixed) design belongs to the full factorial designs with some factors at more than two levels. This type of screening design is called 'full' because all possible corners are investigated. The main effects and all interactions can be determined independently and are not confounded.

To statistically evaluate the regression analyses of the model four parameters were used: the coefficient of determination (R^2), the goodness of prediction (Q^2), the validity of the model and the reproducibility value (Chap. 8.2.2.5).

5.1.5 Spheronization of 500µm extrudates – CCC-design

The formulation contained 80 % lactose monohydrate and 20 % κ-carrageenan. The moisture content of the extrudates was preliminary determined and was between 97.2 % and 100.2 % for 27 samples with one exception of 105.1 %.

The extrusion of κ-carrageenan through a die plate with 500 µm diameter orifices was successful in every run. The extrudates with κ-carrageenan showed always a smooth surface. However, the spheronization process of small extrudates was more challenging. Therefore, the spheronization process to produce round micropellets had to be optimized (CCC-design).

Spheronization speed (x_{spd}), residence time (x_{tim}), temperature of the spheronizer wall (x_{temp}) and loading of the spheronizer (x_{loa}) were selected as the influence variables (factors). Three replicates were performed at the zero level. All runs were conducted in a randomized order. The responses aspect ratio, pellet size and yield were measured (Tab. 2).

The chosen spheronization speeds of the Schlueter spheronizer of 800 rpm, 1000 rpm and 1200 rpm are equal to 12.57 m·s⁻¹, 15.71 m·s⁻¹ and 18.85 m·s⁻¹, respectively. A manual scraper was used to prevent the extrudates from adhesion to the spheronizer wall during the process.

Tab. 2: Results of the central composite circumscribed design

Speed [m·s⁻¹]	Time [min]	Temperature [°C]	Loading [g]	Aspect ratio	Pellet size [µm]	Yield [%]
12.57	3	15	400	1.15	625	67.8
12.57	3	25	400	1.16	616	73.2
18.85	3	15	400	1.14	596	82.6
18.85	3	25	400	1.15	574	82.1
12.57	7	15	400	1.13	586	67.6
12.57	7	25	400	1.12	620	61.2
18.85	7	15	400	1.13	547	83.9
18.85	7	25	400	1.14	545	82.0
12.57	3	15	600	1.18	583	49.8
12.57	3	25	600	1.17	637	42.0
18.85	3	15	600	1.18	623	57.1
18.85	3	25	600	1.20	622	37.9
12.57	7	15	600	1.14	675	32.8
12.57	7	25	600	1.14	670	36.2
18.85	7	15	600	1.15	584	62.8
18.85	7	25	600	1.15	581	57.5
15.71	5	12.5	500	1.14	641	52.4
15.71	5	27.5	500	1.15	583	59.4
11.00	5	20	500	1.16	617	60.5
20.42	5	20	500	1.15	567	75.7
15.71	2	20	500	1.19	594	61.5
15.71	8	20	500	1.13	619	54.0
15.71	5	20	350	1.12	555	85.5
15.71	5	20	650	1.17	639	39.1
15.71	5	20	500	1.14	581	61.7
15.71	5	20	500	1.15	609	60.4
15.71	5	20	500	1.13	615	63.2

The complete model equation was:

$$y = b_0 + b_{spd} x_{spd} + b_{tim} x_{tim} + b_{temp} x_{temp} + b_{loa} x_{loa} + b_{spdtim} x_{spd} x_{tim} +$$
$$b_{spdtemp} x_{spd} x_{temp} + b_{spdloa} x_{spd} x_{loa} + b_{timtemp} x_{tim} x_{temp} + b_{timloa} x_{tim} x_{loa} + \quad\quad \text{Eq. (4)}$$
$$b_{temploa} x_{temp} x_{loa} + b_{spdspd} x_{spd}^2 + b_{timtim} x_{tim}^2 + b_{temptemp} x_{temp}^2 + b_{loaloa} x_{loa}^2$$

where y is the response variable, x_i is factor i, b_0 is the constant term, b_i is a model parameter.

The initial evaluations of raw data of particle size and shape distribution showed no major deviations for single batches in the entire investigation series (Fig. 3a, b). The median aspect ratio of the 27 batches varied between 1.12 and 1.20, while the three replicates at the zero point varied between 1.13 and 1.15 (Tab. 2). Thus, all pellets can be rated as good, but not excellent with regard to their shape [Kleinebudde, 1995]. The range of the median of pellet equivalent diameter was rather small spanning from 545 µm to 675 µm, while the range for

15

the replicates was 581 µm to 615 µm. Since the pellets were below 700 µm the pellets were regarded as micropellets (Chap. 1.2.1). The range of yield was broad between 33 % and 85 % with three replicates between 60.4 % and 63.2 %. The 10 %-interval was between 50 % and 71.4 % and therefore qualified as good. Only two exceptions were found: 49 % and 76.2 %.
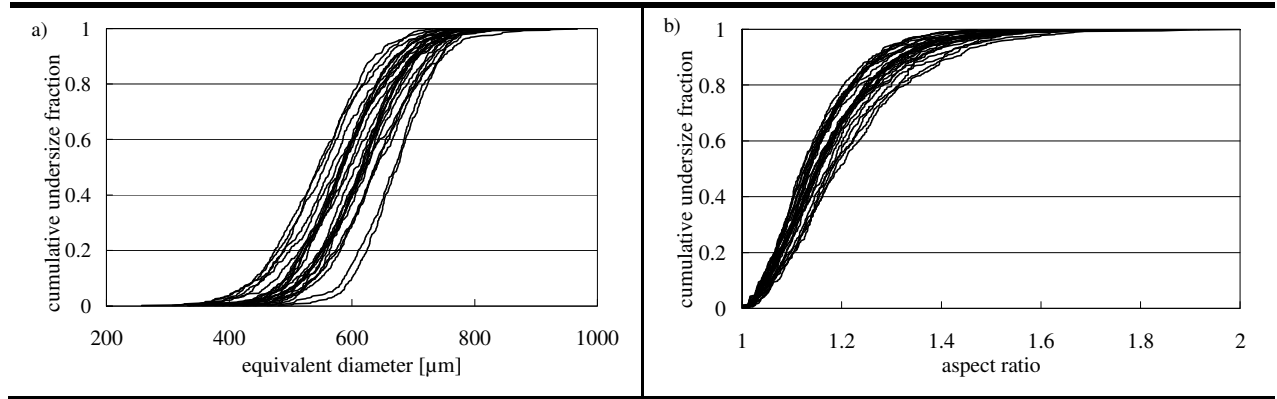
Fig. 3: Evaluation of a) pellet size and b) shape distributions for formulations resulting from the CCC-design

A backward regression was performed to find the most suitable model, which describes all three response variables simultaneously. All coefficients were kept in the model, which were significant ($p < 0.05$) for at least one response variable. The final model was:

$$y = b_0 + b_{spd} x_{spd} + b_{tim} x_{tim} + b_{loa} x_{loa} + b_{spdtim} x_{spd} x_{tim} + b_{timtim} x_{tim}^2 \qquad \text{Eq. (5)}$$

The table of the 'Summary of Fit Plot' shows the reliability of the regression model after pruning (Tab. 3): Here, R_{adj}^2 and Q^2 were not separated by more than 0.2 for aspect ratio and yield indicating that the model was appropriate. Furthermore Q^2 exceeded 0.7 for aspect ratio and yield, while for pellet size Q^2 was only 0.47. For all responses the validity value of the model exceeded 0.25. This was confirmed in the analysis of variance (ANOVA) where $p > 0.05$ for lack of fit in all cases. Therefore, the model error was not significantly larger than the pure error. All responses showed reasonably high reproducibility.

Tab. 3: Table of 'Summary of fit Plot'

Parameter \ Response	Aspect ratio	Pellet size	Yield
R_{adj}^2	0.781	0.601	0.880
Q^2	0.704	0.469	0.840
Model validity	0.891	0.824	0.306
Reproducibility	0.762	0.708	0.991

The results for the final model are shown in the Coefficient Plot (Fig. 4): Spheronizer loading had a significant influence on all three responses. A higher spheronizer load resulted in higher aspect ratios, larger pellets and lower yield. The residence time affected the aspect ratio while

the spheronization speed and the interaction of residence time and spheronization speed had an effect on pellet size and yield. The quadratic effect of the residence time was kept in the model due to a significant effect ($p = 0.042$) on the aspect ratio. The temperature of the spheronizer wall had no effect on the three response variables.
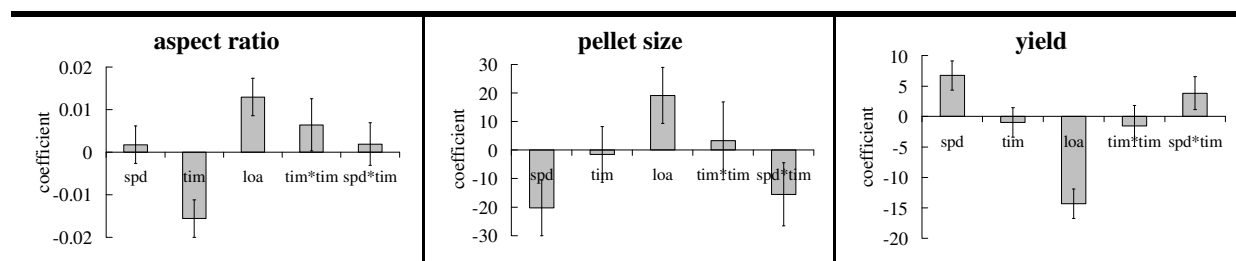
Fig. 4: Coefficient Plot of aspect ratio, pellet size and yield (spd = spheronization speed, mc = moisture content, loa = loading, tim = residence time)

The relationship between factors and response variables are shown in the 4D-Contour Plots (Fig. 5). In terms of aspect ratio (Fig. 5a) longer residence times led to lower aspect ratio. Comparisons of the aspect ratios for the different loads showed that the smallest aspect ratio was obtained with less loading. The specific energy input (energy/mass) at a given spheronizer speed is higher for less loading. This results in lower aspect ratio. However, above a certain limit an uncontrolled granule growth might occur, which was not observed in our study. In addition, at minimum residence time the spheronization does not have an effect on aspect ratio, which is shown by the horizontal graduated lines.

Pellet size, which was dependent on loading, was affected by both residence time and spheronization speed (Fig. 5b). In general, lower loads resulted in smaller pellets. Independent of loading, longer residence times and higher spheronization speeds decreased the pellet size. The two-factor interaction was emphasized by the inverse relationship shown on the 4D-Contour Plot in the lower spheronization speed range. According to Wan and Jeyabalan [1985] cohesive and destructive forces are involved in the spheronization process, whereby an increase of spheronization speed leads to an excess of destructive force. Therefore, the pellet growth is limited and the average pellet diameter decreases.

Yield was affected by all studied factors (Fig. 5c). Lower loads resulted in higher yield. Independent of loading, higher residence times combined with higher spheronization speeds gave higher yield. This is attributed to higher energy input, which more likely converts the extrudates into micropellets. The yield increased due to the achieved pellet properties such as aspect ratio and pellet size. The micropellets obtained are round and small, which are in between the desired sieve mesh range.

From the model, the optimum conditions for the spheronization process were deduced: A loading of 400 g was the best filling rate for the Schlueter spheronizer; higher spheronization speed led to better responses. However, when increasing the spheronization speed up to 1200 rpm (18.85 m·s^{-1}) a longer residence time was required to obtain good aspect ratio as

well as adequate pellet size. For the yield, the residence time was less important. Therefore, the residence time should be adjusted to longer period (defined to 6 min) and the spheronization speed to 18.85 m·s⁻¹.
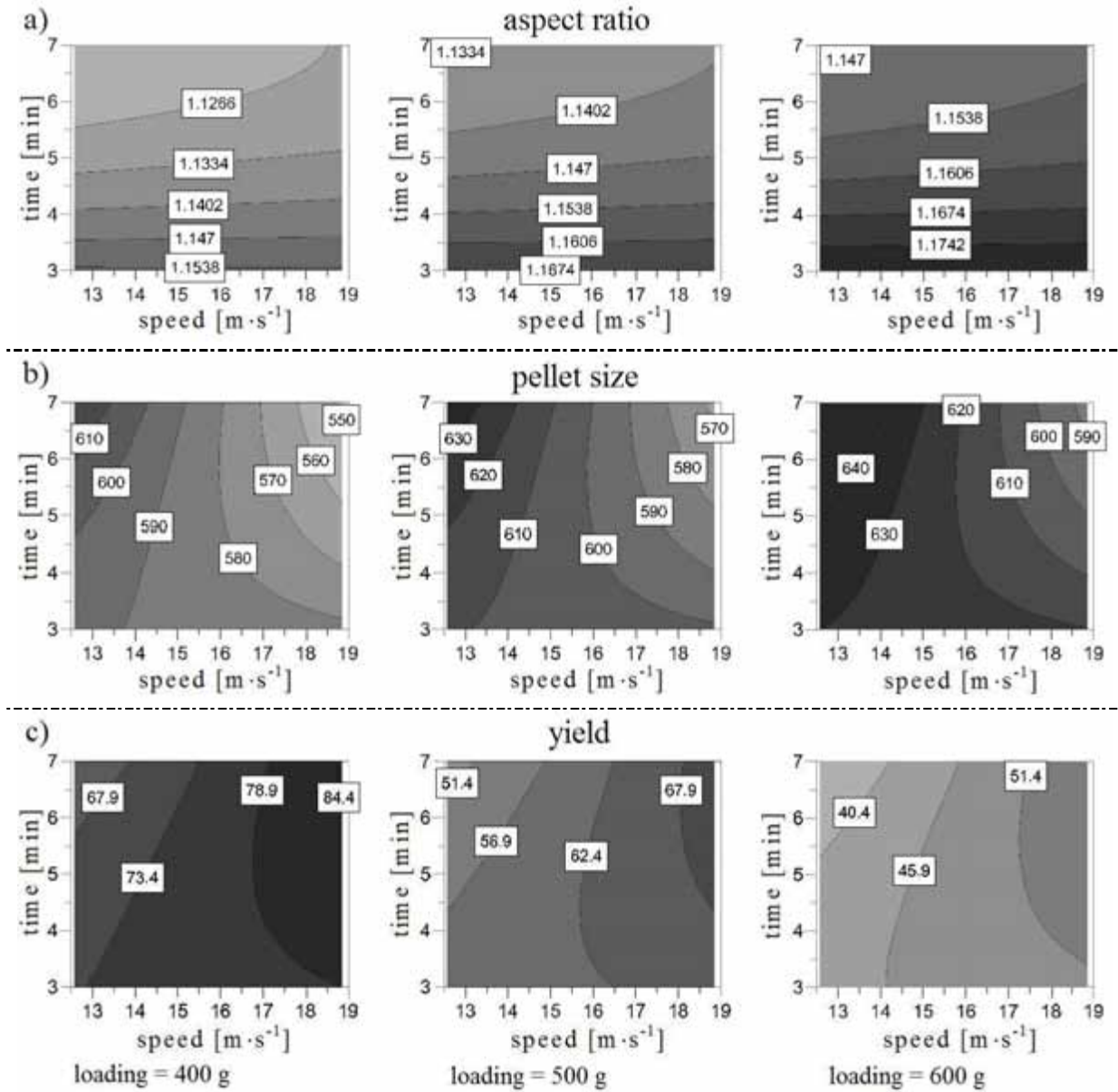
Fig. 5: 4D-Contour Plots of a) aspect ratio, b) pellet size and c) yield at different loading

Two points had to be considered during the following parts of the study: The aspect ratio of the pellets needed to be reduced below the value of 1.1 and the effects of adhesion of the pellets to the spheronizer wall during the spheronization process needed to be addressed. Both issues were related to the moisture content of the extrudates. Therefore, for subsequent experiments, the moisture content was varied.

5.1.6   Comparison between two spheronizers

The formulation used for the spheronizer comparison also contained 80 % lactose monohydrate and 20 % κ-carrageenan. The moisture content of the extrudates varied between 60.1 % and 88.5 %. Extrudates of 400 g were spheronized without using a scraper for 6min at spheronization speeds of 12.57 m·s⁻¹, 15.71 m·s⁻¹ and 18.85 m·s⁻¹. The Schlueter spheronizer was operated at a wall temperature of 25 °C and an inlet air pressure of 0.2 bar. The Nica spheronizer was used without inlet air pressure and without adjustments for the temperature.

Tab. 4: Results of the full factorial (mixed) design for both spheronizers

Moisture content [%]	Speed [m·s⁻¹]	Nica spheronizer			Schlueter spheronizer		
		Aspect ratio	Pellet size [µm]	Yield [%]	Aspect ratio	Pellet size [µm]	Yield [%]
60.5	12.57	1.39	685	97.1	1.30	706	94.3
60.5	15.71	1.23	644	92.3	1.14	642	90.0
60.5	18.85	1.20	663	95.4	1.18	593	89.4
67.9	12.57	1.31	687	92.5	1.20	657	93.8
67.9	15.71	1.21	676	96.1	1.12	625	93.7
67.9	18.85	1.15	609	97.4	1.12	449	93.8
74.6	12.57	1.21	627	85.1	1.17	616	92.1
74.6	15.71	1.16	619	92.9	1.14	605	94.2
74.6	18.85	1.13	593	97.8	1.15	534	95.2
81.5	12.57	-	-	-	-	-	-
81.5	15.71	1.14	618	88.7	1.14	605	92.5
81.5	18.85	1.10	556	96.1	1.12	567	96.6
88.5	12.57	-	-	-	-	-	-
88.5	15.71	1.11	565	80.9	1.15	601	82.7
88.5	18.85	1.10	567	94.3	1.17	544	88.4

The spheronization speed of 12.57 m·s⁻¹ at different moisture content of the extrudates resulted in insufficient roundness of the pellets. This is in line with the results from the CCC-design experiments, which showed that higher spheronization speeds gave better responses. Therefore, extrudates at higher moisture content were only spheronized at spheronization speeds above 12.57 m·s⁻¹. Instead of a twisted-rope movement during the spheronization process the material moved more irregularly in both spheronizers.

To reduce adhesion of the pellets to the spheronizer wall and simultaneously improve the aspect ratio, three different spheronization speeds (x_{spd}) were studied to evaluate the effect of the moisture content of the extrudates (x_{mc}). Responses (aspect ratio, pellet size, and yield) were evaluated using a full factorial (mixed) design for each spheronizer type (Tab. 4).

The complete model equation was:

$$y = b_0 + b_{spd} x_{spd} + b_{mc} x_{mc} + b_{spdmc} x_{spd} x_{mc} + b_{spdspd} x_{spd}^2 + b_{mcmc} x_{mc}^2 \qquad \text{Eq. (6)}$$

The median aspect ratio of the 15 batches for each spheronizer varied in the range from 1.10 to 1.39 for the Nica and 1.12 to 1.30 for the Schlueter spheronizer. Thus, depending on the moisture content of the extrudates not all pellets could be rated as good (ar < 1.20). The range of the median of pellet equivalent diameter was rather small for the Nica spheronizer (556 µm to 687 µm), while the range for the Schlueter spheronizer was wider (534 µm to 706 µm). A batch from the Schlueter spheronizer with 449 µm median pellet size showed an atypical size distribution and was excluded from further investigations. The yield for the Nica and Schlueter spheronizers ranged from 80.9 % to 97.8 % and 88.4 % to 96.6 %, respectively. Although the maximum yield was slightly lower, the range of yield for the Schlueter spheronizer was smaller. The 10 %-interval for the Nica spheronizer was good (53.2 % to 68.2 %), while for the Schlueter spheronizer only most of the values ranged from 52.2 % to 69.2 %. Three batches were below 50 % (18.4 %, 38 % and 43.4 %), definitely assignable in Fig. 6. So far, the Schlueter spheronizer can be considered to be more sensitive to the variation of process settings than the Nica spheronizer.
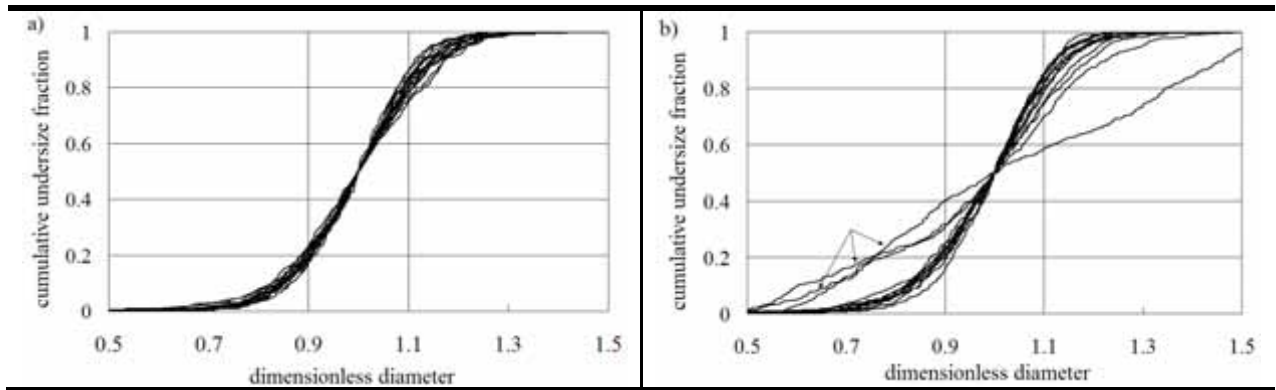
Fig. 6:   **Size distribution of a) Nica spheronizer and b) Schlueter spheronizer**

A backward regression was performed and the final model was equal for both spheronizers:

$$y = b_0 + b_{spd} x_{spd} + b_{mc} x_{mc} + b_{spdmc} x_{spd} x_{mc} + b_{mcmc} x_{mc}^2 \qquad \text{Eq. (7)}$$

The results of the final models are shown in the Coefficient Plots (Fig. 7a, b). For the Nica spheronizer, spheronization speed and moisture content of the extrudates had a significant influence on all three responses (aspect ratio: R^2_{adj} = 0.935; Q² = 0.8603; pellet size: R^2_{adj} = 0.763; Q² = 0.538; yield: R^2_{adj} = 0.919; Q² = 0.840). Increasing the spheronization speed and moisture content of the extrudates led to a decrease in aspect ratio and pellet size. In general, kappa-carrageenan requires more moisture content to be spheronized compared to MCC. This is related to the better water binding capacity of kappa-carrageenan. An additional difference to conventional spheronization studies is the size of the micropellets. The small micropellets have a lower mass, which is relevant for the spheronization. The increased evaporation from extrudates with higher moisture content led to a condensation film on the spheronizer wall,

which prevents the extrudates from adhering to the wall. The extrudates break into smaller pieces right at the beginning. Due to the higher moisture content the pieces are slipping from one another in the spheronizer. Further, during the process moisture movement from the interior to the outer surface of the micropellets is hypothesized. Thus, the pellet growing is prevented. In terms of yield, an increase in spheronization speed led to an increase in yield and an increase in moisture content of the extrudates led to a decrease in yield. The lower yield at higher moisture content can be attributed to agglomerate building during the drying process. As a result the agglomerates were larger than the desired yield of pellet size.
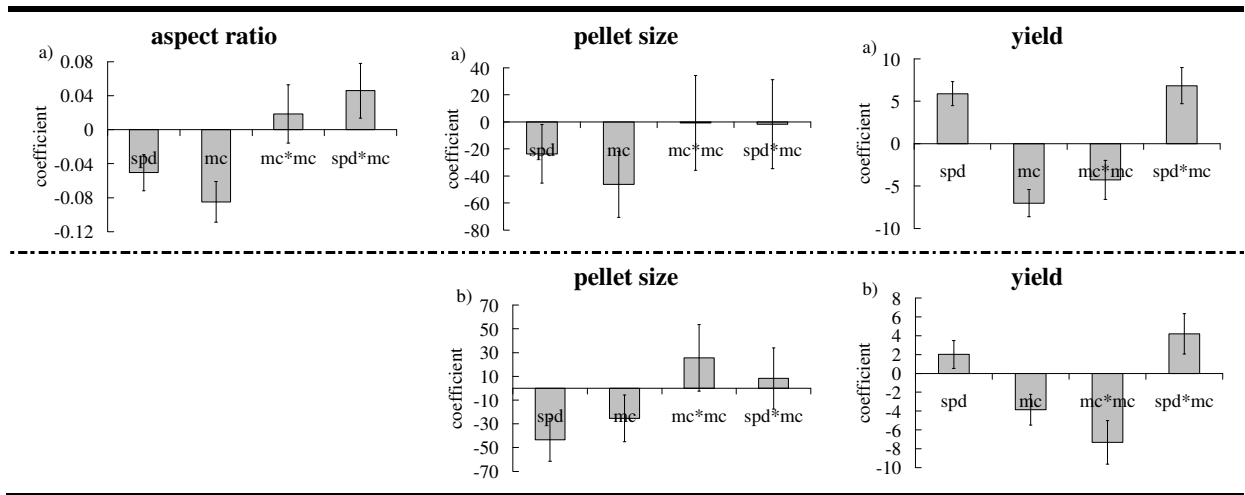
Fig. 7: Coefficient Plots of a) Nica spheronizer and b) Schlueter spheronizer (spd = spheronization speed, mc = moisture content)

For the Schlueter spheronizer, the aspect ratio was largely unaffected by the other factors (R^2_{adj} = 0.422; Q² = -0.736). However, the influence of the spheronization speed on the pellet size (R^2_{adj} = 0.874; Q² = 0.740) and the influences of the spheronization speed as well as the moisture content of the extrudates on the yield (R^2_{adj} = 0.863; Q² = 0.675) were similar to the Nica spheronizer.

The Contour Plots for the Nica spheronizer confirmed the results from the first part of this study (Fig. 8a). Keeping the residence time at 6 min and the loading of the spheronizer at 400 g, higher spheronization speeds resulted in the better aspect ratios and pellet sizes when the moisture content of the extrudates was increased. In addition, higher spheronization speed offset the influence of the moisture content of the extrudates on the yield. At constant moisture content of the extrudates, higher spheronization speed led to decreased aspect ratio and pellet size but increased yield. For the Schlueter spheronizer different profiles of the Contour Plots were obtained (Fig. 8b). The smallest pellet size was obtained at medium moisture content of the extrudates combined with medium to higher spheronization speeds: 12.57 m·s⁻¹ > 18.85 m·s⁻¹ ≈ 15.71 m·s⁻¹. At a constant spheronization speed of 18.85 m·s⁻¹, the pellet size decreased with increasing moisture content up to 78 % before increasing again.

At low and medium moisture content of the extrudates the spheronization speed had marginal effects on the yield. However, when the moisture content of the extrudates was changed to higher values, the yield decreased significantly with lower spheronization speed.
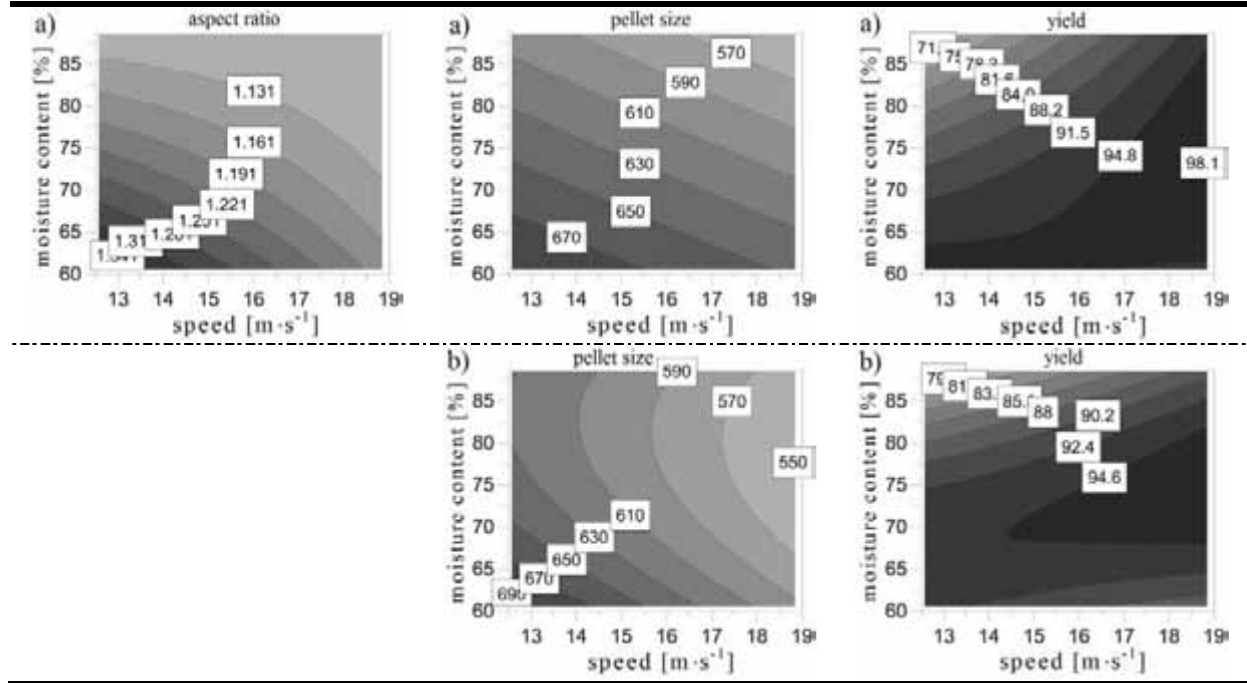
Fig. 8:   Contour Plots of a) Nica spheronizer and b) Schlueter spheronizer

The two spheronizers differed in two respects: First, in the Nica spheronizer a condensation film on the spheronizer wall was obtained by increasing the moisture content of the extrudates. This could be attributed to the absence of inlet air pressure. The condensation film reduced adhesion, which led to lower aspect ratio and increased yield. Second, the friction plate in the Schlueter spheronizer was more clogged, which was related to the different geometry of the friction plates. The Schlueter spheronizer is equipped with bigger truncated pyramids on the friction plate. Therefore, the surface is rougher than that of the Nica spheronizer resulting in a more effective transfer of energy [Schmidt and Kleinebudde, 1998]. Thus, at constant moisture content of the extrudates, the better energy transfer into the product led to more lubrication on the friction plate of the Schlueter spheronizer. As a result, the yield decreased slightly and the pellet size was smaller compared to pellets obtained from the Nica spheronizer.

In this part of the study the optimum conditions for spheronization processes shown in the CCC-design experiments were confirmed on two different spheronizers. Furthermore, by increasing the moisture content of the extrudates the adhesion of the pellets to the spheronizer wall was reduced effectively, especially for the Nica spheronizer. Nevertheless, the trends observed were similar for both spheronizers. Although all factors were adjusted to achieve comparable conditions during the spheronization process, the statistical models were better for the Nica spheronizer.

22

5.1.7 Adaptation of the additional spheronizer process variables

The formulation for this experiment contained 10 % spironolactone (SpL) as API, 70 % tricalcium phosphate as filler and 20 % κ-carrageenan as pelletization aid (Tab. 5). Extrudates of 400 g were spheronized without the use of a scraper for 6 min at spheronization speeds of 15.71 m·s^{-1} and 18.85 m·s^{-1}. The moisture content of the extrudates was between 144.2 % and 146.6 %. The Schlueter spheronizer was used. The additional spheronizer process variables for the Schlueter spheronizer such as temperature of the spheronizer wall and the inlet air pressure were adapted to the conditions of the Nica spheronizer. Both process variables were related to the appearance of the condensation film on the spheronizer wall, which had positive effects on the pellet properties and yield. The temperature of the spheronizer wall was set to 25 °C, 15 °C or left without control resulting in a temperature of approximately 30 °C. The spheronization was performed without inlet air pressure or at 0.2 bar, respectively.

Tab. 5: Results of the full factorial (mixed) design for the adaptation evaluations

Speed [m·s^{-1}]	Temperature [°C]	Inlet air pressure [bar]	Aspect ratio	Pellet size [µm]	Yield [%]
15.71	15	0	1.08	576	77.8
15.71	15	0.2	1.07	597	80.9
18.85	15	0	1.08	554	76.4
18.85	15	0.2	1.07	554	75.5
15.71	25	0	1.08	583	83.7
15.71	25	0.2	1.11	595	87.9
18.85	25	0	1.08	560	80.7
18.85	25	0.2	1.09	553	84.5
15.71	30	0	1.10	583	86.5
15.71	30	0.2	1.11	588	87.7
18.85	30	0	1.08	550	83.6
18.85	30	0.2	1.10	542	88.7

The factors were spheronization speed (x_{spd}), spheronizer wall temperature (x_{temp}) and inlet air pressure (x_{inl}). The same responses were measured and evaluated retrospectively using a full factorial (mixed) design. The complete model equation was:

$$y = b_0 + b_{spd} x_{spd} + b_{temp} x_{temp} + b_{inl} x_{inl} + $$
$$b_{spdtemp} x_{spd} x_{temp} + b_{spdinl} x_{spd} x_{inl} + b_{tempinl} x_{temp} x_{inl}$$

Eq. (8)

The median aspect ratio of the 12 batches was found to vary between 1.07 and 1.11. Thus, most of the pellets could be rated as excellent. The range of the median of pellet equivalent diameter was also small (542 µm to 597 µm) and although the yield was below 90 %, the range was still adequate (75.5 % to 88.7 %). The 10 %-interval for most values was good ranging from 60.2 % to 74.8 %, whereby four values exceeded 75 % (75.2 %, 75.8 %, 76.6 % and 82.4 %) and therefore were excellent.

After performing the backward regression the final model was:

$$y = b_0 + b_{spd} x_{spd} + b_{temp} x_{temp} + b_{inl} x_{inl} + b_{spdinl} x_{spd} x_{inl} + b_{tempinl} x_{temp} x_{inl} \qquad \text{Eq. (9)}$$

The Coefficient Plot shows the results of the final models (Fig. 9).

For the aspect ratio (R^2_{adj} = 0.713; Q^2 = 0.394), the temperature of the spheronizer wall and the two-factor interaction between the temperature and the inlet air pressure showed significant influences. For the pellet size (R^2_{adj} = 0.947; Q^2 = 0.792), the spheronization speed and the two-factor interaction between the spheronization speed and the inlet air pressure were significant. Higher spheronization speed decreased the pellet size. For the yield (R^2_{adj} = 0.89; Q^2 = 0.639), all three factor variables showed significant influences. Therefore, by adapting the additional spheronizer variables Q^2 and R^2_{adj} were improved, although Q^2 was still below 0.5 for the aspect ratio. Nevertheless, most aspect ratios were below 1.1. Turning off the inlet air pressure at higher spheronization speeds and temperatures had positive effects on the aspect ratio, while a spheronizer wall temperature of 15 °C resulted in the best aspect ratio. The benefit of low temperatures is the formation of a condensation film on the spheronizer wall, which prevents the extrudates from sticking to the wall and thus being excluded from the spheronization process. As previously mentioned, the moisture content in the extrudates is a major determinant of the pellet shape and the level of adhesion to the spheronizer wall. This means, the wet-massing during the extrusion process has the highest impact on the pellet properties.
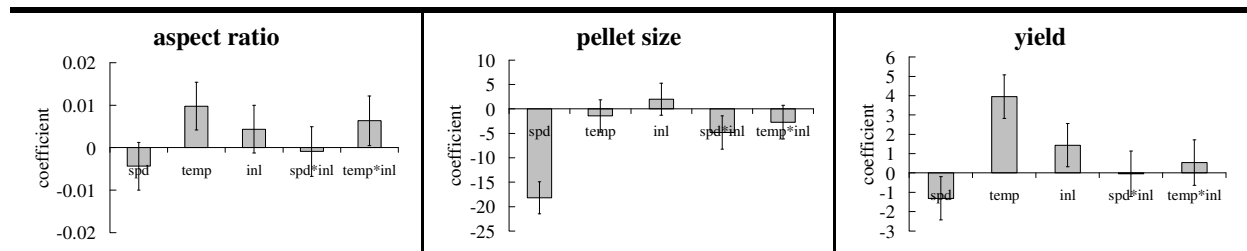
Fig. 9: **Coefficient Plots for adaptation of the additional spheronizer process variables (spd = spheronization speed, temp = temperature of the spheronizer wall, inl = inlet air pressure)**

Due to the better transfer of energy, the water content necessary for the formulation was reduced when the Schlueter spheronizer was used [Schmidt et al., 1997; Schmidt and Kleinebudde, 1998]. Therefore, in studies that used a die plate with 1 mm diameter the high moisture content in the extrudates caused adhesion during the spheronization process. It was thus unexpected that for a die plate with 500 µm diameter higher moisture content was needed to obtain a spheronization process without adhesion. As a result, it was not necessary to reduce the temperature to 15 °C because a sufficient moisture content of the extrudates led to the production of a condensation film on the spheronizer wall when the inlet air pressure was

turned off. This can be explained according to Ghebre-Sellassie [1989b], who elucidated the plasticity of the surface by the enforced moisture movement from the interior to the outer surfaces during spheronization. Thus with higher moisture content of the extrudates, the condensation film arises easily at the beginning. Thus, a spheronization process without adhesion was obtained.

Hence, the adaptation of the additional spheronizer process variables of the Nica to the Schlueter spheronizer resulted in aspect ratios below 1.1. Therefore, both types of spheronizer can be used to produce micropellets.

5.1.8   Summary

Conversion of 500 µm diameter of the extrudates based on κ-carrageenan into micropellets requires higher moisture content of the extrudates to obtain appropriate pellet properties. The optimum conditions for the Schlueter spheronizer was found to be as follows: Spheronization speed of 18.85 m·s^{-1}, spheronizer load of 400 g and residence time of 6 min. Furthermore, to prevent adhesion during the spheronization process, the temperature of the spheronizer wall and the inlet air pressure should not be adjusted if the moisture content in the extrudates is sufficient. There were no significant differences between the Nica and Schlueter spheronizers for spheronization of 500 µm extrudates containing κ-carrageenan.

5.2 Micropellets containing spironolactone as API

5.2.1 Introduction and objective

To evaluate the drug release of micropellets based on κ-carrageenan, spironolactone was used as the first API due to certain requirements. The detailed specifications of the requirements are listed in Chap. 5.3.1.1. First, Spironolactone was used as a model drugs.

The objective of this part of work was to determine i) the properties of the micropellets containing spironolactone as API in different fractions in the formulations; ii) the effect of the filler and; iii) the dissolution behavior of the API in different dissolution media.

5.2.2 Evaluation parameters

5.2.2.1 Introduction

Besides the parameters to characterize the pelletization process and the micropellets (Chap. 5.1.3), the dissolution behavior was the main focus to evaluate the entire product in this part of the work. Micropellets with the best aspect ratio and yield were taken from each formulation for dissolution tests. In addition, the mechanical stability of micropellets containing different ratios between API and pelletization aid were evaluated.

5.2.2.2 Drug release

To evaluate the pharmaceutical availability of the drugs from the micropellets, dissolution profiles were constructed in which the percentage of drug release is drawn against the time. The dissolution rates of micropellets in different media were compared graphically up to 6 h. For a detailed comparison the mean dissolution time (MDT) was calculated (Chap. 8.2.2.5).

5.2.2.3 Similarity of the dissolution profiles

The criteria for deciding the difference or similarity between dissolution profiles are unclear [Shah et al., 1998]. Besides the exploratory data analysis methods, various mathematical comparison methods were used to evaluate the difference between the drug release per unit time for a reference and a test formulation. The 'similarity factor' (f_2 equation) was first described by Moore and Flanner [1996]. It is endorsed by the US Food and Drug Administration (FDA) in the scale-up and post-approval changes-modified release (SUPAC-MR) guidance as an acceptable method for dissolution profile comparison [FDA, 1997b].

The value of f_2 is 100 when the profiles of the reference and the test dissolutions are identical. For an average difference of 10 % at all measured time points f_2 was 50. Values between 50 and 100 ensure sameness of equivalence of the two dissolution profiles [FDA, 1997b] (Chap. 8.2.2.9).

5.2.2.4 Mechanical stability

Micropellets are usually bulk ware to be further processed into tablets or capsules. Therefore, micropellets must be mechanical stable. Mechanical stability is another variable for characterization. Different methods were derived, of which the evaluation by the tensile strength (σ) was suitable to describe the firmness of the micropellets. The tensile strength is calculated by the determining the fracture force to the pellet size (Chap. 8.2.2.4).

5.2.3 Choice of filler

5.2.3.1 Introduction

The micropellets production depends upon the formulation contents. Baert et al. [1991; 1992] evaluated the correlation of extrusion forces and different mixtures, in which the moisture content of the extrudates were dependent on the solubility of the type of filler. In general the drug release of micropellets is mainly dependent on the drug properties such as solubility and particle size. If an insoluble drug was used the dissolution rate from pellets accelerated if water-soluble excipients, surfactants or disintegrants were incorporated [Vervaet et al., 1994]. Santos et al. [2002] investigated the effects of different fillers on the physical properties of pellets containing chitosan. There were no distinctive differences in the dissolution rates between the different formulations.

Hence, to evaluate the dissolution behavior of micropellets comprising κ-carrageenan, different types of fillers with different solubilities were used.

5.2.3.2 Tricalcium phosphate

Tricalcium phosphate ($Ca_5(PO_4)_3OH$) exists in different types and properties [cfb Budenheim, 2008]. In this work two different tricalcium phosphates were used: C13-03 and C53-06 (Tab. 6). While C53-06 is mainly used in pharmaceutics, C13-03 is classified as food grade. However, C13-03 can be used for food as well as for pharmaceuticals. Both types of tricalcium phosphates are food additives and belong to E341 (calcium phosphates).

Tab. 6: Overview of the two different tricalcium phosphates (data provided by Budenheim)

Parameter / Type	C13-03	C53-06
Description	Tri-Cafos PF	Tri-Cafos 30 (TCP 30)
Standard applicable	Food Grade	Ph. Eur
Specification	National Formulary	Ph. Eur
Application	Food Pharmaceutical	Pharmaceutical
Food additive	E341	E341
Molecular weight [g·mol^{-1}]	502	502
P_2O_5 value [%] (Phosphate [%])	41.5 (18)	43.0 (18)
CaO value [%] (Calcium [%])	53.5 (40)	52.0 (40)
Bulk density [g·l^{-1}]	200	200
pH value of 10 % suspension	7.0	5.8
Median particle size (d_{50}) [µm]	5	4

Tricalcium phosphates are chemically stable at room conditions and practically insoluble in water. The chosen tricalcium phosphates basically differ in the proposed applications and the pH value. The difference in pH is related to the different ratio between calcium oxide and phosphorus pentoxide. All measured values were provided as approximate values. Further parameters were investigated (Tab. 7).

Tab. 7: **Measured parameters of the different tricalcium phosphates ($\bar{x} \pm SD$, n = 3, * n = 5)**

Parameter / Type	C13-03	C53-06
ffc value	1.71 ± 0.04	1.84 ± 0.20
Bulk density [g·l^{-1}] *	240 ± 0.01	225 ± 0.01
Helium pycnometric density [g·cm^{-3}]	3.03 ± 0.03	3.12 ± 0.01
Median particle size in air [µm]	3.36 ± 0.03	3.97 ± 0.05
Median particle size in 2-propanol [µm]	-	4.01 ± 0.10
Free calcium conc. [mg·(100ml)$^{-1}$] at:		
pH = 3.03	3.05 ± 0.20	2.35 ± 0.30
pH = 5.02	1.71 ± 0.20	1.12 ± 0.30
deionized water	0.75 ± 0.10	0.37 ± 0.20
Moisture content [%]	1.31 ± 0.10	0.86 ± 0.10
pH value of 10 %-suspension	7.15 ± 0.01	5.73 ± 0.01

The mean moisture content was slightly higher for C13-03. The bulk densities of both types of tricalcium phosphates differed from the provided data, which was probably attributed to handling. The pH values of the 10 % suspensions were similar to the provided data of the manufacturer. In addition, both types of tricalcium phosphate did not substantially differ from one another in the other measured parameters: 1. The flowability was evaluated by the ring shear cell tester (Chap. 8.2.3.9). The ratio of consolidation stress and unconfined yield strength value described the flow behavior of a bulk. It is defined as the flow function (ffc-value). Flow behavior improves with increasing ratio. The flow behavior ranges from non-flowing over cohesive to free-flowing behavior. The ffc-values of both types of tricalcium phosphates were < 2. Hence the flow behavior was categorized as non-flowing and very cohesive. 2. The median particle size was evaluated by the laser light diffraction (Chap. 8.2.3.3). The values differed slightly from the provided data. The median particle size of C53-06 was also investigated as a suspension to determine the effect of the extrusion process on the particle size of tricalcium phosphate (Chap. 8.2.3.3). No substantial difference was obtained to the measurement in air. Hence, it was assumed that the particle size of C53-06 does not change during extrusion. 3. The free calcium concentration was evaluated by complexometric titration (Chap. 8.2.3.7). It is the marginal dissolved calcium amount of a suspension comprising insoluble tricalcium phosphate. Although, with increasing pH the free concentration of calcium ions decreased, the dissolved calcium concentration was < 1 % for all pH values. Hence, it was assumed that the free amount of calcium ions from tricalcium phosphate does not affect the extrusion/ spheronization of κ-carrageenan. Further, the x-ray evaluation showed that the crystalline structure of both types was similar (Fig. 10).
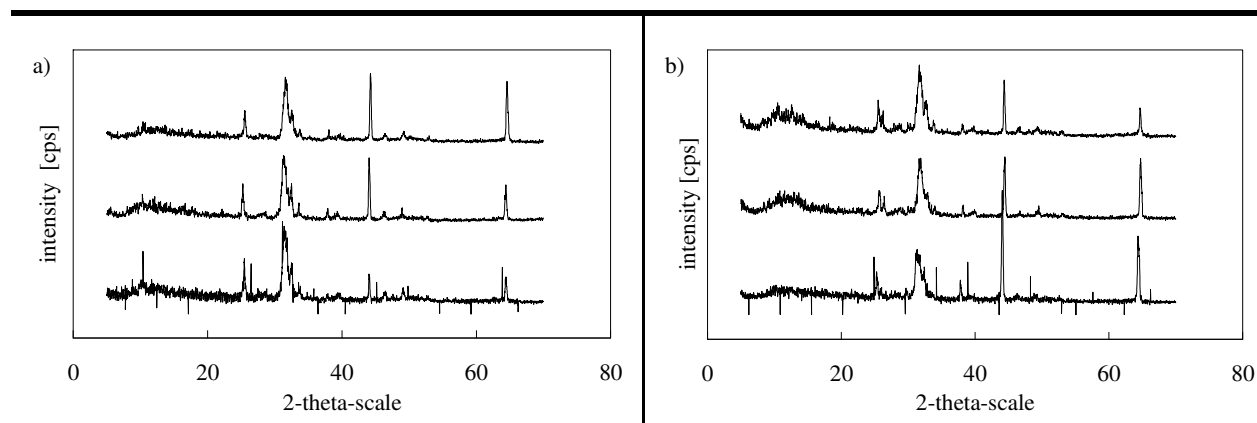
Fig. 10: X-ray pattern of a) C13-03 and b) C53-06 (n = 1)

In summary, both types of tricalcium phosphate differed only in the pH value of a 10 % suspension. Since C53-06 has been explicitly classified for pharmaceutical applications, it was predominantly used in this thesis. C13-03 only served for comparison.

5.2.3.3 Lactose monohydrate

Lactose monohydrate (GL200) is a well-known filler or diluent in pharmaceutical formulations [Wade and Weller, 1994]. It is a natural disaccharide obtained from milk. Lactose is commercially available in various grades, which differ in the physical properties. Hence, lactose exists in two anomeric forms, α- and β-lactose. α-Lactose is generally known as the monohydrate form, but also exists in two anhydrous forms. One of the anhydrous forms of α-lactose is the spray dried lactose, which is available for direct compression.

Lactose monohydrate has a molecular weight of 360.3 g·mol^{-1}, a bulk density around 500 g·l^{-1} (Chap. 8.2.3.10), a mean median particle size (x_{50}) of 30 μm (Chap. 8.2.3.3) and the moisture content is around 5.1 % (Chap. 8.2.2.1). The solubility in water is about 200 g·l^{-1} [Merck Index, 1989].

5.2.4   Extrusion/ spheronization using tricalcium phosphate as filler

5.2.4.1 Production and characterization

Previous production of micropellets containing 10 % spironolactone and 20 % κ-carrageenan was successful (Chap. 5.1.7). For further investigations that ratio in the formulation was taken as '*standard formulation*'. The amount of spironolactone was increased to the binary mixture containing different amount of C53-06 as filler and about 20 % κ-carrageenan as pelletization aid (Tab. 8). The extrusion process differed from the standard conditions by the screw speed (Chap. 8.2.1.2). The extrusion took place at a constant screw speed of 160 rpm. The moisture content of the extrudates varied from batch to batch. The spheronization process was carried out under standard conditions (Chap. 8.2.1.3).

29

Tab. 8: Overview of the formulations containing C53-06 (* $\overline{x}$ ± SD, **x_{50} ± IQR)

Formulation In [%]	I	II[*]	III	IV
Spironolactone	10	25	50	75
C53-06	70	55	30	5
κ-Carrageenan	20	20	20	20
Moisture content [%] *	137.0 ± 0.4	162.6 ± 1.0	134.0 ± 0.9	135.6 ± 1.8
Aspect ratio **	1.11 ± 0.1	1.08 ± 0.1	1.08 ± 0.1	1.10 ± 0.1
Pellet size [µm] **	558 ± 75.1	526 ± 87.0	581 ± 69.7	603 ± 84.6
Yield [%]	87.6	76.0	80.3	54.6
10 %-interval [%]	70.0	58.8	74.2	68.8
Tensile strength [MPa] *	8.13 ± 1.2	14.26 ± 1.8	14.44 ± 2.7	9.70 ± 1.3

All ternary powder mixtures were also extruded and spheronized successfully as with the 10 % spironolactone formulation. The best pellet properties for each formulation are listed in Tab. 8. Compared to the tensile strength values obtained by Thommes [2006], the actual values are higher. This might be attributed to different moisture content since the micropellets were stored under ambient conditions. Changing the ratio between API and pelletization aid, the moisture content of the extrudates were around 135.5 %, with one exception of 162.6 % for Formulation II. Nevertheless, the pellet properties were mainly similar.

To specifically evaluate the effect of C53-06, another type of tricalcium phosphate was used as filler. Therefore both formulations contained 10 % spironolactone, either 70 % C53-06 or C13-03 and 20 % κ-carrageenan as pelletization aid. To exclude an effect of different extrusion screw speeds, the formulation containing C53-06 was produced again. This time the extrusion took place under standard conditions (Chap. 8.2.1.2). The moisture content of the extrudates varied and ranged from 123.5 % to 169.6 % for C53-06 and from 150.0 % to 183.6 % for C13-03. For both formulations the Nica spheronizer was used. Batches of 400 g were spheronized for 6 min at 18.85 m·s^{-1}.

The aspect ratio was 1.11 and 1.16 for the batch with the best pellet properties of each formulation. The micropellets comprising C53-06 had a pellet size of 558 µm, while the pellet size for C13-03 was 515 µm. The yield was 87.6 % and 70.5 %, respectively. Therefore, using C53-06 as filler the micropellets showed better aspect ratio and yield, but the pellet size was bigger than using C13-03. Further, the 10 %-interval was only 70.0 % for C53-06, but 74.2 % for C13-03. Nevertheless, both batches were rated as good. The tensile strength of micropellets based on C13-03 was enhanced (15.20 ± 2.1 MPa) and therefore, the mechanical stability was increased compared to micropellets containing C53-06 (8.13 ± 1.2 MPa). Taken together, the pellet properties of both types of tricalcium phosphates were regarded as similar. Further, the moisture content required for the spheronization of the extrudates containing C53-06 was similar to the moisture content extruded at 160 rpm. However, the moisture content required for the production of the micropellets based on C53-06 and C13-03 varied slightly (Fig. 11).

[*] Actual values: 24.3 % SpL, 54.1 % C53-06, 21.6 % κ-carrageenan
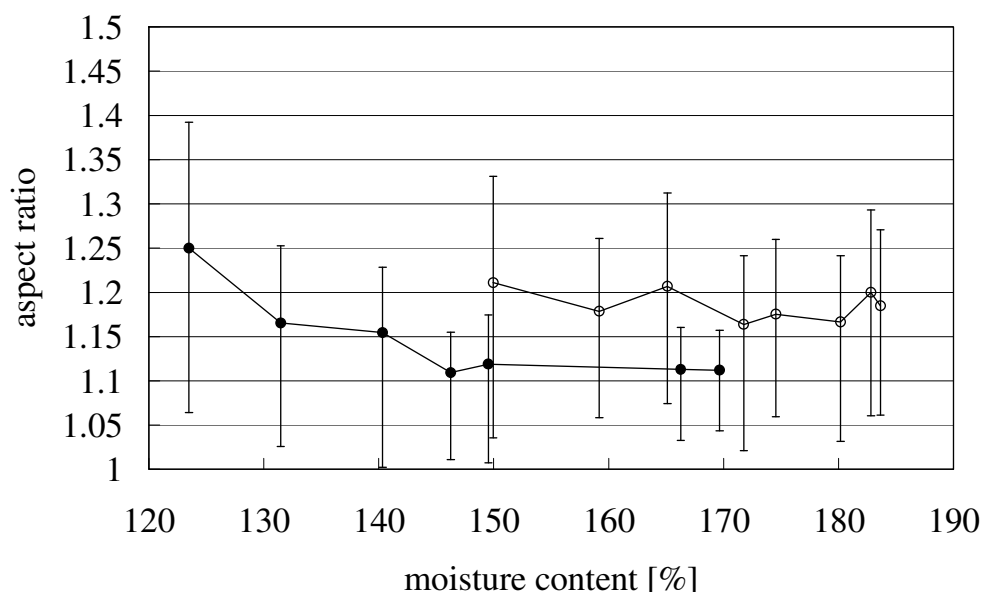
Fig. 11: Micropellet properties of 10 % drug load and different types of filler: —◆— 10 % SpL + 70 % C53-06, —○— 10 % SpL + 70 % C13-03 (x_{50} ± IQR, n = 3)

Although the median aspect ratio values of micropellets containing C53-06 were lower, the interquartile ranges of both formulations were high (Fig. 11). Therefore, the differences were rather insignificant. Nevertheless, due to the exploratory data C53-06 was used for further investigations.

5.2.4.2 Dissolution behavior

Introduction and objective

To evaluate the dissolution behavior on ionic interactions, the gelling behavior of κ-carrageenan was investigated. Not all types of carrageenans are gelling. λ-Carrageenan is a non-gelling type due to the lack of the 3,6-anhydrogalactose residues. The ability of carrageenans to form gels is generally dependent on the presence of the 3,6-anhydrogalactose residue and strongly affected by ion treatments [te Nijenhuis, 1997]. Therefore, the addition of ions such as potassium or calcium ions leads to gelling. However, weak gels were also obtained under salt-free conditions [Hossain et al., 2001].

κ-Carrageenan is a gel-forming polysaccharide. The polymeric network originates from physical cross-linkage by ionic interactions [Hennink and van Nostrum, 2002]. It is an anionic polymer and therefore interacts with cations to create so called 'ionotropic' hydrogels, which absorb and retain large amounts of water. κ-Carrageenan forms thermoreversible gels on cooling, which are typically hard, strong and brittle [Bubis, 2000].

Dependent on the type of ions, κ-carrageenan passes through several stages of conformational transitions. Various descriptions are reported in the literature, whereupon nowadays the largely accepted view is the 'domain'-model [Morris et al., 1980]. To investigate the cationic interactions on micropellets containing κ-carrageenan, different chloride salts were used.

31

In general, the interest in hydrogels and the ionic interactions, which were involved in the cross-linking effects, increased to produce drug delivery systems [Hoffman, 2002]. Miyazaki et al. [1981] reported sustained drug release in the presence of hydrogels due to drug diffusion. Besides, if cross-linking effects were involved, the strength of the cross-linked matrix played an essential role in drug release [Tayade and Kale, 2004]. Further, the dissolution rates were dependent on the dissolution media investigated on cross-linked calcium-pectin gel-coated pellets [Sriamornsak and Kennedy, 2007].

These observations were transmitted to the micropellets containing κ-carrageenan. So far, the production did not show any effects of the calcium compound in the formulation. Therefore, the primary objective was to determine the cationic interactions on drug release in i) different dissolution media containing different types and amounts of dissolved ions; ii) different ratios between API and κ-carrageenan in the formulations and; iii) two different types of tricalcium phosphates. Therefore, micropellets containing spironolactone as API, tricalcium phosphate as filler and κ-carrageenan as pelletization aid were used in the following dissolution investigations.

Fast dissolving media

First, the drug release was investigated in some commonly used dissolution media such as deionized water and 0.1 M HCl. Depending on the amount of drug load, the micropellets floated in the dissolution media. The weighted sample of 10 % drug load (~75 mg) mostly sank to the ground of the vessel, while the weighted sample of higher drug loads (~10 mg) mainly floated. Due to the high amount of insoluble tricalcium phosphate in the standard formulations, deionized water became turbid and the tricalcium phosphate partly accumulated on the filter. To compare the dissolution profiles, only the drug release of the standard formulations in deionized water was normalized, which means that the data points of the equilibrium were considered to 100 %. Each absorption value per unit time was calculated upon the steady state (Eq. 10):

$$ndr = \frac{Abs_{(t)}}{\sum_{i=n-4}^{n} \frac{Abs_{(i)}}{5}} * 100 \qquad \text{Eq. (10)}$$

where ndr is the normalized drug release, Abs is the absorption value at the time (t) and the mean absorption value of the last five values at the steady state respectively.

Even though the dissolution behavior differed dependent on the media, the dissolution profiles obtained for all formulations were fast. The drug release in deionized water was completed within 15 min and in 0.1 M HCl within 20 min, which was attributed to the longer lag time (Fig. 12a, b). The reason for the longer lag time of 50 % drug load was unclear.
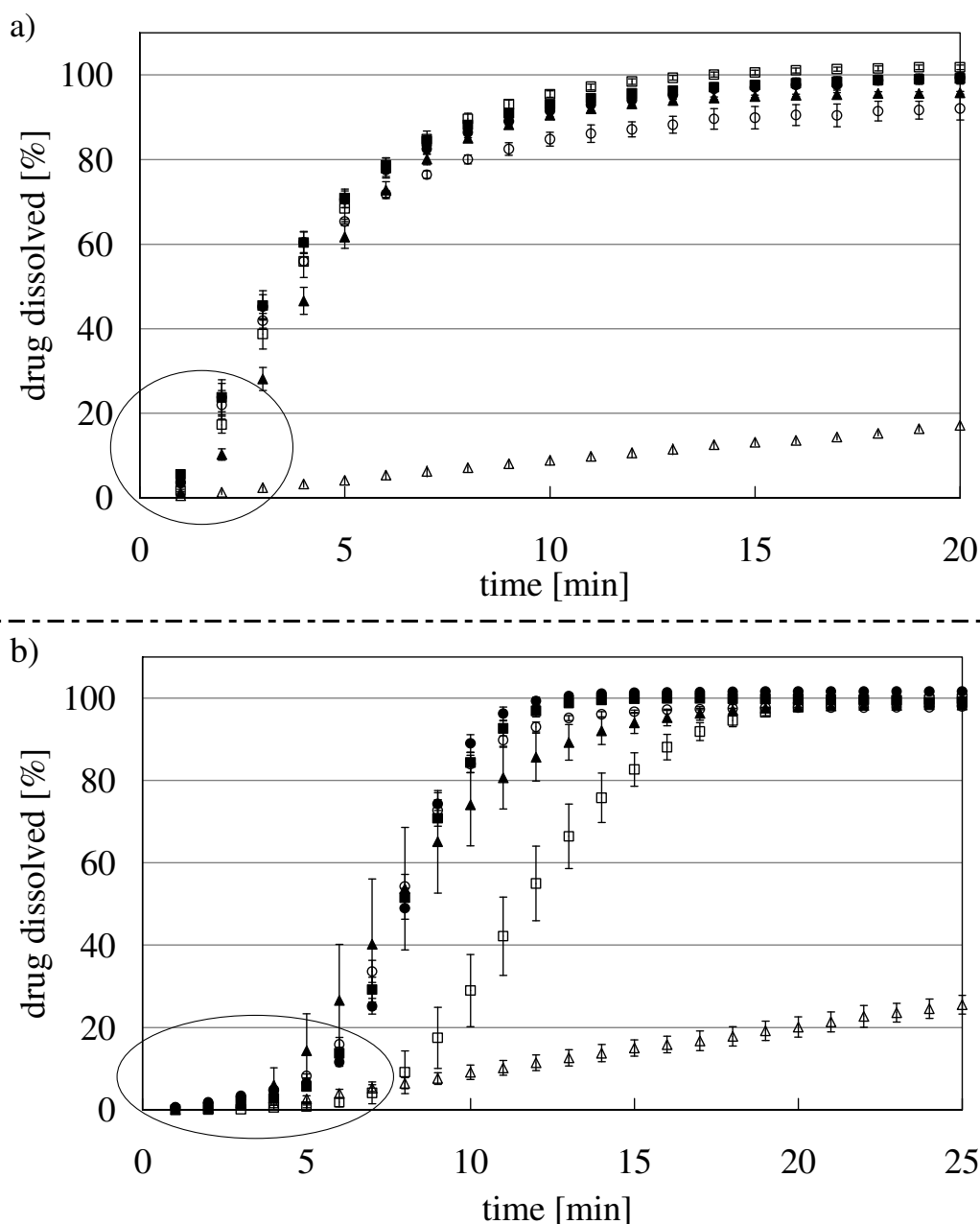
Fig. 12: Release profiles of different formulations in a) deionized water and b) 0.1 M HCl: ⬟ 10 % SpL + 70 % C53-06, ◔ 10 % SpL + 70 % C13-03, ■ 25 % SpL + 55 % C53-06, □ 50 % SpL + 30 % C53-06, ▲ 75 % SpL + 5 % C53-06, △ SpL-powder ($\bar{x} \pm$ SD, n = 3)

The lag time of each dissolution profile was related to the solubility of the API [Ragnarsson et al., 1992]. Hence independent of the media, the drug load affected the dissolution behavior. Therefore, the lag time of the drug outweighed the dissolution behavior of the micropellets. With respect to sink-conditions, pure spironolactone powder of approximately 7.5 mg was spread into the dissolution medium under the same dissolution conditions (Chap. 8.2.2.5). The delayed increase in drug amount at the beginning was attributed to the poor wettability of the drug. In fact, spironolactone powder always floated independent of the medium. Even though the micropellets also partially floated, the drug release was fast. This was attributed to the improved wettability of the drug in the presence of κ-carrageenan. The dominant effect of κ-

33

carrageenan was substantially observed in 0.1 M HCl (Fig. 12b). Further, it was observed that increasing the amount of drug showed higher deviations, which was referred to floating. A difference in density between the micropellets comprising 10 % drug load and 50 % drug load might be the reason.

Likewise to the exploratory analysis, the similarities of the dissolution profiles were proven by the 'similarity factor'. The formulations containing different ratios between API and κ-carrageenan were calculated based on the standard formulation in deionized water. The similarity of the dissolution profiles was only confirmed for micropellets with 25 % drug load ($f_{2\,(25\,\%\,API)}$ = 57.1, $f_{2\,(50\,\%\,API)}$ = 49.6, $f_{2\,(75\,\%\,API)}$ = 43.7). In 0.1 M HCl the dissolution profiles were similar except for the 50 % drug load ($f_{2\,(25\,\%\,API)}$ = 79.6, $f_{2\,(50\,\%\,API)}$ = 27.1, $f_{2\,(75\,\%\,API)}$ = 51.9). Even though, some dissolution profiles were not similar to the standard formulation, the difference might not be of therapeutic relevance due to the fast drug release.

The dissolution behavior of micropellets in 0.1 M sodium chloride solution as dissolution medium was expected to be fast due to the dissolving effect of the sodium ions on κ-carrageenan [Bubis, 2000]. The drug releases of the micropellets comprising C53-06 were completed within approximately 30 min and therefore, the dissolution in 0.1 M sodium chloride solution was substantially longer than in deionized water or 0.1 M HCl. This was related to the time required for the sodium ions to interact with κ-carrageenan (Fig. 13). Furthermore, it was observed that an increase in drug load slightly enhanced the lag time.
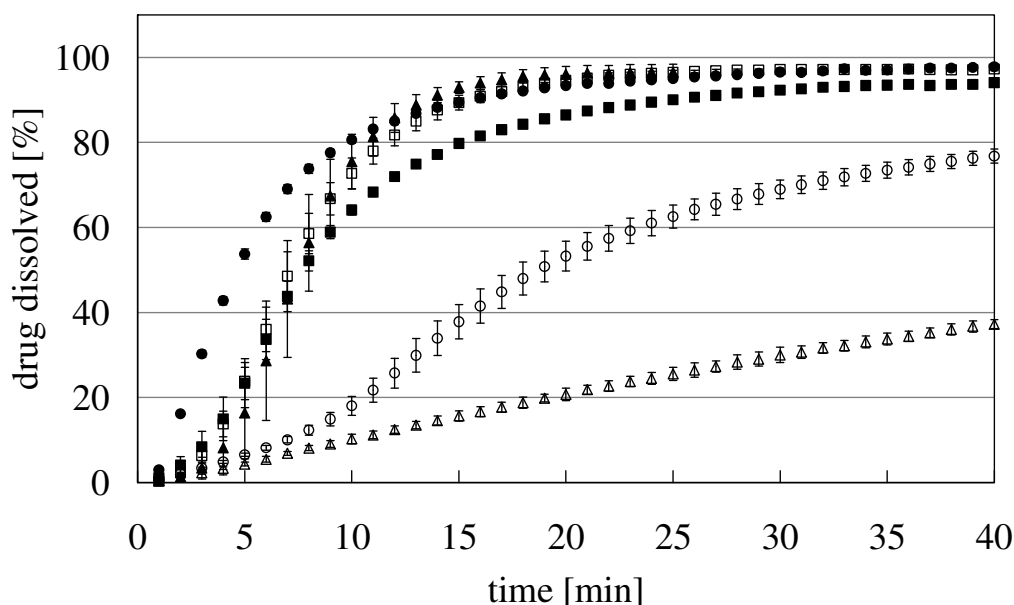
Fig. 13: **Release profiles of different formulations in 0.1 M sodium chloride:** ⬤ **10 % SpL + 70 % C53-06,** ◇ **10 % SpL + 70 % C13-03,** ■ **25 % SpL + 55 % C53-06,** ☐ **50 % SpL + 30 % C53-06,** ▲ **75 % SpL + 5 % C53-06,** △ **SpL-powder ($\bar{x} \pm SD$, n = 3)**

The similarity factors did not confirm the sameness of equivalence to the standard formulation with 10 % drug load based on C53-06 ($f_{2\,(25\,\%\,API)}$ = 43.6, $f_{2\,(50\,\%\,API)}$ = 48.2, $f_{2\,(75\,\%\,API)}$ = 44.3),

which was expected due to the time dependence of the ionic interactions. Nevertheless, with respect to the dissolving profile of the powder, κ-carrageenan improved the drug release independent of the ratio between API and κ-carrageenan. Further, the drug release within 30 min was still in the range of therapeutic importance.

Regarding the dissolution profile of the micropellets based on C13-03, the drug releases in deionized water and 0.1 M HCl were similar to the standard formulation comprising C53-06 (Fig. 12a, b; $f_{2\ (water)} = 56.8$, $f_{2\ (0.1\ M\ HCl)} = 67.3$). However, the dissolution profiles were not similar in 0.1 M sodium chloride solution (Fig. 13; $f_2 = 18.7$). Although the reason was unclear, the drug release was always improved in the presence of κ-carrageenan compared to the dissolving profiles of the powder.

Due to the reproducible dissolution behavior, the micropellets comprising C53-06 were used for further investigations.

Chloride salts with different cations

The ionic interactions between cations and κ-carrageenan were investigated using chloride solutions with different cations as dissolution media. The gel promoting ions were investigated using different concentrations of calcium or potassium chloride solutions to evaluate the attraction between the dissolved ions and κ-carrageenan. In addition, a 0.1 M combination of both ions as well as of calcium and sodium chlorides were analyzed. With regard to the ratio between API and pelletization aid, the cross-linking effects of the dissolved ions on the micropellets were observed on drug release. Fig. 14 showed the dissolution profiles of all formulations in 0.1 M calcium chloride solution.
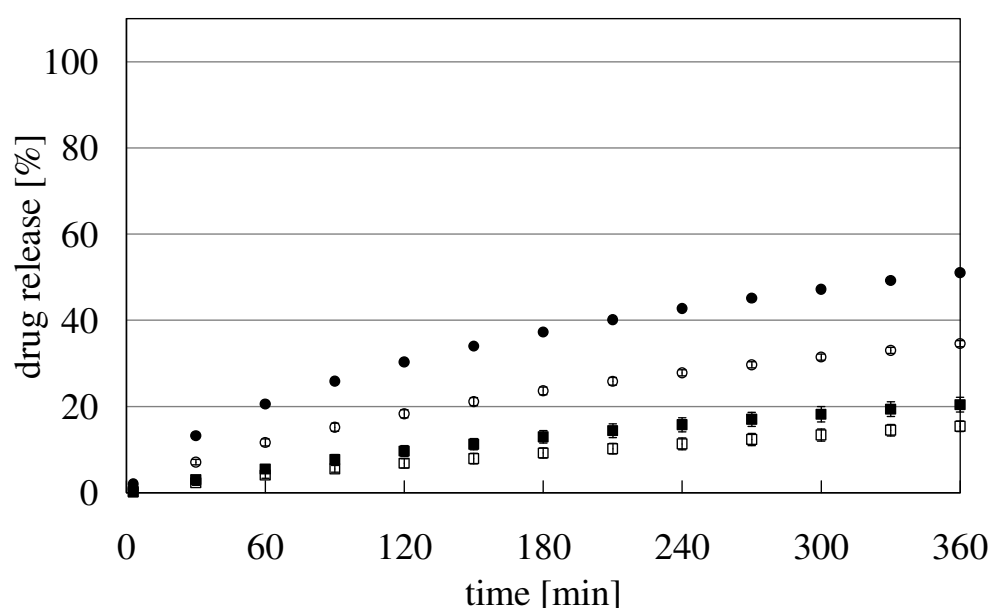
Fig. 14: **Release profiles of different formulations in 0.1 M calcium chloride solution:** ◆ **10 % SpL + 70 % C53-06,** ○ **25 % SpL + 55 % C53-06,** ■ **50 % SpL + 30 % C53-06,** □ **75 % SpL + 5 % C53-06 ($\bar{x} \pm$ SD, n = 3)**

Depending on the ratio between spironolactone and κ-carrageenan, the dissolution profiles varied: While 10 % drug load resulted in the fastest dissolution, 50 % of drug load showed prolonged drug release ($f_2 = 31.4$). The difference between 50 % and 75 % drug load was marginal. In fact, the mathematical comparison evaluated the f_2-value of 70.9. Therefore, further investigations on ionic interactions were performed by comparing the dissolution behaviors of micropellets containing 10 % with 50 % drug load.
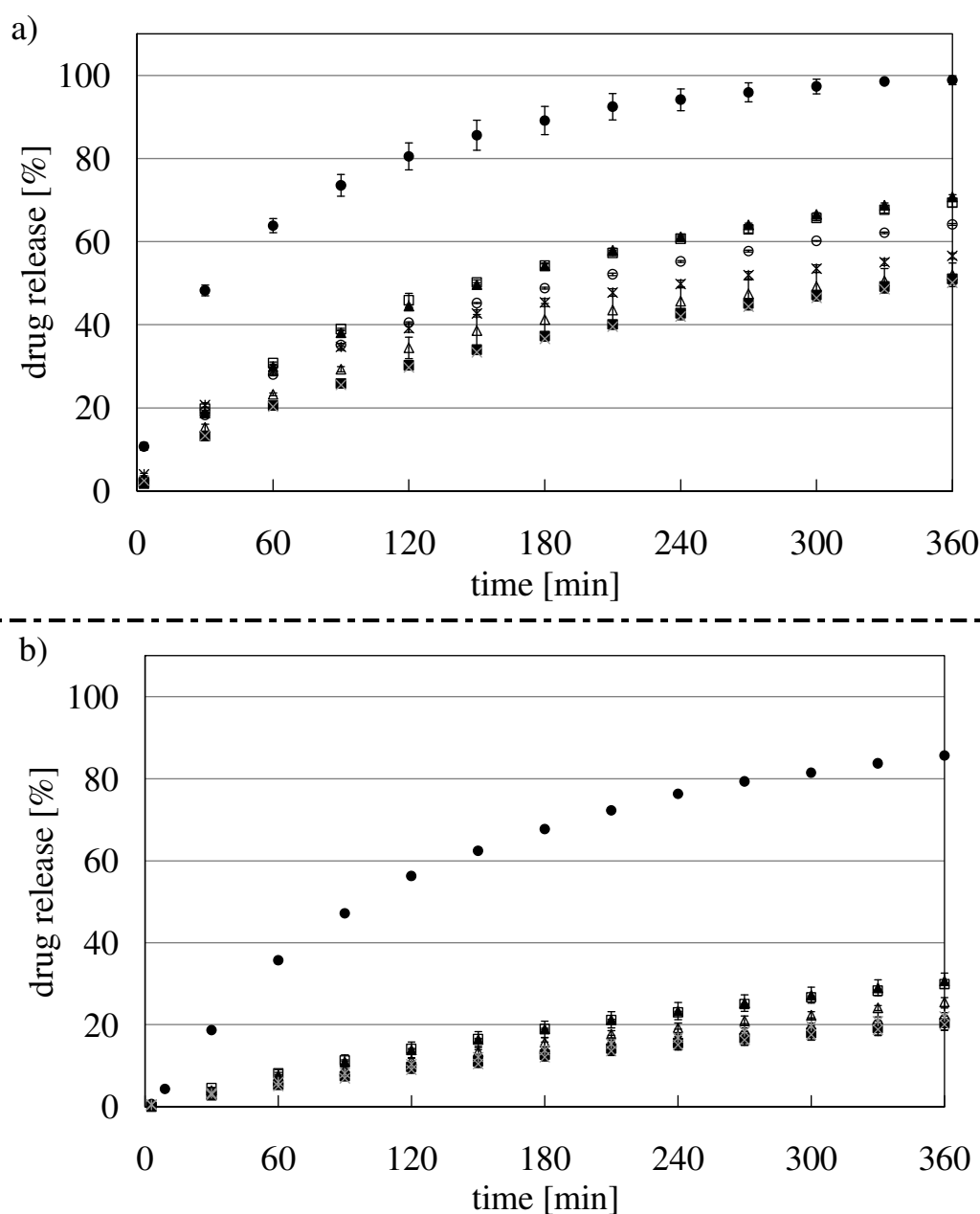
Fig. 15: Release profiles of a) 10 % drug load and b) 50 % drug load: ◕ 0.01 M calcium chloride (for 50 % n = 2), ○ 0.05 M calcium chloride, ■ 0.1 M calcium chloride, □ USP-buffer (pH = 6.8), ▲ 0.05 M potassium chloride, △ 0.1 M potassium chloride, ✕ 2x0.05 M calcium + potassium chloride, ✳ 2x0.05 M calcium + sodium chloride ($\bar{x}$ ± SD, n = 3)

The dissolution profiles differed depending on the concentration of dissolved ions and the ratio between spironolactone and κ-carrageenan: While 10 % drug load resulted in the fastest

dissolution in all media, 50 % drug load hardly reached 50 % drug release within 6 h except in 0.01 M calcium chloride solution (Fig. 15a, b).

All formulations showed similar ranking regarding the media: For each drug load 0.05 M potassium chloride and USP-buffer ($f_{2\ (10\ \%\ API)} = 94.4$, $f_{2\ (50\ \%\ API)} = 98.2$) as well as 0.1 M calcium chloride and 0.1 M potassium chloride showed similar dissolution profiles ($f_{2\ (10\ \%\ API)} = 74.9$, $f_{2\ (50\ \%\ API)} = 74.9$), respectively. For drug load of 50 % or higher 0.05 M calcium chloride solution resulted in dissolution profiles equal to 0.1 M calcium chloride ($f_2 = 98.6$); below 50 % drug load the drug release in 0.05 M calcium chloride was faster ($f_2 = 48.1$) (Fig. 15a, b). Furthermore, the dissolution in 0.05 M potassium chloride solution (or USP-buffer) was always faster than in media containing 0.1 M calcium or potassium chloride solution. With regard to the dissolution profiles of 0.1 M calcium or potassium chloride solution, the combination of both ions was expected to show similar dissolution behavior as the pure 0.1 M calcium chloride solution due to the fact that both ions had similar gelling effects on κ-carrageenan (Tab. 10) [Bubis, 2000]. However, the combination of calcium and sodium ions also showed similar dissolution profile as in 0.1 M calcium chloride solution (Tab. 10), which was attributed to a greater effect of calcium ions rather than to sodium ions. Therefore, the fast dissolving effect of sodium ions was suppressed.

Referring to the fast dissolving media, the dissolution profiles of 0.1 M sodium chloride solution were not similar for the micropellets containing either C53-06 or C13-03. Therefore, the dissolution behavior of the micropellets based on C13-03 was investigated in several dissolution media containing different cations. To calculate the similarity factor (Tab. 9), the dissolution profiles of micropellets based on C53-06 in each dissolution medium was used as reference.

Tab. 9: Similarity factor of the comparison between both tricalcium phosphates in different media

Medium	0.05 M Calcium	0.05 M Potassium	0.1 M Calcium	2x0.05 M Calcium + potassium	USP-buffer
f_2-value	82.2	75.3	76.4	76.3	71.3

Independent from the type and amount of ions in the dissolution media, the dissolution profiles of the micropellets based on C13-03 were similar to the dissolution profiles of the micropellets containing C53-06. Especially the comparison of the dissolution profiles in 0.1 M calcium chloride solution indicated that the drug release of the micropellets comprising either type of the tricalcium phosphates will behave similar in the presence of other 0.1 M gel-promoting ions. In addition, to exclude the effect of the pH of both types on the dissolution behavior of the micropellets, the pH values of the different dissolution media were measured before and after the dissolutions (Chap. 8.2.3.12). No substantial differences were obtained for the micropellets comprising either of the tricalcium phosphates. In fact, all measured pH values were around 6. Hence, the dissolution behavior of C53-06 micropellets was sufficient for future comparison of dissolution profiles.

Besides the investigated ions, κ-carrageenan contains various counter-ions itself such as magnesium, lithium and ammonium ions (Chap. 1.3.3). Therefore, dissolution media containing 0.1 M of these cation chloride solutions were investigated. The comparison of all media containing concentrations of 0.1 M different ions varied in the dissolution profiles (Fig. 16a, b). It was confirmed that 0.1 M of sodium and lithium chloride showed the fastest dissolutions independent of the drug load.
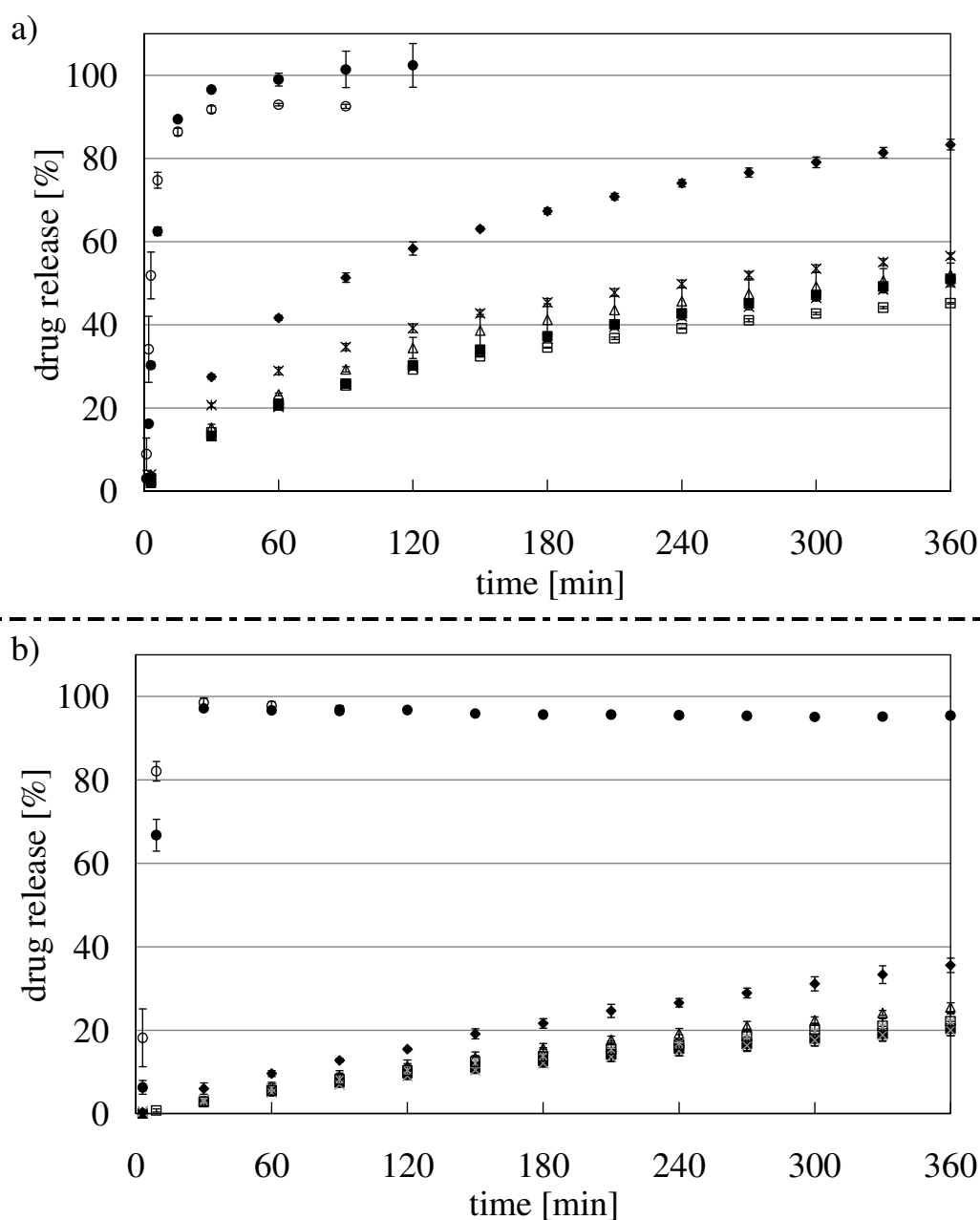
Fig. 16: **Release profiles in different 0.1 M media a) 10 % drug load and b) 50 % drug load: ⬤ sodium chloride, ○ lithium chloride, ■ calcium chloride, □ magnesium chloride, ◆ ammonium chloride, △ potassium chloride, ✕ 2x0.05 M calcium + potassium chloride, ✳ 2x0.05 M calcium + sodium chloride ($\bar{x} \pm SD$, n = 3)**

For drug load of 50 %, the dissolution profiles of 0.1 M in gel-promoting ions were similar in the exploratory and mathematical comparison methods (Tab. 10). However, all the drug releases were below 50 % within 6 h (Fig. 16b).

Tab. 10: Similarity factor of different 0.1 M gel-promoting ions to calcium ions in the dissolution media

0.1 M Medium \ f_2-value	$f_{2\,(10\,\%\,API)}$	$f_{2\,(50\,\%\,API)}$
Potassium chloride	74.9	74.9
Calcium + potassium chloride	96.4	96.2
Calcium + sodium chloride	56.0	91.7
Magnesium chloride	74.2	91.5
Ammonium chloride	27.7	51.0

For 10 % drug load, the dissolution profiles of 0.1 M gel-promoting ions ranged within 10 % difference of the drug release, which was also observed in the f_2-values (Tab. 10). Even though the values of f_2 differed more than the values of 50 % drug load, the dissolution profiles were still similar except the dissolution in 0.1 M ammonium chloride. Compared to 50 % drug load the difference to the 0.1 M ammonium chloride solution was striking and did not confirm the sameness of equivalence. The reason was unclear.

Taken together, the dissolution behavior of the micropellets comprising different ratios between API and κ-carrageenan depend on the amount of gel-promoting ions in the medium. To exclude the effect of the moisture content of the micropellets, more dissolution experiments were performed. The moisture content of the micropellets was evaluated by Karl-Fischer titration (Chap. 8.2.3.3). Micropellets containing 75 % drug load were used to investigate the possible effect of moisture content in the different dissolution media (Tab. 11). The difference in moisture content between the measurements of intact and comminuted micropellets was negligible. Hence for further investigations, the moisture content of the micropellets was evaluated by the comminuted micropellets.

Tab. 11: Moisture content [%] of the micropellets containing 75 % drug load ($\bar{x} \pm SD$, n = 3)

Medium \ Micropellets	0.1 M Calcium	2x0.05 M Mix[†]	0.1 M HCl	Deionized water	0.05 M Calcium	0.05 M Potassium	0.1 M Sodium	0.01 M Calcium	USP-buffer
Comminuted	5.5 ± 0.04	5.5 ± 0.04	5.9 ± 0.05	5.9 ± 0.05	5.9 ± 0.26	5.9 ± 0.26	5.6 ± 0.04	5.3 ± 0.08	5.3 ± 0.08
Intact	5.4 ± 0.15	5.4 ± 0.15	-	-	-	-	-	-	-

Although, the moisture contents of the micropellets were similar, the difference in the dissolution profiles was observed dependent on the dissolution media. Therefore, the moisture content of the micropellets did not affect the dissolution behavior in the different media.

[†] 2x0.05 M Calcium + potassium chloride

Further, to exclude the moisture content effect of the micropellets containing different ratios between API and κ-carrageenan in the presence of calcium ions, the dissolution of each batch was repeated with simultaneous evaluations of the moisture content by Karl-Fischer titration (Tab. 12).

Tab. 12: **Moisture content of different drug loads in 0.1 M calcium chloride solution ($\bar{x} \pm SD$, n = 3)**

Drug load [%]	10	25	50	75
Moisture content [%]	5.5 ± 0.11	5.9 ± 0.20	5.6 ± 0.07	5.5 ± 0.04

The moisture contents of the micropellets containing different ratios between API and κ-carrageenan were similar. Therefore, the moisture content of the micropellets did not affect the dissolution behavior in 0.1 M calcium chloride solution. Hence, the differences in the dissolution profiles were attributed to i) the ratio between API and κ-carrageenan and; ii) the ionic interactions between the dissolved ions and κ-carrageenan.

Discussion of ionic interactions

Differences in the dissolution behavior of micropellets comprising κ-carrageenan were obtained with regard to the dissolution media. This was attributed to ionic interactions. Therefore, two aspects had to be considered: i) the ionic interactions between the κ-carrageenan and dissolved univalent ions with respect to the type and the concentration and; ii) the cationic effects of divalent ions with regard to the univalent ions.

Due to the ionic nature of κ-carrageenan, gelling is substantially affected by the presence of electrolytes, which based on molecular entanglements and secondary forces such as ionic and hydrogen-bonding forces. The gelling mechanism is not perfectly defined at present. However, gelling of κ-carrageenan is nowadays considered to be a two step process in which i) the coil to helix transition leads to the formation of a double helix conformation followed by ii) aggregation and network forming [Morris et al., 1980]. Hence, gels can be empirically classified by the strength of cross-linkages with regard to the concentration of polymers and cations [Mancini et al., 1999].

In general, the gelling reaction occurs when the cations diffuse into the hydrocolloid solution. The gel structure depended on the cross-linkage of the 3D-network beginning at the surface of a sample and immerses [Mammarella and Rubiolo, 2003]. However, in this part of work, κ-carrageenan was processed into micropellets before being exposed to the dissolved ions. Therefore, the starting conditions of κ-carrageenan differed. Hence, the numerous known explanations of the ionic interactions on the κ-carrageenan solution must be transferred with care to the dissolution behavior.

κ-Carrageenan shows selective binding sites for alkali ions such as potassium, rubidium, cesium and ammonium ions [Grasdalen and Smidsrod, 1981; Rochas and Rinaudo, 1984; Piculell et al., 1989]. Therefore, these univalent ions were also called 'specific' ions, which

induced the stability of the helix, promoted the aggregation and increased the gelling ability. In fact, low concentrations were sufficient enough to promote gelling [Rochas and Rinaudo, 1980; Nilsson and Piculell, 1991]. Other cations such as sodium, lithium, tetramethyl ammonium were classified as 'non-specific'. Referring to the dissolution profiles, the 'specific' ions like potassium and ammonium ions showed prolonged drug release with respect to 10 % drug load. The dissolution profiles of 'non-specific' ions such as sodium and lithium ions showed fast drug release independent of drug load. Therefore, the dissolution profiles indicated that at least the ionic interactions were certainly taken place on the surface area of the micropellets. The ionic interactions of the interior micropellets were not defined. However, referring to the hydrocolloid solution, the gel structure of the cross-linked 3D-network depended on the cation diffusion. Hence, the continuous immersion of the solution into the micropellets might be considered as well. The good water affinity of the fillers supported the immersion.

To compare the dissolution behavior of micropellets in media containing different **univalent** ions, not only the specific binding was important but also the shielding of the charge of κ-carrageenan molecules. For sulfated polysaccharides, two types of intramolecular interactions with metal ions were possible i) ion-ion interactions to form ion pairs (Coulomb interaction) and; ii) coordination interactions, which depended on the type of ion [Tako and Nakamura, 1986; Tako et al., 1987]. Besides the ionic bonding between potassium ion and the sulfate group of the one D-galactose component, an electrostatic bond between the potassium ion and the anhydro-O-3,6-ring of the adjacent D-galactose component was proposed. Sodium and lithium ions were determined to be too small. Therefore, 'specific' cations were able to neutralize the Coulomb repulsion force between the polymer chains in the junction zone [Rochas and Rinaudo, 1980]. In addition to the coordination interaction, hydrogen-bondings were also reported to stabilize the system [Bubis, 2000]. Regarding the Coulomb interactions, the Coulomb force (F) is defined as the ratio between the product of the single charges and the squared distance (Eq. 11):

$$F = \frac{Q_1 Q_2}{4\pi\varepsilon_0\varepsilon_r r^2}$$
Eq. (11)

where Q is the single charge point, r is the distance, ε_0 is the absolute and ε_r is the relative dielectric constant of the medium. Therefore, oppositely charges decrease the distance and led to stronger attraction. In fact, higher affinity of potassium ions compared to sodium ions led to shorter distances between the charges and more effective shielding, which were attributed to the relative activity coefficients [Rochas and Rinaudo, 1980].

To conclude on the univalent ions in the dissolution media, the conformational changes of the κ-carrageenan molecules are dependent on the effective shielding of the charge density and the proper distance of the charged polymer chains to promote gelling. For example potassium

ions, which belong to the group of 'specific' ions, shield effectively the charge density of κ-carrageenan by its size and simultaneously affects the coordinative distance of the polymer chain to create gelling. A widespread order of univalent ions to form gels was established for chloride salts [Payens and Snoeren, 1972; Rochas and Rinaudo, 1980], which was similar to the Hofmeister series [Kunz et al., 2004]:

$$Li^+ < Na^+ < N(CH_3)_4^+ < NH_4^+ < K^+ < Cs^+ < Rb^+$$
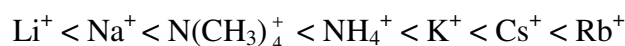
Referring to the micropellets, κ-carrageenan was cross-linked at the surface area to a 3D-network in the presence of potassium ions in the dissolution media. Thus, a matrix system occurred, which showed prolonged drug release compared to the other dissolution profiles of the media containing univalent ions. Furthermore with respect to the Hofmeister series, the use of only one anion was important. In this context, the choice of chloride salts was preferred, because chloride ions were reported to show less perturbation to the water structure [Mancinelli et al., 2007] and also marginal effects on κ-carrageenan [Norton et al., 1984].

The prolonged drug release in the dissolution media of ***divalent*** ions was attributed to the different valency and the high charge density of the divalent ions. Although, the ionic radii of magnesium ions (r = 72 pm) and calcium ions (r = 100 pm) were smaller compared to sodium ions (r = 106 pm) or potassium ions (r = 136 pm), the calculated surface charge densities of the divalent ions were at least twice as high as the ones for univalent ions [Collins, 1997]. Consequently, the charge shielding of the κ-carrageenan molecules was considered to be effective and similar to potassium ions. Besides the possible intramolecular interactions with hydrogen-bonding or the adjacent D-galactose component, divalent ions were also considered to bridge intermolecular, which was exampled for ι-carrageenan [Tako et al., 1987]. Thus, the dissolution behavior of divalent ions was comparable to potassium ions (Fig. 16).

With respect to the different concentrations of calcium ions in the dissolution media, the drug release was slower with increasing amount of calcium ions. This indicated the strengthening effect of the cross-linking 3D-network. However, the ratio between API and κ-carrageenan was also important. Drug load of 50 % showed no further effects in drug release by increasing the calcium concentration from 0.05 M to 0.1 M calcium chloride solution. Hence, the concentration of 0.05 M calcium chloride solution was already sufficient to obtain the strongest interactions between calcium ions and κ-carrageenan (Fig. 15b, $f_2 = 98.6$).
However for 10 % drug load, the dissolution profiles differed on the calcium concentrations (Fig. 15a, $f_2 = 48.1$), indicating that 0.05 M calcium chloride solution did not reach the required concentration for complete interactions. The difference was attributed to the ratio between spironolactone and κ-carrageenan. Decreasing the amount of drug load from 50 % to 10 % the ratio changed in favor to κ-carrageenan. Therefore, in the micropellets containing 10 % spironolactone more κ-carrageenan molecules per API were available. The hypothesis

arose that in the presence of the same amount of calcium ions, the shielding of the charge of the κ-carrageenan in the micropellet was insufficient. Hence, the conformational changes of the polymer chains would not be optimally arranged to form a complete 3D-network. Therefore, it could be that the matrix system retained larger amounts of water [Montero and Perez-Mateos, 2002], which probably improved the wettability of the drug and led to faster drug release. However, the increase in size of the micropellets caused by swelling could not be measured. Even though the evaluation of the drug release mechanism was not completely classified, it was evident that the ratio between API and κ-carrageenan was essential for the drug release.

The ionic interactions between the dissolved calcium ions and κ-carrageenan were evaluated by differential scanning calorimetry (DSC) analysis (Chap. 8.2.3.1). The impurity of ι-carrageenan in the batch of κ-carrageenan was obtained. Ridout et al. [1996] investigated the heating and cooling data of pure and mixed ι- and κ-carrageenan gels. The melting and setting of the carrageenan gels were related to the conformational transitions. The thermoreversible transition of ι-carrageenan was around 60 °C without showing hysteresis. The transitions of the melting and the setting temperature of κ-carrageenan were displaced. In the presence of potassium ions, the melting peak of κ-carrageenan was shifted towards the higher temperature of ι-carrageenan.
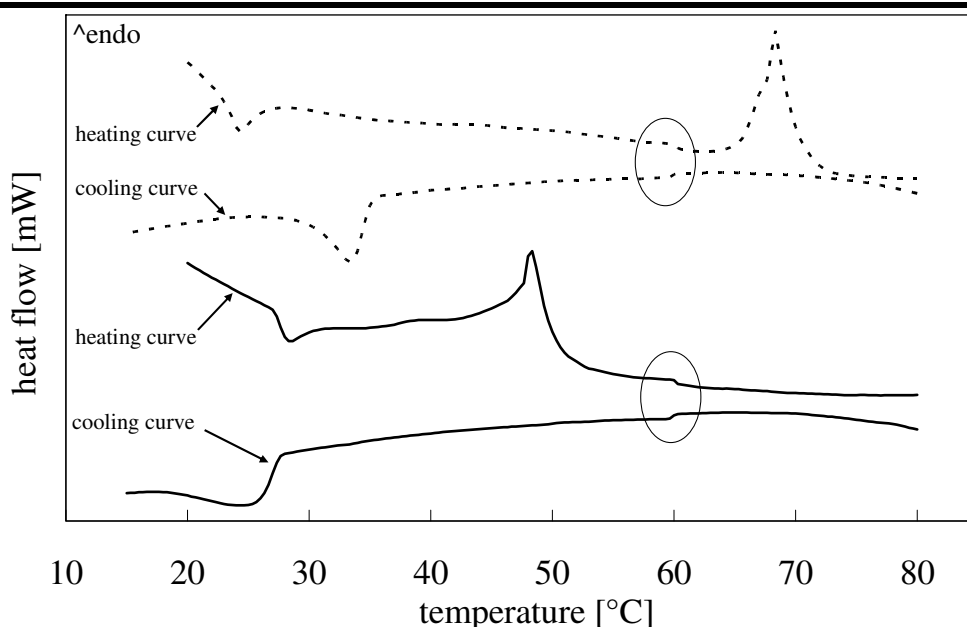
Fig. 17: DSC thermogram of 2 % κ-carrageenan gel (⎯⎯) after 24 h under room condition, (⋯⋯) exposure for 1 h in 0.1 M calcium chloride (n = 1)

According to Ridout et al. [1996], the different transition peaks could be assigned to ι- and κ-carrageenan. However, an additional setting peak was observed at the beginning, which was only present in the first heating curve and not in the second run. The heat treatment of the gel

was performed to verify the first gelling of κ-carrageenan. A slight increase of the melting peaks was observed for the treated gel. This was attributed to the better rearrangement of the κ-carrageenan molecules. Nevertheless, both melting peaks were still around 50 °C. Therefore, Fig. 17 only contains the first measurements. For the sake of orientation, the consistent transition of ι-carrageenan around 60 °C was assigned. The exposure of the gel in 0.1 M calcium chloride solution appeared in the shift of the melting peak about 20 °C, which confirmed the conformational transition of the κ-carrageenan molecules. Even though calcium ions are well-known to prefer ι-carrageenan for ionic interactions, the amount of ι-carrageenan in the κ-carrageenan seemed to be not affected. The setting temperature of the cooling curve was not shifted for ι-carrageenan compared to κ-carrageenan.

Further, the dependency of the calcium concentration on the ionic interactions between the dissolved calcium ions and κ-carrageenan were observed on the surface area of the micropellets for different media (Fig. 18a-d).
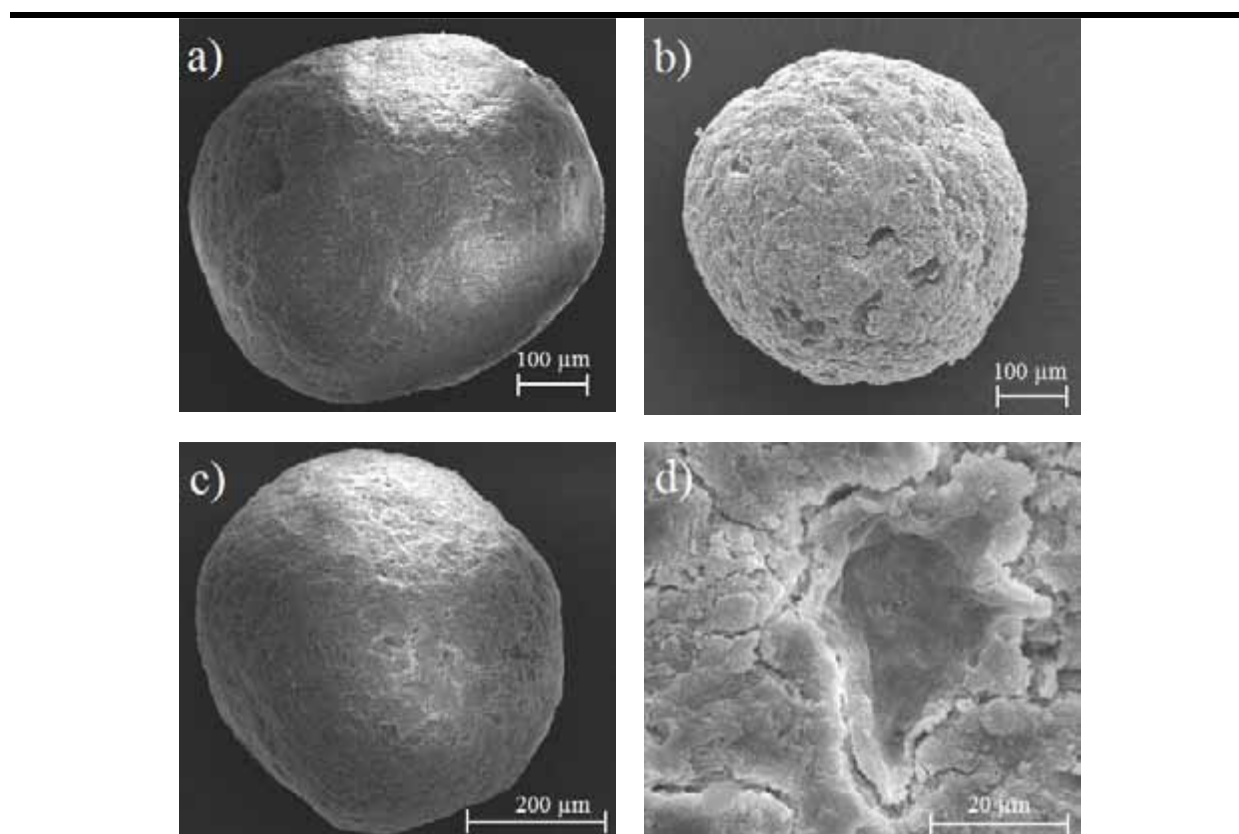
Fig. 18: **SEM-pictures of micropellets containing 10 % drug load: a) untreated, b) after 6 h in 0.05 M calcium chloride, c) after 6 h in 0.1 M calcium chloride, d) magnification of c)**

An untreated micropellet showed a relatively smooth surface area (Fig. 18a). A micropellet containing 10 % drug load showed a rougher surface area after 6 h in 0.05 M calcium chloride solution (Fig. 18b). With increasing amount of calcium in the dissolution media, the surface area was smoother again (Fig. 18c). The rougher surface area in 0.05 M calcium chloride was attributed to erosion processes. Nevertheless, in the presence of calcium ions punctual pore

openings and more cracks were observed, which increased with higher amounts of calcium ions in the dissolution media (Fig. 18c, d). Due to the fact that the micropellets remained intact after 6 h in the dissolution media, the appearance of a polymer network was evident. The 3D-network was considered as a matrix system. Consequently, the dissolution behaviors were evaluated by the Higuchi equation (Fig. 19).
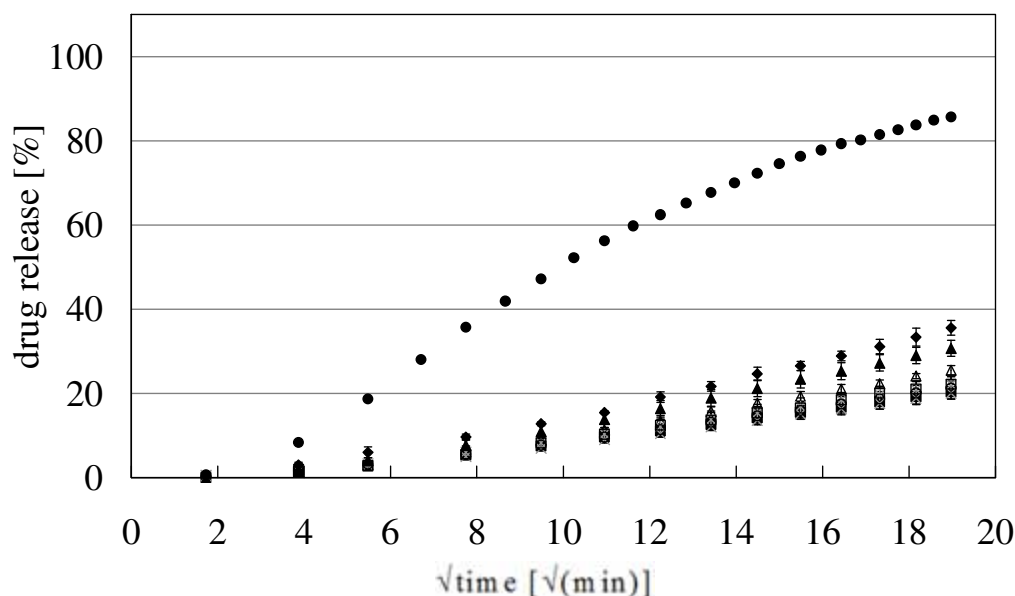
Fig. 19: **Release profiles of 50 % drug load: ✦ 0.01 M calcium chloride, ○ 0.05 M calcium chloride (n = 2), ■ 0.1 M calcium chloride, □ 0.1 M magnesium chloride, ▲ 0.05 M potassium chloride, △ 0.1 M potassium chloride, ◆ 0.1 M ammonium chloride, ✕ 2x0.05 M calcium + potassium chloride, ✳ 2x0.05 M calcium + sodium chloride ($\bar{x} \pm SD$, n = 3)**

The dissolution profiles suggested a square root of time profile which describes a diffusional process. However, even by disregarding the lag time, the dissolution profiles were slightly bended. Therefore, the evaluation by Korsmeyer and Peppas was considered (Chap. 3.3). For the formulation with 10 % spironolactone, the kinetics (n) up to 60 % in different cation chloride solutions ranged from 0.44 to 0.69 (Tab. 13). Therefore, all dissolution mechanisms were anomalous (non-Fickian) diffusions, where different processes such as swelling, diffusion and erosion simultaneously occurred.

Tab. 13: Evaluation by Korsmeyer and Peppas for 10 % drug load in different media

Medium	Parameter	n	log k	R^2
0.01 M	Calcium chloride	0.56	+0.84	0.9776
0.05 M	Calcium chloride	0.59	+0.35	0.9757
0.1 M	Calcium chloride	0.56	+0.29	0.9810
0.05 M	Potassium chloride	0.69	+0.21	0.9695
0.1 M	Potassium chloride	0.49	+0.48	0.9621
0.1 M	Magnesium chloride	0.44	+0.50	0.9665
0.1 M	Ammonium chloride	0.66	+0.42	0.9798
	USP-buffer (pH = 6.8)	0.65	+0.29	0.9685

Tab. 14 shows the parameters for the formulations with 50 % drug load. The kinetics showed values between 0.43 and 1.04. Therefore, the dissolution mechanisms were mostly anomalous (non-Fickian) diffusions except 0.01 M calcium chloride, which showed a zero-order kinetic. However, the drug release in 0.05 M, 0.1 M calcium and 0.1 M potassium chloride solutions were not up to 60 % and thus the final values might differ.

Tab. 14: Evaluation by Korsmeyer and Peppas for 50 % drug load in different media

Parameter Media	n	log k	R^2
0.01 M Calcium chloride	1.04	-0.35	0.9665
0.05 M Calcium chloride	0.77	-0.64	0.9872
0.1 M Calcium chloride	0.75	-0.62	0.9731
0.05 M Potassium chloride	0.79	-0.55	0.9528
0.1 M Potassium chloride	0.77	-0.60	0.9674
0.1 M Magnesium chloride	0.62	-0.27	0.9832
0.1 M Ammonium chloride	0.76	-0.41	0.9846
USP-buffer (pH = 6.8)	0.73	-0.43	0.9389

In the double logarithmic plot of drug release as a function of time for formulation with 50 % API, the dissolution profiles for each media showed a linear slope in the middle of the time phase (Fig. 20, for several media). At the beginning, the slopes increased slowly indicating the effect of time required for water penetration into the micropellets, while the slopes down showed the changes in the kinetic. For a better overview, the standard deviations were excluded in this plot due to the good reproducibility of the dissolution profiles (SD < 3).
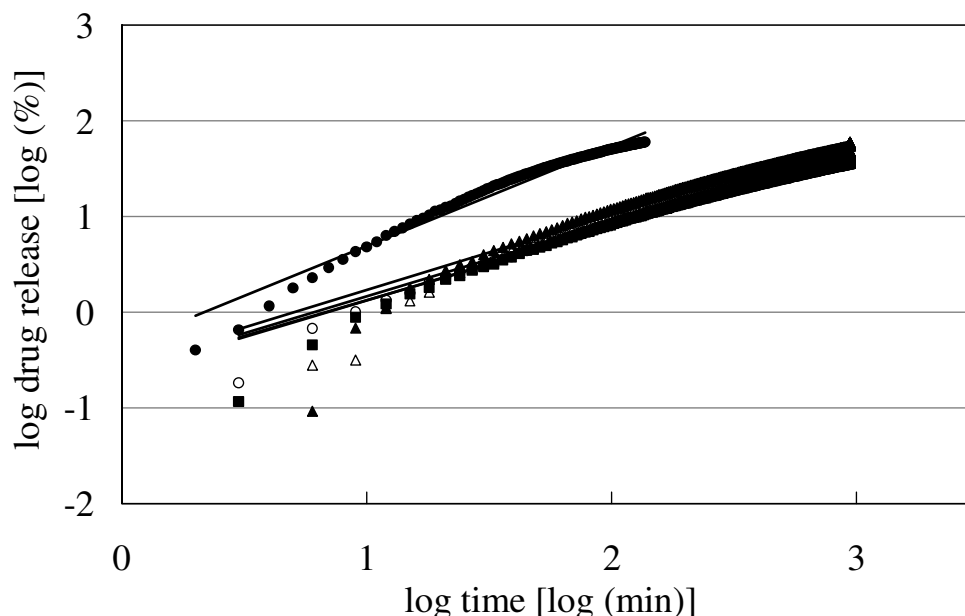
Fig. 20: Release profiles of 50 % drug load: ● 0.01 M calcium chloride, ○ 0.05 M calcium chloride (n = 2), ■ 0.1 M calcium chloride, ▲ 0.05 M potassium chloride, △ 0.1 M potassium chloride ($\bar{x}$, n = 3)

Combined media

After investigating the effects of different cation chlorides, a combination of 0.1 M calcium chloride solution was investigated to evaluate the effect of acidic pH. Thus, calcium chloride was dissolved in 0.1 M HCl to a concentration of 0.1 M. Further, a combination of 0.1 M calcium chloride solution with an addition of surfactant (0.05 % Brij® 35P) was investigated. In general, surfactants improve the wettability of the drug. Therefore, faster drug release was expected. For both investigations micropellets containing 50 % drug load were used (Fig. 21).
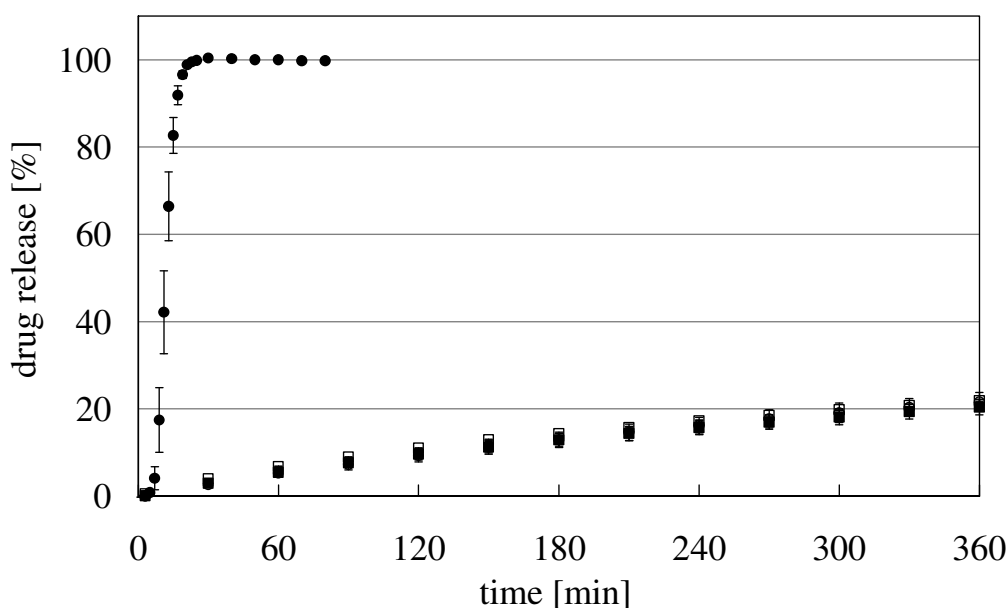
Fig. 21: **Release profiles of 50 % drug load in different combined media: ◆ 0.1 M HCl, ○ 0.1 M calcium chloride in 0.1 M HCl, ■ 0.1 M calcium chloride, □ 0.1 M calcium chloride + 0.05 % Brij® 35P ($\overline{x} \pm$ SD, n = 3)**

For the dissolution process there was no improvement by dissolving the amount of 0.1 M calcium chloride in 0.1 M HCl compared to pure 0.1 M calcium chloride solution ($f_2 = 96.7$). Also, the addition of a surfactant showed hardly any effect on the dissolution behavior ($f_2 = 87.8$). An improvement of wettability by the surfactant and therefore a better dissolution rate was suppressed. Hence, the ionic interactions on κ-carrageenan were attributed to the solely effect of dissolved calcium ions in the media.

The investigations of combined media emphasized that the appearance of the 3D-network by cross-linking the κ-carrageenan molecules with calcium ions constructed a complete matrix system.

FeSSIF medium

In general the dissolution tests (in vitro) are important analytical methods to characterize the drug delivery performance. Only dissolved drug can be absorbed in the GIT and is bioavailable [Dressman and Reppas, 2000], so that the solubility of the drug and the dissolution rate are determinant for in vivo dissolution behavior. Hence to closely reflect the

physiological conditions in the GIT as possible, different research groups investigate the optimization of the in vitro/in vivo correlations (IVIVC), which are still ongoing.

An important effect of the drug release and the bioavailability is the condition of the GIT. Therefore, various biorelevant media were developed to simulate fasted or fed state conditions to predict the effects of food or enzymes etc. on the formulation and the dosage form. Although the revisions of the media are further ongoing [Jantratid et al., 2008], the perfect biorelevant media are still lacking. On the other hand, investigations were performed on the classification of the drugs by the Biopharmaceutics Classification Scheme (BCS) to define the suitable biorelevant media for drug release [Amidon et al., 1995; Galia et al., 1998].

In this part of the study a Fed State Simulating Intestinal Fluid (FeSSIF) was used as medium to simulate the proximal small intestinal conditions in the fed state. This state included diverse factors such as changes in pH, buffer capacity, osmolality and bile output, which had to be considered. Therefore, acetate buffer was used to achieve the required conditions of the buffer and osmolality. The concentration of sodium taurocholate and lecithin reflected the biliary response to meal intake. The dissolution medium was produced according to Marques [2004] (Chap. 8.2.2.8).

First, micropellets containing 10 % spironolactone were investigated (Fig. 22). The dissolution behavior in the FeSSIF medium was carried out twice for 30 min. The stirring was continued to evaluate if the dissolution was completed. The last sample was taken out after 240 min. Each sample was analyzed three times in the HPLC (Chap. 8.2.2.7; 8.2.2.8, FeSSIF). The dissolution profiles were compared to those obtained in 0.1 M sodium chloride solution.
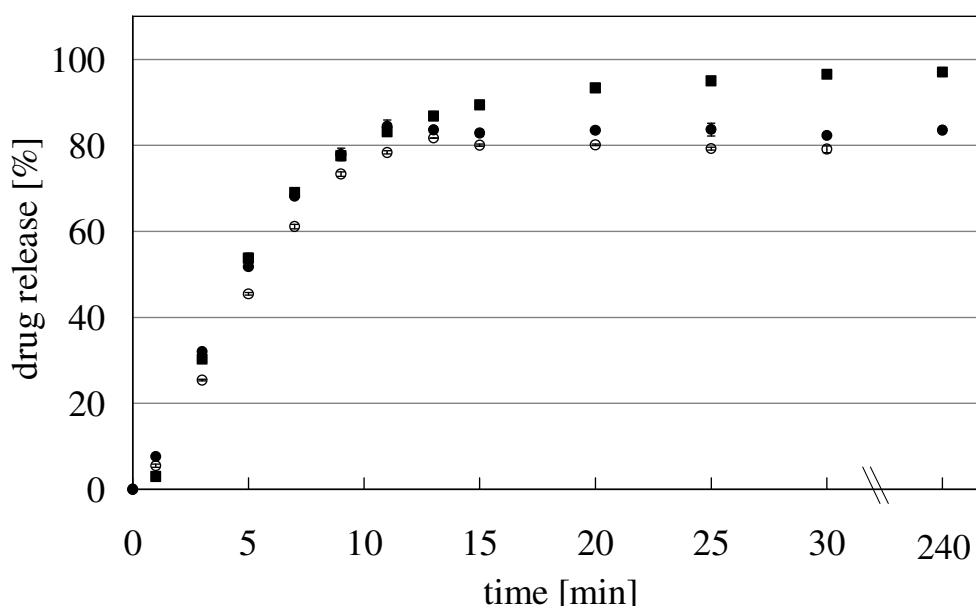
Fig. 22: Release profiles of 10 % drug load in FeSSIF medium compared to 0.1 M sodium chloride: ● 1st run, ○ 2nd run, ■ 0.1 M sodium chloride ($\bar{x}$ ± SD, n = 3)

Fast dissolution behavior was obtained in the FeSSIF medium. In fact, the dissolution rate was similar to the dissolution behavior in 0.1 M sodium chloride solution. The difference in the total concentration was attributed to the lack of sample preparation. However the dissolution profiles observed provided evidence that addition of sodium taurocholate or lecithin did not affect the dissolution behavior of the micropellets. Moreover, only the ionic interactions between sodium ions and κ-carrageenan seemed to be decisive in FeSSIF medium.

Further, micropellets containing 50 % spironolactone were investigated (Fig. 23). The dissolution behavior in the FeSSIF medium was carried out twice for 120 min. Overnight stirring was continued to evaluate if the dissolution was completed. The last sample was taken out after 1320 min. Each sample was analyzed three times in the HPLC (Chap. 8.2.2.7; 8.2.2.8, FeSSIF). The dissolution profiles were compared to the dissolution behavior in 0.1 M sodium chloride solution.

In general, the dissolution curves of 50 % drug load were only decent. However, the dissolution curves were still observed and therefore both runs were used for the evaluations. Nevertheless, the first run in the FeSSIF medium was faster than the second run. The difference between both runs in the FeSSIF medium and the outliers of several data points were attributed to the lack of sample preparations. The samples were taken out by a pipette without filtration. Therefore lumps of the micropellets were able to be transferred into the sample vials, which may alter the drug amount of the sample. Further preparation such as centrifugation of the samples may lead to further uncontrolled interactions between the drug and the compounds. The lumps could be destroyed during centrifugation and increased the concentration in the sample.
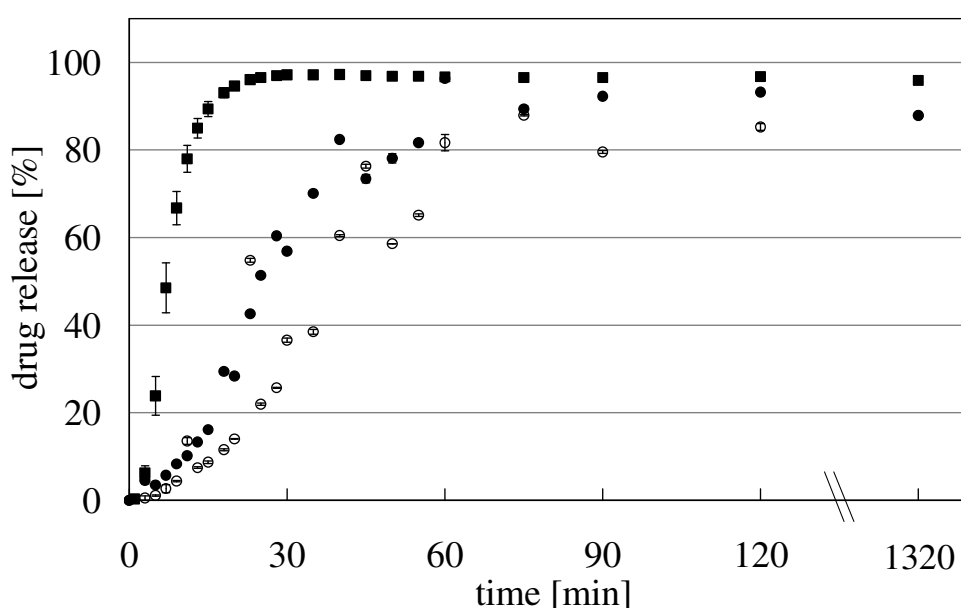

Fig. 23: Release profiles of 50 % drug load in FeSSIF medium compared to 0.1 M sodium chloride: ● 1st run, ○ 2nd run, ■ 0.1 M sodium chloride ($\bar{x} \pm SD$, n = 3)

Especially at the beginning, slower dissolution rates were obtained compared to the dissolution behavior of 0.1 M sodium chloride solution. The complete drug release was achieved after approximately 90 min, while the drug release in 0.1 M sodium chloride solution was completed within 20 min. Therefore, the slower drug release was attributed to additional interactions between the FeSSIF medium and the micropellets containing 50 % drug load, which were not indicated for micropellets containing 10 % drug load. Hence, the ratio between API and κ-carrageenan was decisive. Enhancing the ratio towards κ-carrageenan led to less interaction. As a result, the drug release of micropellets comprising 10 % drug load was faster compared to 50 % drug load in the FeSSIF medium. However, the evaluations must be proceeded with caution due to the few data provided.

Milk medium

Another biorelevant medium for dissolution investigations is milk. It is generally a food-simulating medium and therefore a model of food interactions. Klein et al. [2004] compared different liquid meals to the standard FDA breakfast and evaluated that the physical parameters such as pH, density, buffer capacity, etc. were comparable for the milk but not as good as for the other liquid meals. However, in the population milk is rather regarded as a calcium donating drink than a meal replacement. Besides, the milk is not only just a drink; it is also used in cooking. Due to the versatile use in daily nourishment, the milk was used as dissolution medium to investigate the effects of the milk on the drug release of the micropellets comprising κ-carrageenan.

The milk, as a natural product, showed many disadvantages as a dissolution medium independent of the type of milk. Stability problems and the variations in source and seasons must be considered, which affects the composition of each batch of the milk. Hence, the milk is not a reproducible dissolution medium and the sample preparation is important.

The milk (long-life, 3.5 % fat) contains about 3.3 wt% protein, of which 2.6 wt% are different types of caseins and 0.65 wt% of mineral components. Caseins in milk showed the tendency to associate into micelles, where κ-casein was mostly located on the periphery. Even though casein molecules were important on the dissolution behavior, Macheras et al. [1989] reported that the solubility of the drug in milk was not predictable by the pure casein solutions. Therefore, the complex nature of the milk affected the drug release. Numerous investigations about the effects of milk on the dissolution behavior showed different results such as: i) formulation-dependency [Macheras et al., 1987]; ii) slower drug release compared to aqueous solutions; iii) drug-binding to milk components independent of the drug concentration but on the other hand; iv) drug-binding dependency to the fat content with respect to the API properties [Macheras et al., 1990]. Further, the temperature affected the drug-binding capacity and the distribution in milk [Macheras et al., 1988]. Besides the particular position in daily food, the milk was an interesting dissolution medium due to the different ions. The nutritional values in 100 ml milk were summarized in **Tab. 15** [Souci et al., 1986].

Tab. 15: Nutritional values in milk for 100 ml

Calcium [mg]	Potassium [mg]	Magnesium [mg]	Sodium [mg]	Chloride [mg]
120	157	12	48	102

The intake of 100 ml milk is equal to the daily demand of 15 % calcium for adults [CIAA, 2007]. Moreover, the calcium concentration in milk (1.2 g·l^{-1}) was comparable to the aqueous 0.01 M calcium chloride solution. Due to the additional presence of potassium and magnesium ions, no effects of sodium ions were expected. Hence, the objective was to determine the dissolution rate at the beginning and to compare the dissolution profile to the dissolution behavior in aqueous calcium chloride solutions.

First, micropellets containing 10 % spironolactone were investigated (Fig. 24). The dissolution behavior in the milk medium was carried out twice for 6 h. Each sample was analyzed twice in the HPLC (Chap. 8.2.2.7; 8.2.2.8, milk). The dissolution profiles were compared to 0.01 M and 0.1 M calcium chloride solutions.
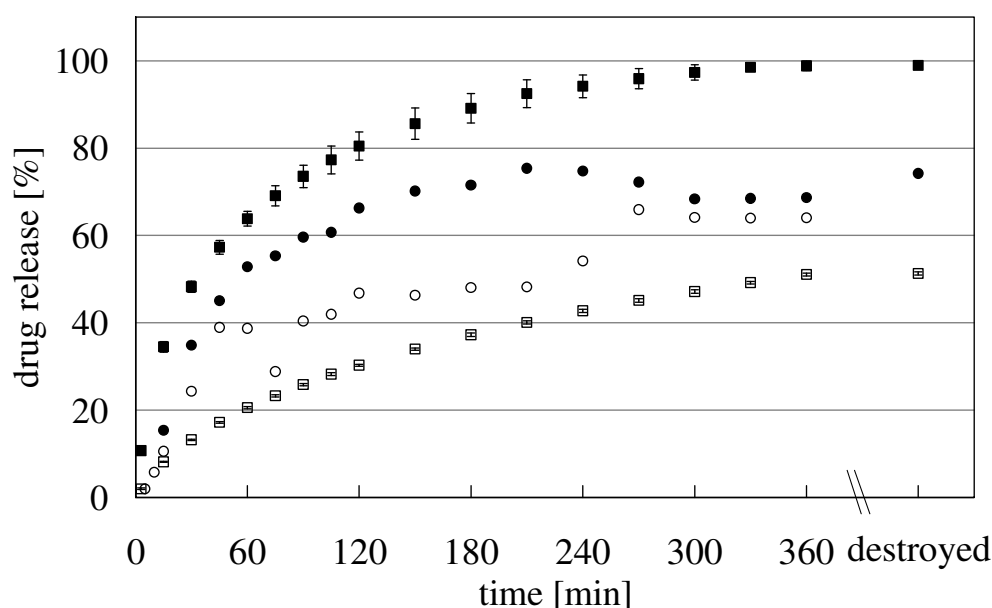
Fig. 24: Release profile of 10 % drug load in milk media compared to calcium chloride solutions: ◆ 1st run, ○ 2nd run (n = 2), ■ 0.01 M sodium chloride, □ 0.1 M calcium chloride ($\bar{x}$ ± SD, n = 3)

Even though both runs in the milk differed during the dissolution, the profiles were still comparable. After 60 min approximately the half of drug load was released. The deviation between the dissolution profiles after 60 min was unclear. The reason must be in the laborious sample preparation (Chap. 8.2.2.8, milk). However, since the dissolution behavior at the beginning as well as at the end was comparable, no further investigations were performed. The dissolution profiles of the micropellets containing 10 % API were located between the dissolution profiles of 0.01 M and 0.1 M calcium chloride solutions. The intermediate range of the dissolution behavior in milk was expected due to the presence of the other gel-

promoting ions. The additional ionic interactions were rather attributed to the potassium than the magnesium ions with respect to the concentration (~0.02 M potassium and $6*10^{-4}$ M magnesium). The dissolution profile in milk indicated that the cross-linkage was incomplete compared to the dissolution profile in 0.1 M calcium chloride solution.

The dissolution profiles of 50 % drug load differed to 10 % drug load (Fig. 25). Although, both runs were similar to each other ($f_2 = 73.9$), the dissolution behavior in milk differed substantially from the dissolution profiles in 0.01 M calcium chloride solution. In fact, the comparison to the 0.1 M calcium chloride solution was similar ($f_{2\ (1st\ run)} = 72.8$, $f_{2\ (2nd\ run)} = 78.9$). After destroying the micropellets in the milk, the total concentration obtained was below 80 %. In the pre-investigation test of spiking, spironolactone was completely regained (Chap. 8.2.2.8, milk). However, the spiking was performed without the presence of κ-carrageenan. The residues of the sample in the HPLC vial did not dissolve completely in the 1 ml mobile phase even after 24 h. Hence, the incomplete recovery was attributed to the interactions between milk compounds and κ-carrageenan assuming an entrapment of API in the complex.
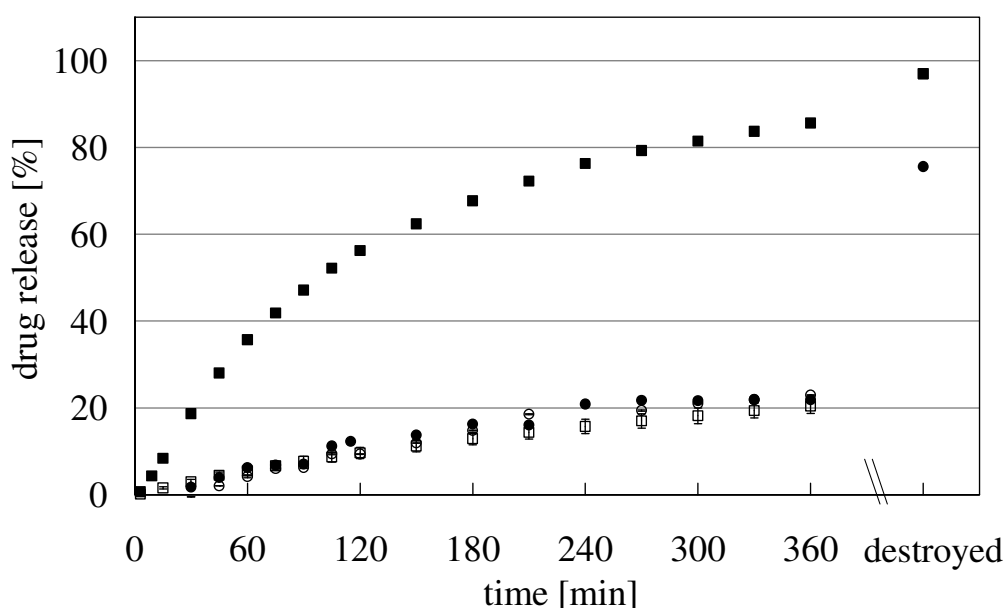
Fig. 25: Release profile of 50 % drug load in milk media compared to calcium chloride solution: ◆ 1st run, ○ 2nd run, ■ 0.01 M sodium chloride (n = 2), □ 0.1 M calcium chloride ($\bar{x} \pm$ SD, n = 3)

In general, the discussion concerning the interactions between κ-carrageenan and the milk compounds based on similar discussions between κ-carrageenan and the aqueous univalent solutions. A precise description of the interactions between κ-carrageenan and milk compounds was not established in the literature as well. Langendorff et al. [2000] investigated the interactions between milk and the three different types of carrageenans (κ, ι, λ). Due to the shielding of the charge density, the interactions to the micelles were dependent on the

temperature for the gelling carrageenan types, while λ-carrageenan was highly charged enough to shield without the temperature-dependent configuration of the carrageenan molecules. However, independent of the various discussions on the interactions between κ-carrageenan and the milk proteins, the presence of calcium, potassium and magnesium ions definitely promoted gelling.

The similarity of the dissolution profiles of micropellets with 50 % drug load in milk compared to 0.1 M calcium chloride solution indicated a dissolution profile of complete matrix system in the milk medium. Besides the calcium concentration, the amount of the presence of further gel-promoting ions (potassium, magnesium, and κ-casein) was sufficient for the micropellets containing 50 % drug load to create the complete 3D-network in contrast to 10 % drug load. Therefore, in case of the same type and amount of gel-promoting compounds in the dissolution medium, the dissolution behavior of micropellets comprising κ-carrageenan was dependent on the ratio between API and pelletization aid (Chap. 5.2.4.2, discussion). However, the evaluations must be proceeded with caution due to the few data provided.

5.2.4.3 Summary

The moisture content required for the spheronization process was not affected by the different extrusion screw speeds. The micropellets comprising C53-06 had better pellet properties and required less moisture content in contrast to the production based on C13-03. Thus, C53-06 was the preferred filler.

The dissolution profiles of micropellets based on κ-carrageenan were related on two different issues: i) the dissolution media and ii) the ratio between API and pelletization aid.

Regarding the dissolution media, the drug release was dependent on the type and amount of ions in the dissolution media rather than pH or surfactant addition. Further investigations to evaluate the strength of the matrix system will be discussed later (Chap. 5.2.8). Varying the ratio between API and κ-carrageenan in favor to the pelletization aid, the dissolution behavior was faster. In addition, the ratio-dependent dissolution behavior indicated further interactions in the biorelevant media such as FeSSIF and milk. Therefore, food interactions must be considered on the administration of micropellets comprising κ-carrageenan. To verify the observations further investigations will follow using different drugs (Chap. 5.3).

5.2.5 Extrusion/ spheronization using dicalcium phosphate as filler

5.2.5.1 Introduction and objective

The objective was to evaluate the effect of calcium contained fillers. Therefore, another calcium compound was used for the comparison. The standard formulation of spironolactone (Chap. 5.2.4.1) contained C92-14, a dicalcium phosphate type (Di-Cafos) as a filler.

The different types of dicalcium phosphates vary among other parameters in the amount of hydrates. C92-14 is a dihydrate. It is one of the most widely used tableting excipients. In

addition, it is used for compression or wet granulation. C92-14 also belongs to the food additive E341 (calcium phosphates). Therefore, besides the standard applicable in the pharmacopoeia it is listed in the FCC [cfb Budenheim, 2008].

C92-14 is practically insoluble in water. The concentration of calcium oxide is 32.5 % and of phosphorus pentoxide 41.5 %. The molecular weight is 172.09 g·mol^{-1}.

5.2.5.2 Production and characterization

The wet extrusion/ spheronization process took place under standard conditions (Chap. 8.2.1.2, 8.2.1.3). The moisture content varied in the range from 103.0 % to 117.1 %. The production of micropellets based on C92-14 was successful.

The batch with the best pellet properties was used for further investigations. It showed an aspect ratio of 1.14, a pellet size of 573 µm and a yield of 76.4 %. The 10 %-interval of 57.8 % was good. The moisture content of the extrudates was 103.0 %. Hence, the production of micropellets comprising C92-14 required less moisture content of the extrudates. However, micropellets based on C53-06 showed better pellet properties compared to C92-14.

5.2.5.3 Dissolution behavior

First, the dissolution behavior of the micropellets based on C92-14 was investigated in fast dissolving media according to the dissolution evaluations of micropellets containing C53-06 (Chap. 5.2.4.2, fast dissolving media). Even though the dissolution behavior differed dependent on the media, the dissolution profiles obtained for all formulations were fast (Fig. 26). The drug releases in deionized water and 0.1 M sodium chloride solution were completed within 15 min. Due to the longer lag time in 0.1 M HCl, the drug was released within 20 min.
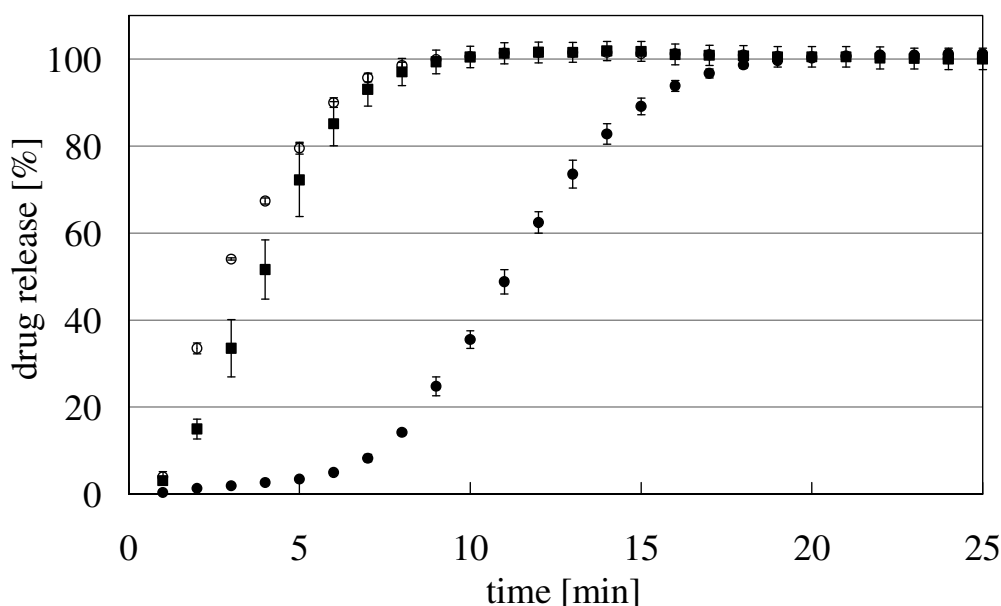
Fig. 26: **Release profiles of micropellets comprising 10 % SpL and 70 % C92-14 in different dissolution media: ◆ 0.1 M HCl, ◇ deionized water, ■ 0.1 M sodium chloride ($\bar{x}$ ± SD, n = 3)**

The mathematical comparison showed that the dissolution profiles in 0.1 M sodium chloride was similar to deionized water ($f_2 = 56.3$), while the dissolution profile of 0.1 M HCl was not similar ($f_2 = 14.8$). Moreover, the dissolution profile of the micropellets comprising C92-14 in deionized water was similar to the dissolution profile of the micropellets based on C53-06 ($f_2 = 57.5$). The similarity was not confirmed for the dissolution profiles in 0.1 M HCl ($f_2 = 30.7$). The mathematical comparison was not performed on 0.1 M sodium chloride solution due to the different times required to complete drug release. Despite the different times required to complete drug release, the availability of the drug was in the range of therapeutic relevance.

Further, different ionic dissolution media were investigated (Fig. 27). The drug releases were prolonged. The dissolution profiles were compared to the dissolution behavior of the micropellets based on C53-06 with 10 % drug load (Chap. 5.2.4.2, chloride salts with different cations).
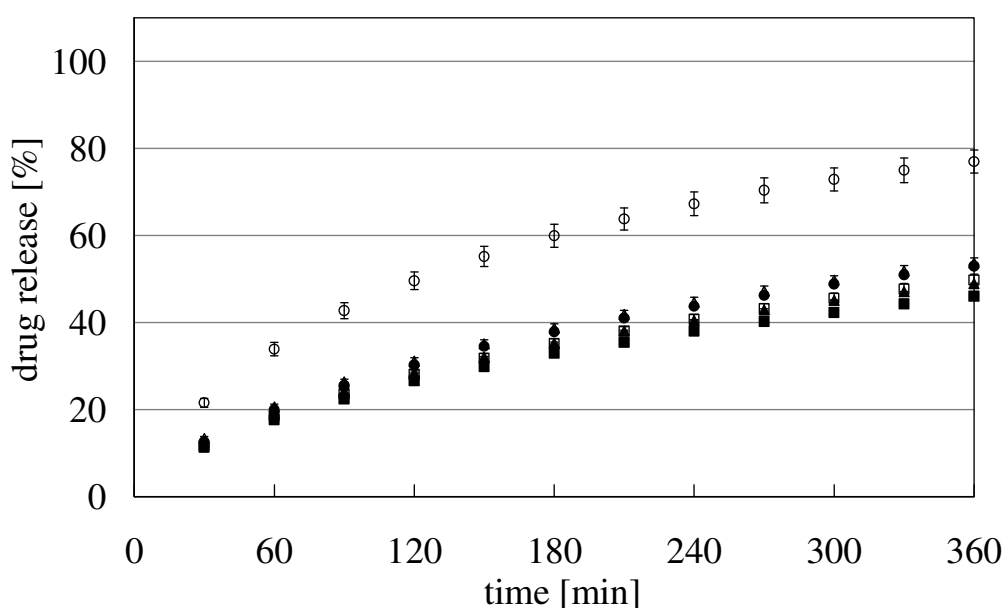
Fig. 27: **Release profiles of micropellets comprising 10 % SpL and 70 % C92-14 in dissolution media with different ions: ◆ 0.05 M calcium chloride, ◇ 0.05 M potassium chloride, ■ 0.1 M calcium chloride, □ 0.1 M magnesium chloride, ▲ 2x0.05 M calcium + potassium chloride, △ 2x0.05 M calcium + sodium chloride ($\bar{x} \pm$ SD, n = 3)**

The mathematical comparison of the different dissolution media based on 0.1 M calcium chloride solution as reference. The similarity was confirmed except for 0.05 M potassium chloride solution (Tab. 16). While the micropellets containing C53-06 showed different drug releases dependent on the amount of calcium ions in the media, no difference in the dissolution profiles of micropellets comprising C92-14 in 0.05 M and 0.1 M calcium chloride solution was obtained ($f_2 = 65.2$). Further, the micropellets based on C92-14 showed the fastest drug release in 0.05 M potassium chloride solution.

Tab. 16: Similarity factor of the micropellets based on C92-14 compared to 0.1 M calcium chloride

Medium	0.05 M Calcium	0.05 M Potassium	0.1 M Magnesium	2x0.05 M Calcium + potassium	2x0.05 M Calcium + sodium
f_2-value	65.2	29.9	79.8	80.4	62.0

The mathematical comparison of the dissolution profiles referred to the dissolution profiles of the micropellets based on C53-06. The dissolution profiles of both standard formulations in the same dissolution media were similar except for 0.05 M calcium chloride solution (Tab. 17). However, since the value was marginally below 50, the absence of sameness of equivalence is disputable.

Tab. 17: Similarity factor of the comparison between the filler in different media

Medium	0.05 M Calcium	0.05 M Potassium	0.1 M Calcium	0.1 M Magnesium	2x0.05 M Calcium + potassium	2x0.05 M Calcium + sodium
f_2-value	49.5	63.1	68.8	80.6	89.7	59.7

Hence, the main difference in the dissolution profiles was obtained in the 0.05 M calcium chloride solution between both types of filler in the micropellets. With the exception of 0.05 M potassium chloride solution, less deviation between the dissolution profiles of the micropellets comprising C92-14 in the different media was obtained compared to the dissolution profiles of micropellets containing C53-06.

5.2.5.4 Summary

The production of micropellets containing C92-14 required less moisture content of the extrudates than C53-06 as filler. However, the micropellets based on C53-06 showed better pellet properties than micropellets comprising C92-14.

The dissolution profiles in the different media were similar to the dissolution profiles of the micropellets based on C53-06. However, the dissolution behavior of micropellets containing C92-14 showed less deviation between the prolonged drug releases of the different media than the dissolution profiles of the micropellets containing C53-06.

The exchange of the type of filler did not substantially affect the properties of micropellets comprising κ-carrageenan.

5.2.6 Extrusion/ spheronization using lactose monohydrate as filler

5.2.6.1 Introduction and objective

The ratio between API and pelletization aid had an effect on the dissolution behavior in different media, while the type of filler – even though it contained calcium ions – seemed to be insignificant. Both issues were related to the ionic interactions between the dissolved ions in media and the amount of κ-carrageenan. The objective was to evaluate the effect of the filler.

5.2.6.2 Production and characterization

The ratio between API and pelletization aid with regard to another type of filler was varied. Tricalcium phosphate was replaced by lactose monohydrate (GL200), which showed a lack of calcium and good solubility in water. For the sake of comparison, additional formulations of 40 % drug load were investigated besides the standard formulation. Therefore, a formulation containing 40 % spironolactone and 40 % C13-03 was also produced. The amount of κ-carrageenan in all formulations was 20 %. Further, to evaluate the effect of κ-carrageenan on the formulation based on lactose monohydrate as filler, a formulation containing 40 % spironolactone, 20 % GL200 and 40 % κ-carrageenan was also investigated (Tab. 18).

Extrusion took place under standard conditions (Chap. 8.2.1.2). The Schlueter spheronizer was used, but the spheronization process differed from the standard conditions (Chap. 8.2.1.3): Batches of 400 g were spheronized for 6 min at 15.71 m·s^{-1} with a constant temperature of the spheronizer wall at 25 °C and an inlet air pressure of 0.2 bar. All ternary powder mixtures were extruded and spheronized successfully.

Tab. 18: Overview of the different formulations (* $\bar{x}$ ± SD, ** x_{50} ± IQR)

Formulation In [%]	I	II	III	IV
Spironolactone	10	40	40	40
GL200	70	40	20	-
C13-03	-	-	-	40
κ-Carrageenan	20	20	40	20
Moisture content [%] *	101.2 ± 1.1	101.6 ± 1.1	131.9 ± 5.3	120.8 ± 1.4
Aspect ratio **	1.12 ± 0.1	1.13 ± 0.2	1.19 ± 0.2	1.18 ± 0.2
Pellet size [µm] **	578 ± 92.6	631 ± 84.0	558 ± 104.7	569 ± 119.8
Yield [%]	87.5	89.3	95.5	94.6
10 %-interval [%]	61.0	66.6	52.4	48.0
Tensile strength [MPa] *	10.97 ± 2.0	9.69 ± 1.4	28.32 ± 5.0	11.22 ± 1.7

Tab. 18 contains the data of the batch with the best pellet properties of each formulation. The values were in the ranges of each parameter (ar < 1.2, pellet size < 700 µm, 10 %-interval > 50 %). However, the pellet properties were regarded as decent due to the poor spheronization conditions. Although the product adhered substantially to the spheronizer wall, high yield was obtained.

Regarding the extrudates containing lactose monohydrate, the moisture content of the extrudates based on 20 % κ-carrageenan were similar (101.2 % and 101.6 %, respectively). The moisture content of the extrudates containing 40 % κ-carrageenan was 131.9 %. Thus, an increase of the pelletization aid led to higher moisture content to produce suitable micropellets. The moisture content of the extrudates containing tricalcium phosphate was 120.8 % and therefore enhanced compared to the same formulation comprising lactose monohydrate. Consequently, the exploratory data confirmed that the formulation containing insoluble components such as tricalcium phosphate as filler required more moisture content than the same formulation containing lactose monohydrate (Chap. 5.2.3). The mechanical stability was

slightly increased for micropellets based on 40 % C13-03 compared to the micropellets with 40 % GL200. However the most impact on the tensile strength was observed in the different formulations comprising lactose monohydrate. The mechanical stability was enhanced for micropellets based on 40 % κ-carrageenan (Tab. 18).

5.2.6.3 Dissolution behavior

The dissolution profiles of the micropellets based on C53-06 and C13-03 were mostly similar (Chap. 5.2.4.2). Hence, the comparison of the standard formulation referred to the normalized dissolution profile of the micropellets based on C53-06.

The dissolution behavior of micropellets containing lactose monohydrate varied depending on the dissolution media. In the fast dissolving media the dissolution profiles differed in the drug release rate. However, complete drug releases were reached within 15 min (Fig. 28a, b).
In deionized water, the dissolution profiles of micropellets containing 10 % API and either 70 % GL200 or C53-06 were similar (Fig. 28a, $f_2 = 64.3$). The dissolution profiles of Formulation II and IV were also similar ($f_2 = 64.9$). But, the drug release rate per unit time was reduced compared to 10 % drug loads. Therefore, the comparison of the dissolution profiles of Formulation I and II was not confirmed by the sameness of equivalence ($f_2 = 42.4$). In addition, increasing the pelletization aid in the formulation reduced the drug release rate per unit time. Hence, the dissolution profile of Formulation III was similar to the one of Formulation II ($f_2 = 64.4$) but not to the dissolution profile of Formulation I ($f_2 = 38.3$). However independent of the type of filler, all drug releases were fast and therefore, the differences in the dissolution profiles might not be of therapeutic relevance.

In 0.1 M HCl solution the dissolution profiles varied depending on the ratio and type of filler (Fig. 28b). Micropellets containing lactose monohydrate were faster independent of the ratio. However, an increase in drug load led to slower dissolution profiles. In addition, the different amount of pelletization aid did not show any effects on the dissolution. Comparing the dissolution profiles of the micropellets comprising lactose monohydrate, only the dissolution profiles of Formulation II and III were similar ($f_2 = 76.3$). The main difference in the dissolution profiles of the micropellets containing lactose monohydrate or tricalcium phosphate was obtained at the beginning of the dissolution. The lag time was longer for the micropellets containing tricalcium phosphates independent of the type and amount. Although the dissolution profiles comprising tricalcium phosphate were similar ($f_2 = 54.8$), after approximately 9 min the dissolution profile of the micropellets with 10 % drug load showed enhanced drug release. This was attributed to the faster disintegration of micropellets with higher amount of insoluble filler.
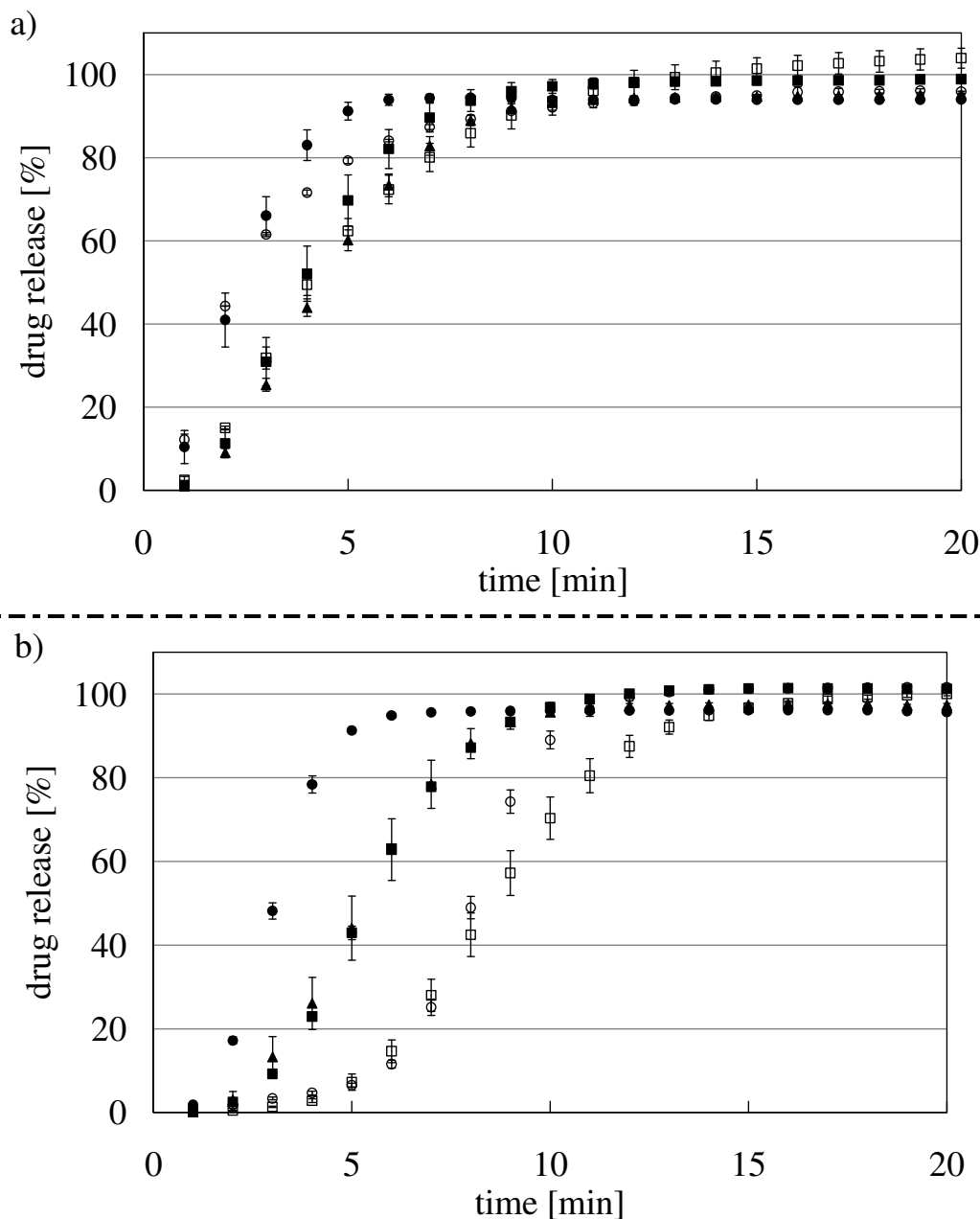
Fig. 28: Release profiles in a) deionized water and b) 0.1 M HCl: ⬥ 10 % SpL + 70 % GL200, ◌ 10 % SpL + 70 % C53-06, ■ 40 % SpL + 40 % GL200, □ 40 % SpL + 40 % C13-03, ▲ 40 % SpL + 20 % GL200 ($\bar{x} \pm SD$, n = 3)

Depending on the ratio between API and pelletization aid, the dissolution profiles varied in the dissolution media containing 0.1 M gel-promoting ions (Chap. 5.2.4.2). To evaluate the effects of the solubility of the fillers on the different ratios, 0.1 M calcium chloride solution was used as representative for all media containing 0.1 M gel-promoting ions (Fig. 29).

Micropellets containing lactose monohydrate showed faster dissolution profiles compared to micropellets based on tricalcium phosphate. In addition, an increase in ratio between API and pelletization aid in favor to κ-carrageenan led to faster dissolution independent of the type of filler. This was referred to the hypothesis of the ionic interactions of κ-carrageenan (Chap. 5.2.4.2, discussion). The cross-linking κ-carrageenan molecules constructed a 3D-network, in

which the interior of the micropellet is able to retain lager amounts of water dependent on the effective shielding of the polymer charge. The located water increased the viscosity in the matrix system and improved the wettability of the API. In addition, the good solubility of lactose monohydrate led to a change in the ratio between the solid and liquid phase of the matrix, which also supported the dissolution of the API. As a result, the dissolution of spironolactone was faster.
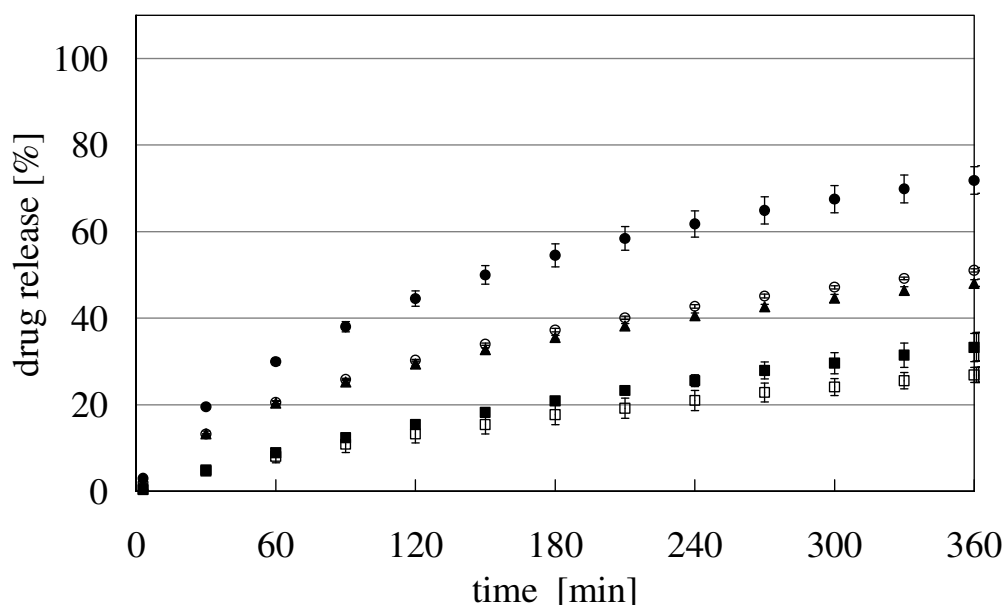
Fig. 29: Release profiles in 0.1 M calcium chloride solution: ✦ 10 % SpL + 70 % GL200, ○ 10 % SpL + 70 % C53-06, ■ 40 % SpL + 40 % GL200, □ 40 % SpL + 40 % C13-03, ▲ 40 % SpL + 20 % GL200 ($\bar{x}$ ± SD, n = 3)

Nevertheless, the ionic interactions between calcium ions and κ-carrageenan were also observed with lactose monohydrate as filler: Decreasing the amount of lactose monohydrate reduced the drug release. The differences in the time-dependent dissolution profiles containing either 70 % lactose monohydrate or tricalcium phosphate were neglected by increasing the amount of API in the formulations and therefore decreasing the content of filler (Fig. 29). Thus, small amount of filler affected less the dissolution independent of the type of filler. Due to that the dissolution profiles of the Formulation II and IV were almost identical (f_2 = 90.5). Therefore, with increasing amount of API the properties of the filler such as solubility seemed to be negligible. Compared to that, Formulation III showed faster drug release than Formulation II and therefore, the dissolution profiles were not similar (f_2 = 29.6). The increase of κ-carrageenan relaxed the 3D-network with regard to the hypothesis. More water was located in the matrix, which improved the wettability of the API. As a result, the drug release increased. The dissolution profiles was similar to the dissolution profile of the micropellets with the standard formulation comprising C53-06 (f_2 = 84.0).

5.2.6.4 Summary

The production of micropellets containing lactose monohydrate required less moisture content of the extrudates than tricalcium phosphate as filler. Increasing the amount of pelletization aid of the micropellets containing higher amount of API led to higher aspect ratio.

Regarding the fast dissolving media, the drug release was completed within 15 min, although the dissolution profiles differed for both media. Besides the effects of the ratio between the API and the pelletization aid, the type and amount of filler was decisive for the dissolution behavior. With high amount of filler the dissolution increased with water soluble fillers. Changing the ratio reduced the dissolution profiles independent of the type of filler. Increasing the amount of pelletization aid improved the dissolution profiles of micropellets containing higher amount of API.

The exchange of the type of filler substantially affected the dissolution behavior of micropellets comprising κ-carrageenan especially in the media containing gel-promoting ions.

5.2.7 Extrusion/ spheronization using calcium lactate as filler

5.2.7.1 Introduction and objective

The dissolution profiles of the micropellets containing spironolactone, tricalcium phosphate or lactose monohydrate and κ-carrageenan were dependent on the type and amount of the filler (Chap. 5.2.6.3). The dissolution behavior of the micropellets based on the standard formulation was affected by the solubility of the filler. Further, the free calcium concentration of the insoluble calcium phosphates was marginal and insignificant during the extrusion process. In the following investigation, the filler combined both important properties: The good solubility of lactose monohydrate and the presence of calcium ions as in tricalcium phosphate. Therefore, calcium lactate was used as filler. The objective was to evaluate i) the production process in the presence of dissolved calcium ions and ii) the dissolution behavior of the product.

Calcium lactate is soluble in water [Ph.Eur. 6, 2008]. The aqueous solution of calcium lactate has a pH of 6 - 7 [DAB-10 Kommentar, 1994]. It is used in foods (E327), pharmaceuticals and in cosmetics as acidity regulator, preserving or sapidity agent. Besides the calcium ions, magnesium or alkali metal ions can be present up to 1 %. Calcium lactate has a molecular weight of 218.2 $g \cdot mol^{-1}$.

5.2.7.2 Production and characterization

The formulation contained 8.5 % spironolactone, 73.1 % calcium lactate and 18.4 % κ-carrageenan. Even though less API was in the formulation, it was compared to the standard formulation (Chap. 5.2.4.1). The extrusion/ spheronization process took place under standard conditions (Chap. 8.2.1.2, 8.2.1.3). The moisture content varied from batch to batch.

The production of micropellets failed. The extrudates were too sticky and elastic. Nevertheless the long extrudates were transferred into the spheronizer to break them into cylindrical rods of approximately the same size. The impossible conversion into micropellets was attributed to the ionic interactions between the filler and the pelletization aid. Calcium lactate was classified as soluble in water. Hence, it was suggested that κ-carrageenan was mingled with the dissolved calcium ions during extrusion. As a result, κ-carrageenan lost the capacity as pelletization aid. However, to prove the hypothesis further investigation should be performed on different fillers with the same properties.

5.2.7.3 Dissolution behavior

Due to the ionic interactions on the production of the micropellets, the cylindrical extrudates were investigated in different dissolution media (Fig. 30). The lag time of deionized water was prolonged compared to the other media. This was attributed to the conformational changes of the κ-carrageenan during the production. However, the dissolution was still fast.
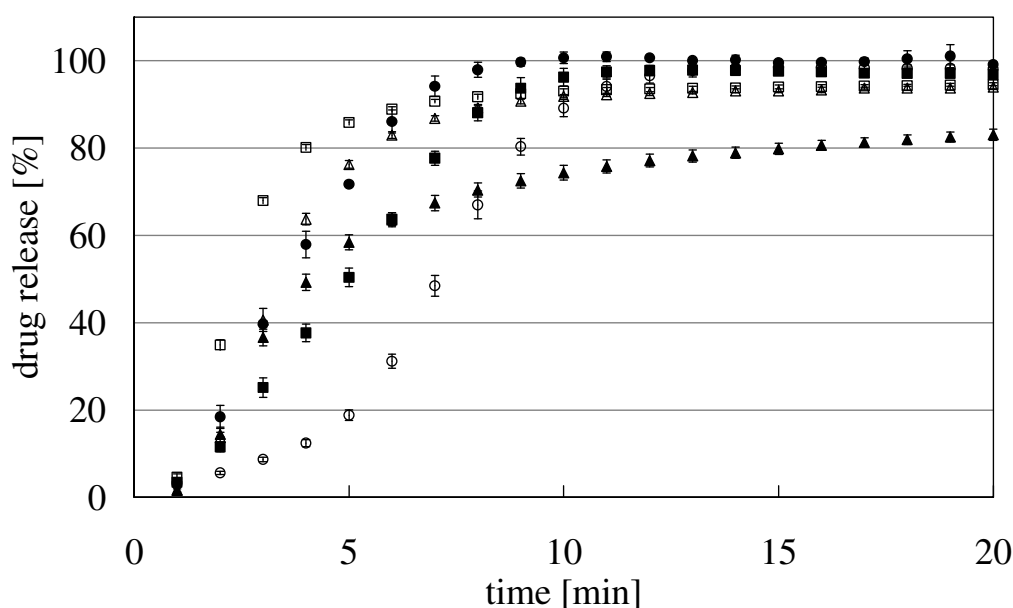
Fig. 30: Release profiles of micropellets containing SpL and calcium lacate in different media: ◆ **0.1 M HCl,** ○ **deionized water,** ■ **0.1 M sodium chloride,** □ **0.05 M calcium chloride,** ▲ **0.1 M calcium chloride,** △ **0.1 M potassium chloride (** $\bar{x} \pm SD, n = 3$ **)**

In the presence of ions the dissolution profiles differed from the dissolution behavior of the micropellets containing spironolactone and the other fillers. Independent of the type and amount of ions, the dissolution was always fast. The drug release was completed within 15 min, except for 0.1 M calcium chloride solution. Nevertheless, the latter medium showed 80 % drug release within the time. Hence, no substantial ionic interactions were observed.

Due to the longer lag time in deionized water, the mathematical comparison was referred to the dissolution profile in 0.1 M HCl. The f_2 equation did not prove the sameness of

equivalence (Tab. 19) except for 0.1 M potassium chloride solution. However, due to the fast drug release, the differences in the dissolution profiles might not be of therapeutic relevance.

Tab. 19: Similarity factor to compare the dissolution profiles in different media to 0.1 M HCl

Medium	Deionized water	0.1 M Sodium	0.05 M Calcium	0.1 M Calcium	0.1 M Potassium
f_2-value	30.0	49.2	48.3	35.1	58.8

The mingling of κ-carrageenan and the dissolved calcium ions during the extrusion abolished further ionic interactions on the dissolution independent of the type and amount of gel-promoting ions.

5.2.7.4 Summary

The production of micropellets failed using calcium lactate as filler. The good solubility of calcium lactate led to ionic interactions between the dissolved calcium ions and κ-carrageenan during the production. Hence, κ-carrageenan lost its capacity as pelletization aid. Further, the drug release was fast and independent of the type and amount of ions in the dissolution media. Taken together, the exchange of the calcium contained filler with good solubility was disastrous on the production of micropellets. Nevertheless, the product showed no further ionic interactions between the dissolved ions and κ-carrageenan during the dissolution.

5.2.8 Extrusion/ spheronization using MCC as pelletization aid

5.2.8.1 Introduction and objective

On the screening of different ratios between spironolactone and κ-carrageenan, different dissolution behavior was observed in each dissolution media (Chap. 5.2.4.2). In the presence of gel-promoting ions the drug release was prolonged, which was attributed to the appearance of a matrix system. The objective was to evaluate the strength of the matrix system. Therefore, micropellets were produced containing MCC as pelletization aid (Chap. 1.3.2).

5.2.8.2 Production and characterization

The dissolution profiles of micropellets comprising κ-carrageenan were dependent on the ratio between API and pelletization aid. The main difference in drug release was obtained with micropellets comprising 10 % and 50 % drug load (Chap. 5.2.4.2). Hence, both formulations were produced with MCC (Tab. 20). The micropellets were compared to the previous produced micropellets containing κ-carrageenan as pelletization aid.

The extrusion process differed from the standard conditions by the screw speed (Chap. 8.2.1.2). The extrusion took place at a constant screw speed of 160 rpm. The moisture content varied from batch to batch. The Schlueter spheronizer was used, varying the standard conditions by the residence time (Chap. 8.2.1.3). Batches were spheronized for 5 min.

In general, the production of micropellets containing 20 % MCC was more challenging. Especially the spheronization process was insufficient, which was attributed to the narrow range in water binding capacity of the MCC [Thommes and Kleinebudde, 2006a]. Adhesion was observed, which produced micropellets with decent properties (Tab. 20).

Tab. 20: Overview of the formulations containing different pelletization aids (* x̄ ± SD, **x_{50} ± IQR)

Formulation In [%]	I	II	III	IV
Spironolactone	10	50	10	50
C53-06	70	30	70	30
κ-Carrageenan	20	20	-	-
MCC	-	-	20	20
Moisture content [%] *	137.0 ± 0.4	134.0 ± 0.9	72.7 ± 1.0	67.3 ± 0.6
Aspect ratio **	1.11 ± 0.1	1.08 ± 0.1	1.11 ± 0.1	1.17 ± 0.2
Pellet size [µm] **	558 ± 75.1	581 ± 69.7	703 ± 61.2	711 ± 79.8
Yield [%]	87.6	80.3	31.4	33.9
10 %-interval [%]	70.0	74.2	84.6	76.6

Extrudates containing MCC required less moisture content than the formulation containing κ-carrageenan, which was in accordance to Thommes and Kleinebudde [2006a]. Compared to Formulation I and II, the micropellets with MCC showed bigger pellet sizes, which must be considered in further dissolution investigations. Although, the micropellet properties were only decent; no further investigations were performed on the production process as it was outlying the objective.

5.2.8.3 Dissolution behavior

Referring to the Higuchi equation, O'Connor and Schwartz [1993] classified the mechanism of drug release from MCC pellets in distilled water as inert matrix dissolution. Micropellets containing κ-carrageenan showed dissolution profiles of matrix systems in the presence of 0.1 M gel-promoting ions (Chap. 5.2.4.2). Therefore, the dissolution profiles of micropellets based on κ-carrageenan were compared to the dissolution behavior of micropellets containing MCC. Besides deionized water, 0.1 M calcium chloride and 0.1 M potassium chloride solution were used as dissolution media to determine the strength of the matrix system in micropellets based on κ-carrageenan. Micropellets comprising MCC were dissolved in deionized water.

Fig. 31 showed the dissolution profiles of the micropellets containing 10 % spironolactone, 70 % C53-06 and either 20 % κ-carrageenan or MCC as pelletization aid. In deionized water the drug release of the micropellets based on κ-carrageenan was fast, whereas micropellets containing MCC showed prolonged drug release. Regarding the dissolution profiles of micropellets based on κ-carrageenan in 0.1 M calcium or potassium chloride solutions, it was observed that the drug release in both media was faster than the dissolution behavior of micropellets containing MCC in deionized water. The mathematical comparison of the

dissolution profiles of the micropellets based on κ-carrageenan in media containing 0.1 M gel-promoting ions to the dissolution profile of the micropellets comprising MCC in deionized water confirmed the absence of similarity ($f_{2\ (0.1\ M\ calcium)} = 49.1$, $f_{2\ (0.1\ M\ potassium)} = 40.1$). Thus, the cross-linking of the matrix system was incomplete. However, regarding the pellet size and therefore the specific surface area of the micropellets based on κ-carrageenan, faster dissolution behavior could be expected.
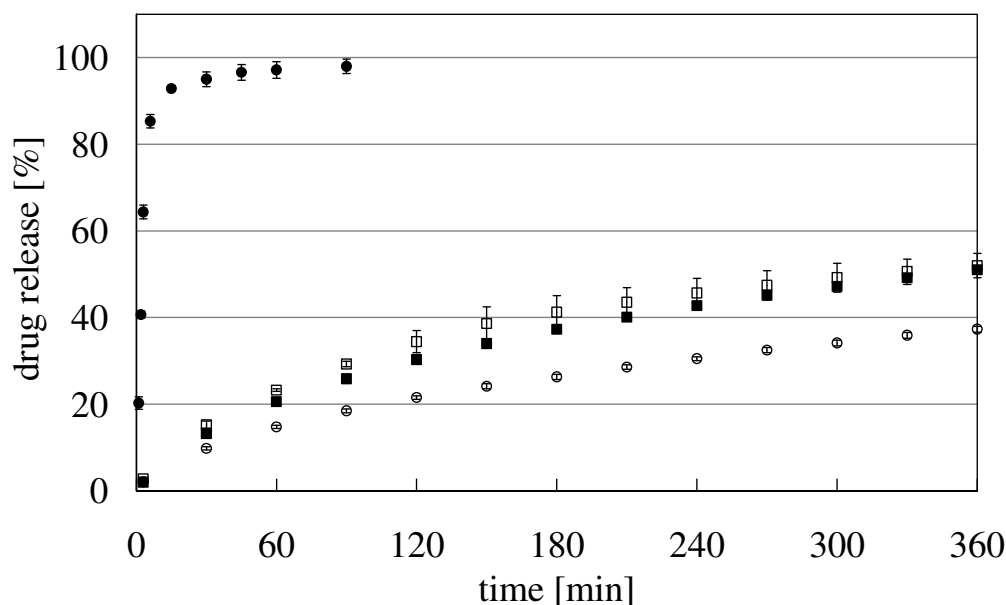
Fig. 31: **Release profiles of 10 % drug load and 20 % pelletization aids in different media: ✦ deionized water (κ-carrageenan), ○ deionized water (MCC), ■ 0.1 M calcium chloride (κ-carrageenan), □ 0.1 M potassium chloride (κ-carrageenan) ($\bar{x} \pm SD$, n = 3)**

The dissolution profiles in deionized water differed for the micropellets comprising 50 % drug load and either κ-carrageenan or MCC (Fig. 32). However, the dissolution profiles of micropellets based on κ-carrageenan in media containing 0.1 M gel-promoting ions were similar to the dissolution profile of MCC micropellets in deionized water ($f_{2\ (0.1\ M\ calcium)} = 90.1$, $f_{2\ (0.1\ M\ potassium)} = 68.3$). Moreover, the dissolution behavior in 0.1 M calcium chloride solution was almost identical to the matrix dissolution of micropellets containing MCC.
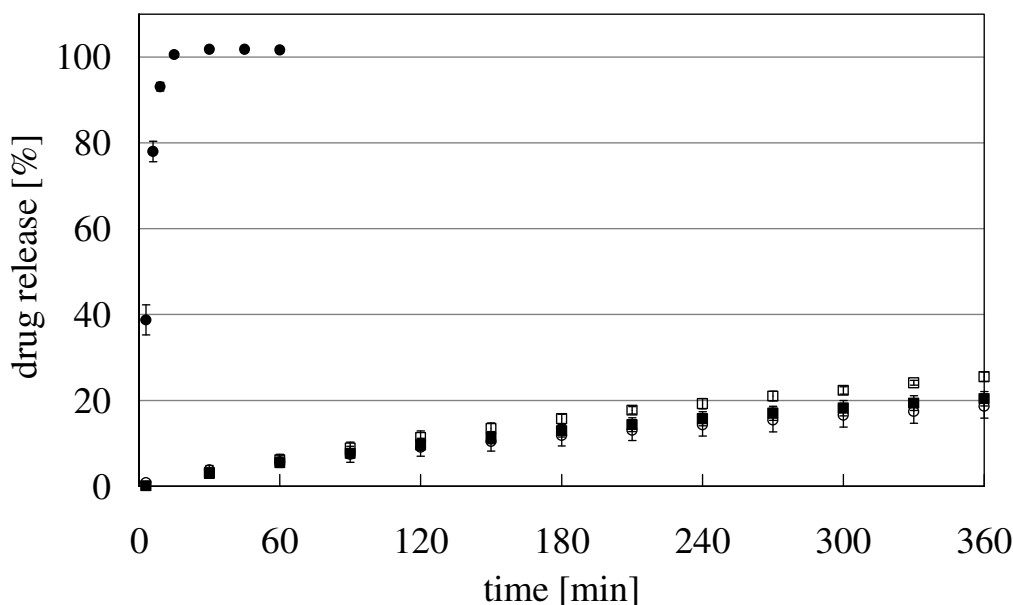
Fig. 32: Release profiles of 50 % drug load and 20 % pelletization aid in different media: ◆ deionized water (κ-carrageenan), ○ deionized water (MCC), ■ 0.1 M calcium chloride (κ-carrageenan), □ 0.1 M potassium chloride (κ-carrageenan) ($\bar{x} \pm SD$, n = 3)

The dissolution of pellets based on MCC is commonly known to follow the Higuchi equation. However in this thesis, the prolonged drug releases of the different micropellets showed a kinetic of anomalous (non-Fickian) diffusion according to the evaluation by Korsmeyer and Peppas (Tab. 21). Hence, the appearance of the cross-linked 3D-network of micropellets based on κ-carrageenan was regarded as inert matrix, when the dissolution profiles were similar to the dissolution profile of the micropellets comprising MCC. Thus the mechanism of drug release in the dissolution media containing 0.1 M gel promoting ions was evaluated as an inert matrix of the micropellets containing 50 % drug load and κ-carrageenan.

Tab. 21: Evaluation by Korsmeyer and Peppas for dissolution of micropellets based on MCC in water

Parameter Formulation	n	log k	R^2
III	0.5161	+0.2424	0.9938
IV	0.6475	-0.3659	0.9993

Consequently, the bigger pellet size of micropellets containing MCC did not affect the dissolution behavior (Tab. 20). Therefore, the faster drug release of micropellets containing 10 % drug load and κ-carrageenan was attributed to the incomplete 3D-network of κ-carrageenan rather than to the pellet size.
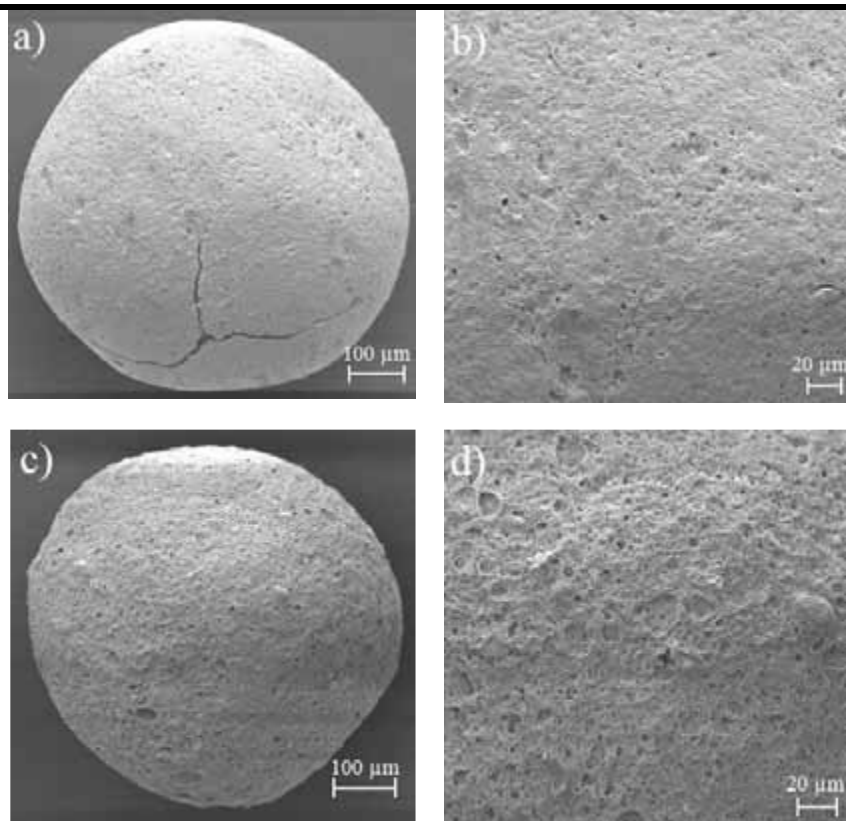
Fig. 33: **SEM pictures of micropellets based on MCC after 18 h in deionized water a)+ b) 10 % drug load, c) + d) 50 % drug load**

Further, the surface area of the micropellets comprising MCC differed depending on the drug load. After 18 h in deionized water, the surface area of micropellets with 10 % drug load was smoother (Fig. 33b) compared to the micropellets of 50 % drug load (Fig. 33d). However, micropellets of 10 % drug load had cracks, while micropellets of 50 % drug load did not burst (Fig. 33a, c). Therefore, the differences in the dissolution profiles comparing both drug loads on the basis of MCC were attributed to the micropellet structures.

Surprisingly, the comparison of the dissolution profiles of the micropellets containing MCC and either 10 % or 50 % API resulted in different dissolution rates as observed for micropellets comprising κ-carrageenan. The drug release of the micropellets based on 10 % drug load was faster than the micropellets with 50 % drug load. The reason was unclear.

5.2.8.4 Summary

Dependent on the ratio between API and κ-carrageenan, the strength of the matrix system in the dissolution media containing 0.1 M gel-promoting ions varied. Comparing the prolonged drug releases of 10 % spironolactone, the micropellets based on κ-carrageenan was faster than the dissolution behavior of the micropellets containing MCC. Therefore, the cross-linkage of the polymer chains was incomplete. Drug load of 50 % constructed an inert matrix system, which showed prolonged drug release almost identical to the dissolution profiles of MCC based micropellets. Additionally, the differences in the studied range of pellet size did not affect the dissolution behavior.

5.3 Micropellets containing different APIs

5.3.1 Choice of model substances as API

5.3.1.1 Specification

Model substances are used to characterize the drug delivery out of the dosage forms. The choice of the model substances are adjusted to the requirements of the investigation.

In this work the requirements of the model substances were defined as followed: i) higher solubility at low pH than in alkali solutions; ii) poor wettability; iii) UV-detectable, iv) a molecular weight around 500 $g \cdot mol^{-1}$; v) highly to dose and; vi) medium to small particle size. The BCS classification is taken from Wu and Benet [2005].

A short introduction of the four selected APIs is given below.

5.3.1.2 Spironolactone

Spironolactone (SpL), introduced in 1962, is an aldosterone antagonist and belongs to the group of diuretica [Rang et al., 1999]. It inhibits the physiological effects of aldosterone by competing for intracellular mineralo-corticoid receptors on the collecting tubules. Therefore potassium ions are retained in the late-distal tubules. Hence, spironolactone is also called a potassium-sparing diuretic, which is only active in the presence of aldosterone. In addition spironolactone is also effective against hypertension and also exhibits antiandrogenic effects.

Spironolactone is metabolized in the body into different metabolites. Canrenone is one of the principal metabolites and pharmacologically active. However, canrenone is able to develop carcinogenic epoxides.

Spironolactone is classified to be practically insoluble in water [Ph.Eur. 6, 2008]. The solubility in water at 25 °C is 28 $mg \cdot l^{-1}$ [Sutter and Lau, 1975]. It belongs to the BCS class II due to the low water solubility and high permeability and is well absorbed from the GIT. Spironolactone is UV-detectable and shows a maximum peak around 240 nm. The molecular weight is 416.59 $g \cdot mol^{-1}$.

5.3.1.3 Griseofulvin

Griseofulvin (GsF) is an antifungal agent which belongs to the subgroup of antibiotics [Roth and Fenner, 2000]. The narrow-spectrum only includes dermatophytes infections. It is fugistatic and accumulates in ceratogenic cells. The mechanism involves an interaction with microtubules and an interfering with the mitosis.

Griseofulvin is classified to be practically insoluble in water [Ph.Eur. 6, 2008]. The wettability is poor and the solubility of water is 20 $mg \cdot l^{-1}$ [Wassvik et al., 20086]. It belongs to the BCS class II due to the low water solubility and high permeability. The absorption of griseofulvin is complicated and varies dependent on the type of preparation and particle size [Roth and Fenner, 2000]. Nevertheless, oral dosage forms can be administered.

Concomitant intake of lipophilic food enhances the drug absorption [Roth and Fenner, 2000]. Griseofulvin is UV-detectable and shows a maximum peak around 291 nm. The molecular weight is 352.77 g·mol^{-1}.

5.3.1.4 Itraconazole

Itraconazole (ICZ) is an antifungal agent which belong to the subgroup of 'azole-derivates' for systemic treatment. It shows a broad spectrum and fungistatic activity. The azoles inhibit the fungal P450 enzymes responsible for the synthesis of ergosterol, which leads to defects in the cell membrane [Rang et al., 1999].

Itraconazole are classified to be practically insoluble in water [Ph.Eur. 6, 2008]. The aqueous solubility of itraconazole was below the detection limit of 1 mg·l^{-1} [Johnson&Johnson, 2004]. It also belongs to the BCS class II and therefore, it is administered in local and oral dosage forms but not parenteral due to the low solubility. Concomitant intake of food enhances the bioavailability and reduces the gastrointestinal side-effects [Roth and Fenner, 2000]. Itraconazole is UV-detectable with a maximum peak around 254 nm. The molecular weight is 705.7 g·mol^{-1}.

5.3.2 Extrusion/ spheronization of theophylline monohydrate

5.3.2.1 Introduction and objective

The dissolution profiles of micropellets containing spironolactone as API showed drug releases dependent on the ratio between the API and the pelletization aid in various dissolution media (Chap. 5.2.4.2). With increasing amount of insoluble API, the dissolution rate decreased. Therefore, the effects of the different ratios between API and κ-carrageenan were investigated on another API, which showed a better solubility compared to spironolactone.

Theophylline monohydrate (ThP) was used as API. It is a bronchodilator. The therapeutic use is in the respiratory diseases like chronic obstructive pulmonary disease or asthma. Besides the smooth muscle relaxant activities, it also shows diuretic and cardiac stimulating effects [Rang et al., 1999]. Due to the narrow therapeutic index, individual doses are recommended [Ph.Eur. 5 Kommentar, 2006]. Hence, for long-term application the prolonged release dosage forms are favored. Compared to the other model substances, theophylline monohydrate is classified as slightly soluble in water [Ph.Eur. 6, 2008]. The solubility in water is 8.3 g·l^{-1} [Merck Index, 1989]. Theophylline is categorized in BCS class I due to the high solubility and permeability. Theophylline monohydrate is UV-detectable with a maximum peak around 271 nm. The molecular weight is 198.2 g·mol^{-1}. With respect to the specification requirements, theophylline monohydrate was beyond the specification. However, the primary objective was to determine i) the effects of the solubility of the API and ii) the development of the matrix system in the presence of gel-promoting ions on the drug release. Hence, theophylline monohydrate was a suitable model substance.

5.3.2.2 Production and characterization

The ratio between API and pelletization aid varied from 10 % to 70 % respectively, while the amount of filler was constant at 20 % (Tab. 22, Formulation I - VII). The mixtures contained C53-06 as filler and κ-carrageenan as pelletization aid. For the sake of comparability the standard formulation (Chap. 5.2.4.1) was also produced with theophylline monohydrate (Tab. 22, Formulation VIII).

Tab. 22: Overview of the formulations containing theophylline monohydrate (* $\bar{x} \pm SD$, ** $x_{50} \pm IQR$)

Formulation In [%]	I	II	III	IV	V	VI	VII	VIII
Theophylline monohydrate	10	20	30	40	50	60	70	10
C53-06	20	20	20	20	20	20	20	70
κ-Carrageenan	70	60	50	40	30	20	10	20
Powder feed rate [g·min^{-1}]	20	25	25	25	33	33	33	33
Extrusion screw speed [rpm]	125	125	125	125	125	125	125	125
Moisture content [%] *	360.7	252.6	280.0	235.7	159.6	111.7	62.6	148.1
	± 1.9	± 2.7	± 3.6	± 1.2	± 3.1	± 0.7	± 1.6	± 0.7
Aspect ratio **	1.13	1.14	1.14	1.14	1.13	1.14	1.12	1.08
	± 0.1	± 0.1	± 0.1	± 0.1	± 0.1	± 0.1	± 0.1	± 0.1
Pellet size [µm] **	403	446	413	463	493	542	644	533
	± 63.4	± 77.1	± 69.3	± 77.8	± 73.8	± 95.8	± 92.2	± 75.9
Yield [%]	96.6	98.1	95.9	87.2	91.1	88.7	70.8	83.8
10 %-interval [%]	59.4	58.0	59.0	57.4	63.2	54.6	65.2	67.2

The extrusion process differed from the standard conditions by the powder feed rate (Chap. 8.2.1.2). Dependent on the ratio, the powder feed rate was adjusted in the rage of 20 g·min^{-1} to 33 g·min^{-1}. The Schlueter spheronizer was used under standard conditions (Chap. 8.2.1.3). All ternary powder mixtures were extruded and spheronized successfully. The best pellet properties of each formulation are listed in Tab. 22. The yield for all formulations was high. Only Formulation VII showed a yield of 70.8 %, which was related to the bigger pellet size. The 10 %-interval of all formulations was good. To obtain higher moisture contents of the extrudates, the filling degree of the extruder was changed. The range of the aspect ratios was narrow (1.12 and 1.14). However, no aspect ratio was below 1.1 except the standard formulation (ar = 1.08). This was attributed to the drying process, where difficulties occurred with increasing moisture content due to the poor movement of the fluid bed. Especially at the beginning it was difficult to set the wet micropellets in motion. Therefore, agglomerates were formed. In addition, micropellets of higher moisture content may deform if colliding with each other during drying. However, the drying process was not part of the objectives and therefore, the pellet properties simply provided the suitable batch of each formulation for further dissolution investigations.

With increasing amount of κ-carrageenan, the optimum moisture content of the extrudates required for spheronization gradually increased ranging from 62.6 % to 360.7 %. The micropellet size decreased, respectively. The moisture content of the standard formulation was 148.1 %. The increase of moisture content was in agreement with the comparison of

micropellets containing 20 % or 40 % κ-carrageenan and lactose monohydrate as filler. In addition, Thommes [2006] also reported that enhancing the amount of κ-carrageenan required higher moisture content of the extrudates to be spheronized.
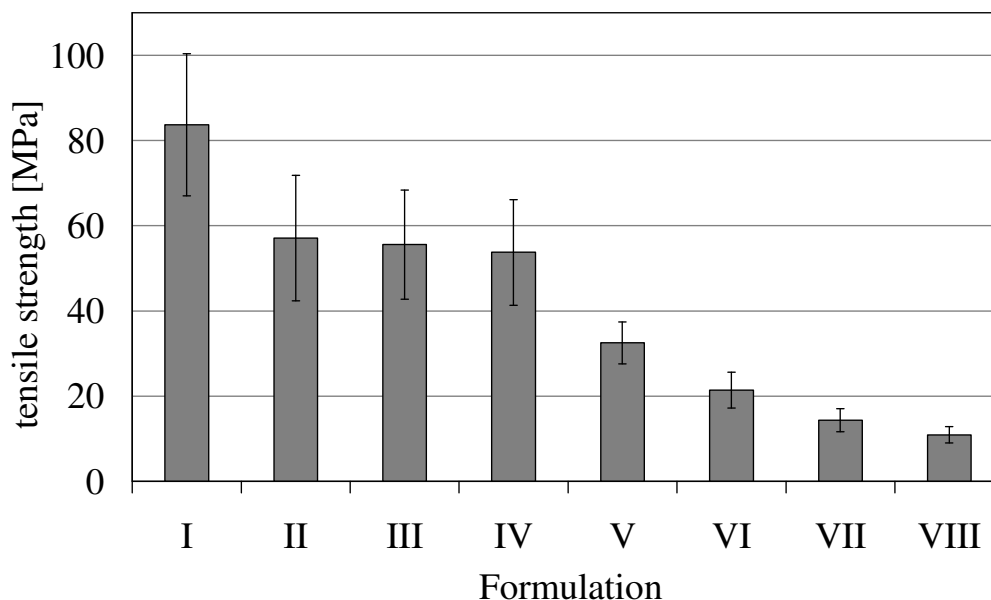
Fig. 34: **Tensile strength of the micropellets containing different ratios between ThP and κ-carrageenan ($\bar{x} \pm$ SD, n = 50)**

In accordance to the investigations on spironolactone (Chap. 5.2.4.1), the tensile strength of the micropellets comprising theophylline monohydrate was dependent on the ratio between API and κ-carrageenan (Fig. 34). With increasing amount of API the tensile strength was decreasing, respectively. The lower mechanical stability of the micropellets containing the standard formulation was related to higher amount of tricalcium phosphate and therefore, probably attributed to differences in densities in the micropellets. The generally higher values of the tensile strength were attributed to ambient storage conditions (Chap. 5.2.4.1).

5.3.2.3 Dissolution behavior

To evaluate the effects of the solubility of the API, micropellets containing theophylline monohydrate were used with regard to the different ratios between API and pelletization aid. The dissolution behavior was investigated in deionized water and 0.1 M calcium chloride solution, which was used as representative of the different gel-promoting ions.

First, each batch of every formulation was evaluated in deionized water. In the fast dissolving medium drug release was completed within 10 min (Fig. 35). No substantial differences in the dissolution profiles of the different ratios were obtained. Moreover, all pellets dissolved completely and the media became slightly turbid. Therefore, the drug release was normalized (Chap. 5.2.4.2). Compared to micropellets containing spironolactone a lag time was not observed, which was attributed to the better solubility of theophylline monohydrate.

71
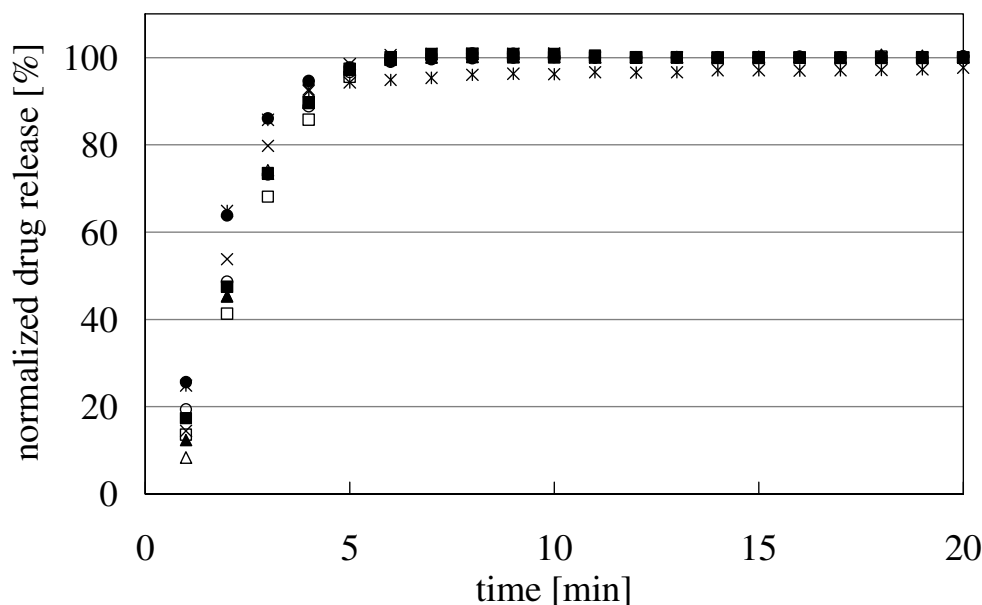
Fig. 35: **Release profiles of formulations containing different amount of ThP and a constant amount of 20 % C53-06 in deionized water: ● 10 %, ○ 20 %, ■ 30 %, □ 40 %, ▲ 50 %, △ 60 %, ✕ 70 %, ✳ 10 % + 70 % C53-06 ($\bar{x}$ ± SD, n = 3)**

The mathematical comparison of the dissolution profiles was also calculated on the normalized data of the drug amount (Chap. 5.2.4.2, fast dissolving media). The values confirmed the sameness of equivalence to the standard formulation (Tab. 23).

Tab. 23: Similarity factor of different ratios compared to the standard formulation in deionized water

Formulation	I	II	III	IV	V	VI	VII
f_2-value	92.1	61.9	61.0	54.5	58.5	57.3	67.0

Secondly, the dissolution behavior of the micropellets in 0.1 M calcium chloride solution was investigated to estimate a dominant effect between the cross-linking κ-carrageenan and the solubility of the API (Fig. 36). The drug was released completely within 15 min. The evaluation by the similarity equation referring to the standard formulation or to 50 % drug load had only 20 time points due to the fast dissolution behavior (Chap. 8.2.2.9). Only formulations up to 30 % were similar to the standard formulation (Tab. 24). The comparison to 50 % drug load showed that drug load of 50 % or higher was similar, while the sameness of equivalence was not given between 50 % and 10 % drug loads. Furthermore, several formulations of either similarity to the dissolution profiles of micropellets comprising 10 % or 50 % drug load existed (Tab. 24).

Tab. 24: Similarity factor compared to micropellets with different drug loads in 0.1 M calcium chloride

Formulation	I	II	III	IV	V	VI	VII	VIII
$f_{2\,(10\,\%\ API)}$-value	88.9	58.7	52.7	43.9	41.2	40.0	43.6	-
$f_{2\,(50\,\%\ API)}$-value	40.3	51.9	58.6	80.6	-	91.1	81.2	41.2
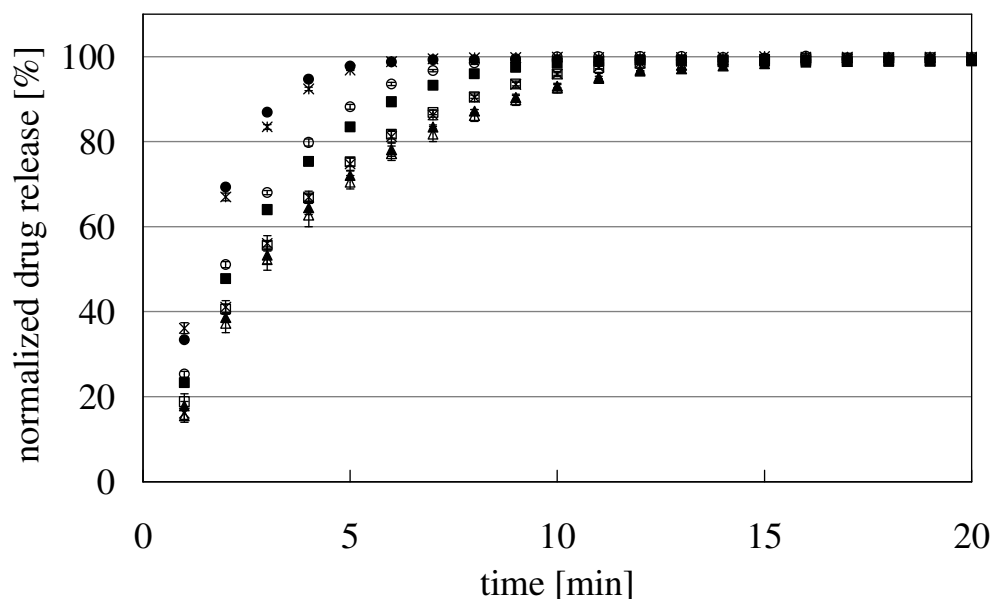
Fig. 36: Release profiles of formulations containing different amount of ThP and a constant amount of 20 % C53-06 in 0.1 M calcium chloride solution: ◆ **10 %,** ○ **20 %,** ■ **30 %,** □ **40 %,** ▲ **50 %,** △ **60 %,** ✕ **70 %,** ✳ **10 % + 70 % C53-06 (x̄ ± SD, n = 3)**

The difference of the dissolution behavior between 10 % and 50 % drug load was given by the calculated comparison. However, the absence of similarity between all formulations was insignificant for the therapeutic relevance due to the fast drug release within 15 min. Therefore, the effect of varying the ratio between API and κ-carrageenan was not confirmed with theophylline monohydrate as observed for spironolactone (Chap. 5.2.4.2). Hence, an increase of hydrophilic matrix, meaning a decrease in API content in the formulations did not improve the drug release of theophylline monohydrate.
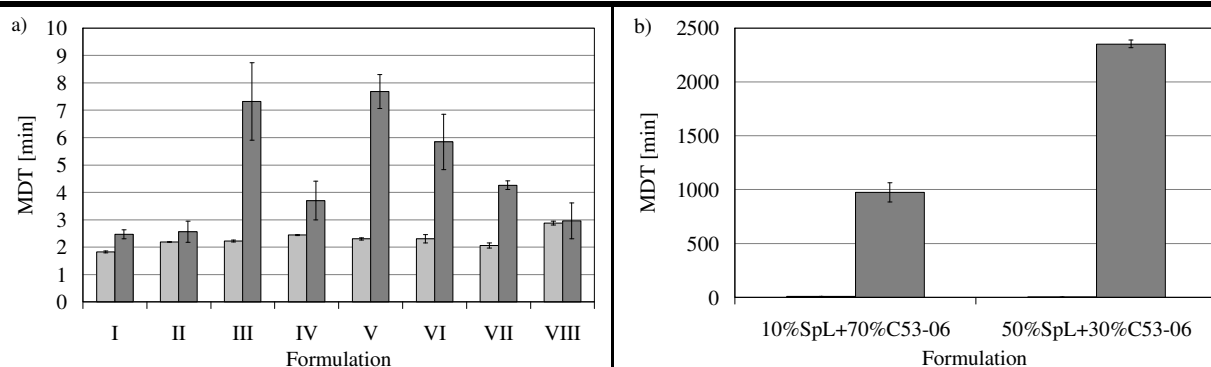
Fig. 37: MDTs of formulations containing different ratios between a) ThP and κ- carrageenan in (▨) deionized water and (▨) 0.1 M calcium chloride solution and; b) SpL in (▨) 0.1 M calcium chloride solution (x̄ ± SD, n = 3)

The MDTs of theophylline monohydrate emphasized the dissolution profiles. All MDT values were below 10 min for both media compared to spironolactone (Fig. 37a, b). Only the MDTs of spironolactone in deionized water were similar to theophylline monohydrate (15 min) and therefore, virtually invisible in Fig. 37b. However, no relation between the ratio and the

MDTs were observed for theophylline monohydrate. Hence, the dissolution of slightly soluble drugs was always fast and therefore, the effects of the ionic interactions between the dissolved ions and κ-carrageenan on the drug release were only obtained for practically insoluble drugs. To exclude further effects of other dissolved ions, the standard formulation with 10 % Theophylline monohydrate was investigated to screen different media (Fig. 38). Independent of the type and concentration of ions in the media, all dissolution profiles were similar and showed drug release within 10 min.
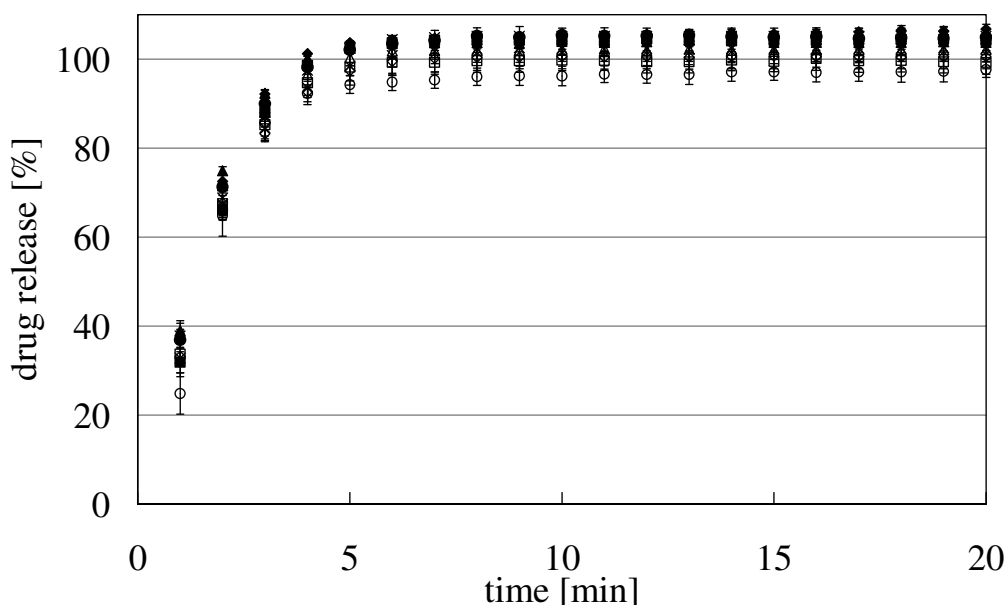
Fig. 38: **Release profiles of 10 % ThP + 70 % C53-06 in different media: ⬤ 0.1 M HCl, ◇ deionized water, ■ 0.01 M calcium chloride, □ 0.05 M calcium chloride, ▲ 0.05 M potassium chloride, △ 0.1 M potassium chloride ◆ 0.1 M sodium chloride, ◇ 0.1 M calcium chloride, ✕ 2x0.05 M calcium + potassium chloride, ✳ 2x0.05 M calcium + sodium chloride ($\bar{x} \pm$ SD, n = 3)**

The evaluation of the calculated similarity based on 0.1 M HCl as reference due to the peculiarity in deionized water. The similarity was confirmed by the f_2-values (Tab. 25). Therefore, comparing the dissolution profiles with the dissolution profiles of the micropellets containing spironolactone (Chap. 5.2.4.2) the effect of the solubility of the API was striking.

Tab. 25: Similarity factor of the standard formulation in different dissolution media to 0.1 M HCl

Medium		f_2-value
	Deionized water	54.2
0.01 M	Calcium chloride	84.5
0.05 M	Calcium chloride	64.7
0.05 M	Potassium chloride	87.1
0.1 M	Potassium chloride	77.9
0.1 M	Sodium chloride	89.3
0.1 M	Calcium chloride	65.9
2x0.05 M	Calcium + potassium chloride	75.2
2x0.05 M	Calcium + sodium chloride	87.3

Theophylline monohydrate is classified to be slightly soluble in water [Ph.Eur. 6, 2008]. With respect to the dissolution profiles, the solubility of theophylline monohydrate in all media was sufficient enough to overcome the ionic interactions between the dissolved ions in media and κ-carrageenan. However, the ionic interactions were still present. Intact or bursted micropellets remained in the vessel after reaching the maximum of drug release (Fig. 39a, b). In contrast, micropellets dissolved completely in deionized water. To assure that the bursted micropellets were not artifacts of the SEM sample preparation, the micropellets in the dissolution media were directly imaged (Chap 8.2.3.5). Independent of the type and amount of API, micropellets containing κ-carrageenan always showed cross-linkages in the presence of gel-promoting ions. In the example above, 60 % theophylline monohydrate were released completely, leaving an empty shell behind containing C53-06 and κ-carrageenan (Fig. 39).
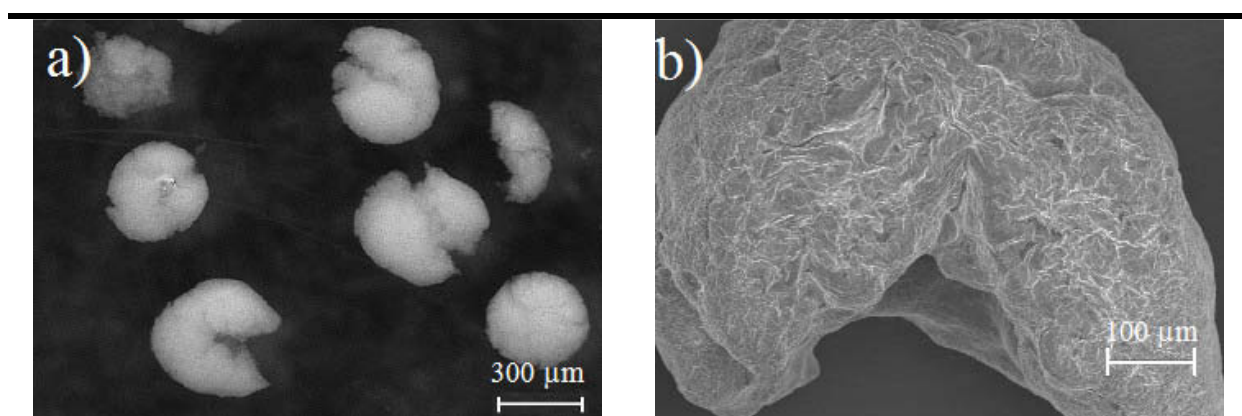
Fig. 39: **Pictures of micropellets containing 60 % ThP after 16 h of treatment in 0.1 M calcium chloride a) microscopic picture b) SEM**

The magnification of the empty micropellet shell revealed structures on the surface area (Fig. 40), which might be hypothetically related to the cross-linked 3D-network of polymer chains. Due to the structures, the surface area appeared to be rather rough. In addition pores and cracks were also observed, which were related to the solubility of the API and bursting effects of the micropellets due to the insoluble tricalcium phosphate.
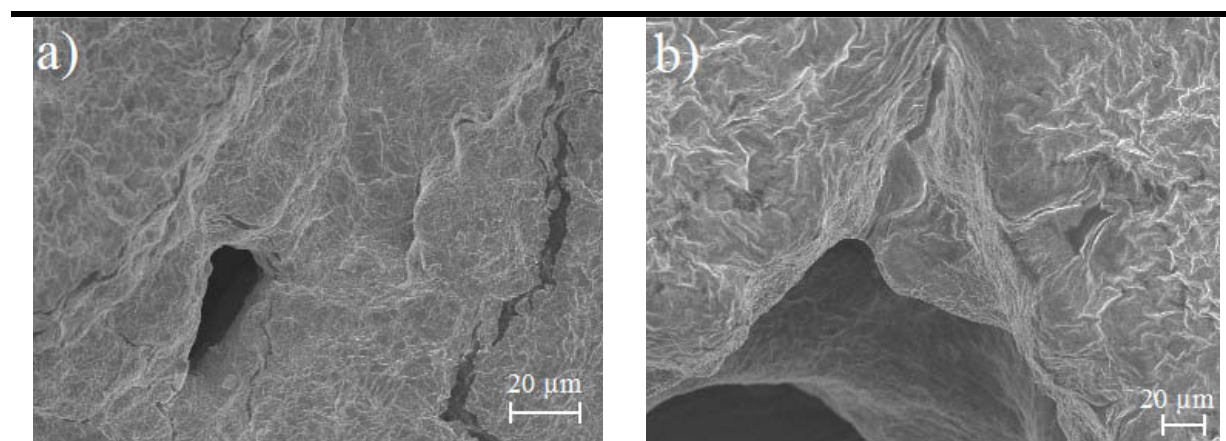
Fig. 40: **SEM pictures of the surface area of micropellets containing 60 % ThP after 16 h treatment in 0.1 M calcium chloride**

5.3.2.4 Summary

In comparison to spironolactone, micropellets containing theophylline monohydrate showed different dissolution behavior. Varying the ratio between API and κ-carrageenan did not show any substantial differences in the dissolution profiles. In addition, the presence of calcium ions in the medium did not affect the dissolution behavior. Therefore, the drug release was mainly dependent on the solubility of the API. Nevertheless a matrix system was obtained in the presence of calcium ions. However, the solubility of theophylline monohydrate was sufficient enough to overcome the ionic interactions and showed fast drug release. Consequently, the bioavailability of slightly soluble drugs is not affected by the ionic interactions with κ-carrageenan.

For further investigations, another API was used with lower solubility.

5.3.3 Extrusion/ spheronization of hydrochlorothiazide

5.3.3.1 Introduction and objective

Due to the superior effect of the solubility of theophylline monohydrate on the dissolution behavior (Chap. 5.3.2.3), further investigations were accomplished. The investigations on the different ratios between API and κ-carrageenan were repeated using another API. The solubility of the chosen drug was between those of spironolactone and theophylline monohydrate. The objectives were i) to evaluate the degree of the solubility role of the API on the dissolution behavior and; ii) to compare once more the ratio between API and κ-carrageenan.

Hydrochlorothiazide (HCT) was used as API. It is a diuretic belonging to the subgroup of 'thiazide-derivates'. Hydrochlorothiazide acts on the early distal tubule. It decreases active reabsorption of sodium and accompanying chloride by binding to the chloride site of the electroneutral Na^+/Cl^- co-transport system and inhibiting its action. The clinical use is in hypertension, in mild heart failure, in several resistant oedema and in nephrogenic diabetes insipidus [Rang et al., 1999].

Hydrochlorothiazide is classified as very slightly soluble in water. The solubility in water at 25 °C is 0.6 $g \cdot l^{-1}$ [Ph.Eur. 4.06 Kommentar, 2005]. It is categorized as BCS class II and is well absorbed from the GIT. Hydrochlorothiazide is UV-detectable and shows a maximum peak around 271 nm. The molecular weight is 297.7 $g \cdot mol^{-1}$.

5.3.3.2 Production and characterization

The dissolution profiles of micropellets containing spironolactone showed the main difference between 10 % and 50 % drug load (Chap. 5.2.4.2). Therefore, the ratio between API and pelletization aid just varied from 10 % to 60 %, respectively. The filler was C53-06 with a constant amount of 20 % and the pelletization aid was κ-carrageenan (Tab. 26).

Tab. 26: Overview of the formulations containing hydrochlorothiazide (*$\bar{x}$ ± SD, **x_{50} ± IQR)

| In [%] / Formulation	I	II	III	IV
Hydrochlorothiazide	10	30	50	60
C53-06	20	20	20	20
κ-Carrageenan	70	50	30	20
Powder feed rate [g·min^{-1}]	25	33	33	33
Extrusion screw speed [rpm]	125	125	125	125
Moisture content [%] *	363.4 ± 2.6	270.4 ± 2.3	184.9 ± 0.4	137.3 ± 7.8
Aspect ratio **	1.14 ± 0.1	1.14 ± 0.1	1.12 ± 0.1	1.12 ± 0.1
Pellet size [µm] **	402 ± 69.0	447 ± 85.4	509 ± 83.6	530 ± 103.4
Yield [%]	95.1	93.3	79.4	74.7
10 %-interval [%]	57.0	52.2	56.8	51.2
Tensile strength [MPa] *	83.39 ± 15.9	54.97 ± 13.3	25.19 ± 4.7	12.49 ± 2.7

The extrusion process differed from the standard conditions by the powder feed rate (Chap. 8.2.1.2). Dependent on the ratio the powder feed rate was adjusted in the range of 20 g·min^{-1} and 33 g·min^{-1}. The moisture content was varied from batch to batch. The Schlueter spheronizer was used under standard conditions (Chap. 8.2.1.3). All ternary powder mixtures were extruded and spheronized successfully. The best pellet properties of each formulation are listed in Tab. 26. The different filling degrees in the extruder did not affect the pellet properties as observed for theophylline monohydrate. Moreover, the aspect ratios were not below 1.1, which was again attributed to the drying process (Chap. 5.3.2.2). The aspect ratio was dependent on the amount of κ-carrageenan and therefore on the moisture content. With increasing amount of κ-carrageenan higher moisture contents of the extrudates were required to obtain optimum spheronization conditions and therefore, to produce micropellets with an aspect ratio below 1.2 (Chap. 5.1.7). The moisture content gradually increased from 137.3 % to 363.4 % respectively. The comparison of the moisture content of the extrudates containing either 60 % theophylline monohydrate (111.7 %) or hydrochlorothiazide (137.3 %) emphasized the effect of the solubility. Hydrochlorothiazide was less soluble and therefore, required higher moisture content for the production of micropellets. With increasing amount of κ-carrageenan, the aspect ratio increased marginally from 1.12 to 1.14, while the pellet size decreased. In addition, the yield increased respectively. The 10 %-interval for all formulations was good. Further, according to theophylline monohydrate (Chap. 5.3.2.2), the mechanical stability was enhanced with increasing amount of κ-carrageenan.

In summary, the micropellet properties containing hydrochlorothiazide did not show substantial differences on the process of production to the micropellets based on theophylline monohydrate.

5.3.3.3 Dissolution behavior

To evaluate the effect of the solubility of the API, the same dissolution media were used as for theophylline monohydrate. Besides, the investigations of the dissolution behavior in deionized water and 0.1 M calcium chloride solution were profitable to observe an effect of the different ratios between API and κ-carrageenan.
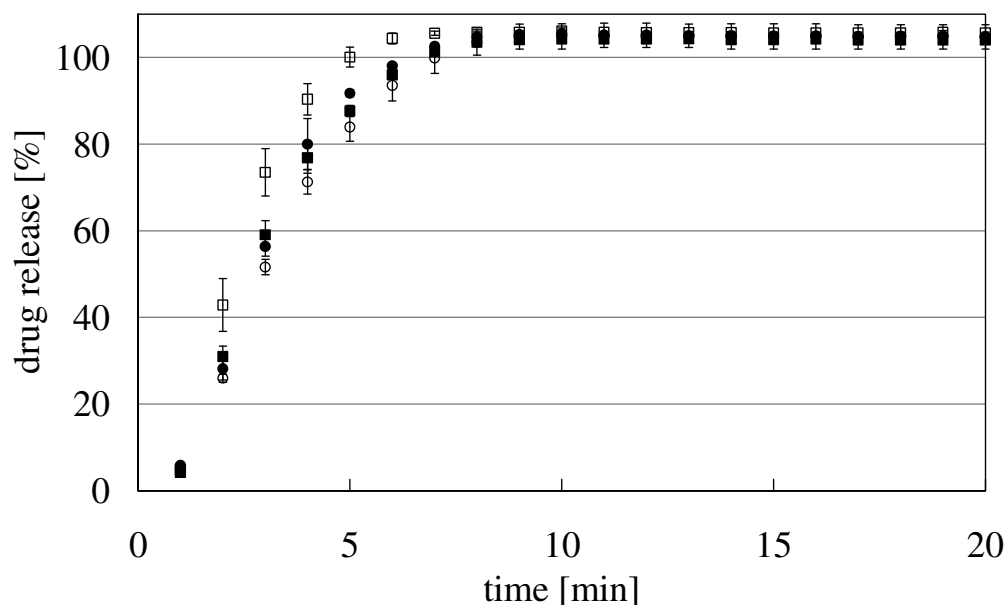
Fig. 41: Release profiles of micropellets containing different amount of HCT and a constant amount of 20 % C53-06 in deionized water: ◆ 10 %, ◇ 30 %, ■ 50 %, □ 60 % ($\bar{x} \pm SD$, n = 3)

First, each batch with the best aspect ratio of every formulation was dissolved in deionized water. All micropellets released the drug within 10 min and dissolved completely (Fig. 41). Independent of the amount of hydrochlorothiazide, no substantial differences in the dissolution profiles were obtained compared to spironolactone or theophylline monohydrate. The lag time of approximately 1 min was marginal. The comparison of the different ratios on the similarity equation referred to the Formulation I. The dissolution profiles were almost identical (Tab. 27).

Tab. 27: Similarity factor compared to the formulation comprising 10 % HCT in deionized water

Formulation	II	III	IV
f_2-value	97.3	99.8	91.2

The use of 0.1 M calcium chloride solution showed different dissolution profiles than the drug release of theophylline monohydrate (Fig. 42). Moreover, the effect of the ratio between API and κ-carrageenan was observed. Changing the ratio towards hydrochlorothiazide, the dissolution rate was slower. Nevertheless, the drug release was completed within 3 h. Therefore, independent of the shorter dissolution time, the effect of the ratio between API and κ-carrageenan was observed as in micropellets containing spironolactone. Thus, drug load of 50 % or higher did not show any differences in the dissolution profiles in 0.1 M calcium chloride solution.
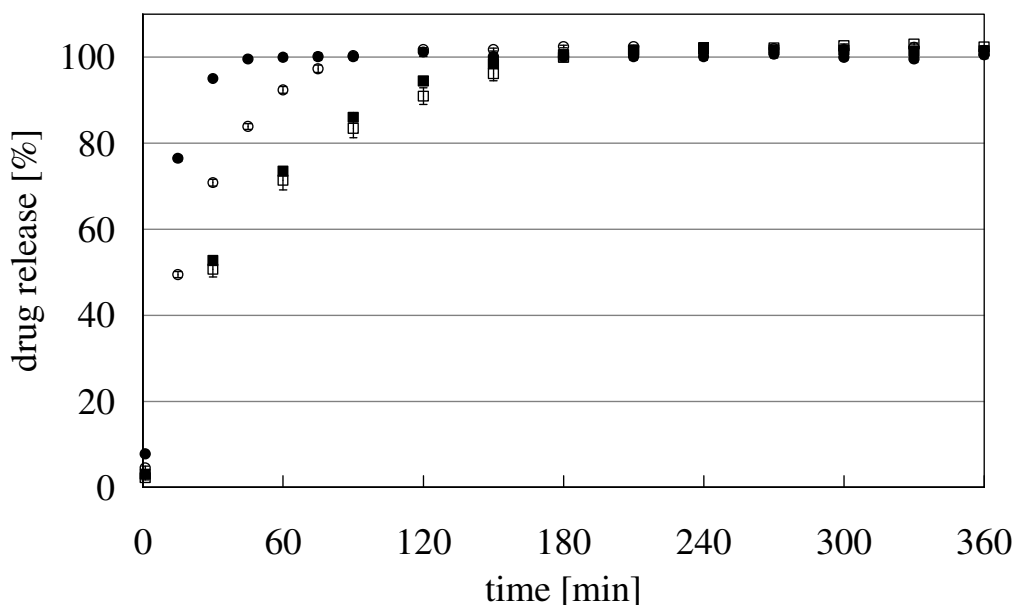
Fig. 42: Release profiles of micropellets containing different amount of HCT and a constant amount of 20 % C53-06 in 0.1 M calcium chloride: ● 10 %, ○ 30 %, ■ 50 %, □ 60 % ($\bar{x}$ ± SD, n = 3)

The mathematical comparison showed that the dissolution profiles of 50 % and 60 % were similar ($f_2 = 83.9$). The similarity evaluation to the Formulation I showed that only the dissolution profile of Formulation II was similar, while higher drug loads were not similar (Tab. 28). Hence, it could be concluded that the drug release of very slightly soluble drugs like hydrochlorothiazide was affected by the ionic interactions between the dissolved ions and κ-carrageenan, while the dissolution behavior of slightly soluble drugs was independent by the ionic interactions.

Tab. 28: Similarity factor compared to the formulation comprising 10 % HCT in 0.1 M calcium chloride

Formulation	II	III	IV
f_2-value	53.3	39.6	38.0

Even though the micropellets containing hydrochlorothiazide showed complete drug release within 3 h, the pellet shape was maintained in the presence of gel-promoting ions in the medium. Therefore, the ionic interactions between the dissolved calcium ions and κ-carrageenan were once more confirmed. The evaluation by Korsmeyer and Peppas showed anomalous (non-Fickian) diffusion for all formulations (Tab. 29), which emphasized the appearance of matrix systems in the presence of 0.1 M calcium chloride solution.

Tab. 29: Evaluation by Korsmeyer and Peppas for micropellets containing HCT

Formulation	Parameter n	log k	R^2
I	0.8885	+0.9414	0.9889
II	0.7835	+0.7762	0.9822
III	0.7295	+0.6656	0.9770
IV	0.7486	+0.6266	0.9642

The ionic interaction between dissolved calcium ions and κ-carrageenan on the different ratios was also reflected in the MDTs (Fig. 43). Decreasing the ratio between API and κ-carrageenan towards the hydrophilic matrix, the MDTs decreased respectively. This was referred to the hypothesis of the ionic interactions of κ-carrageenan (Chap. 5.2.4.2, discussion): The cross-linking κ-carrageenan molecules constructed a 3D-network depending on the effective shielding of the polymer charge. The presence of more κ-carrageenan molecules might disturb the arrangement of the polymer chains and therefore, the interior of the micropellet could retain lager amounts of water. Consequently, the located water would increase the viscosity in the matrix system and improve the wettability of the API.
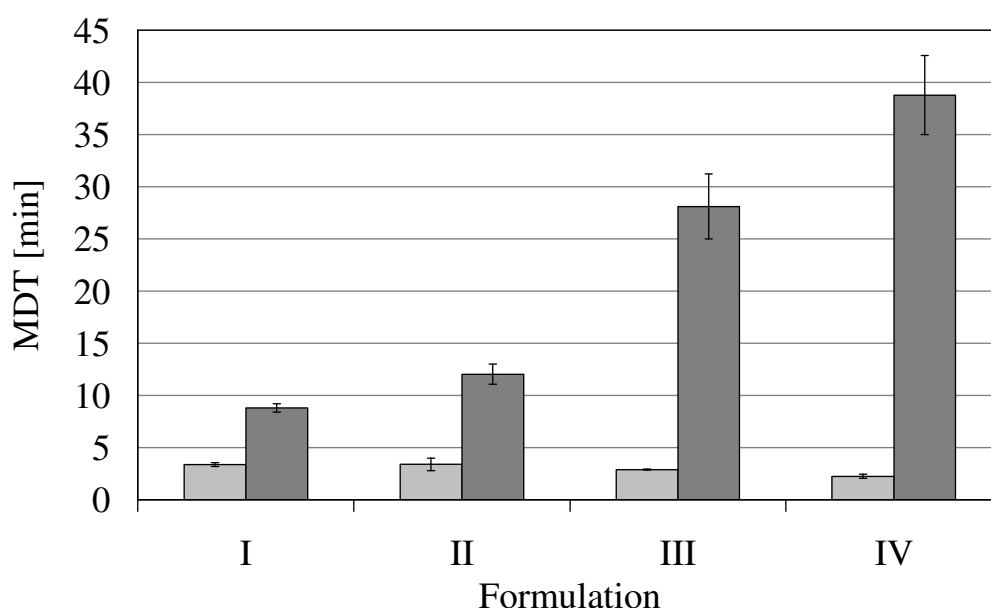
Fig. 43: MDTs of micropellets containing different amount of HCT and a constant amount of 20 % C53-06 in different media (▢) deionized water and (▢) 0.1 M calcium chloride ($\bar{x} \pm SD$, n = 3)

The relation between the ratio and the MDTs were observed for hydrochlorothiazide. Even though the drug release was faster compared to spironolactone, the effect of the ionic interactions between the dissolved ions and κ-carrageenan on the drug release could be extended to very slightly soluble drugs. The main difference in the dissolution profiles was obtained in faster drug release of hydrochlorothiazide.

Due to the presence of ionic interactions between the gel-promoting calcium ions and κ-carrageenan two questions arose rather i) to what extent the solubility of the API was decisive on the dissolution behavior and; ii) what other factors may affect the drug release of the micropellets. All prolonged drug releases showed anomalous (non-Fickian) diffusion. However, the drug release was generally dependent on the solubility of the API. With increasing solubility of the APIs the drug release was enhanced, respectively. Hence, the drug release rate increased in the following order:

spironolactone < hydrochlorothiazide < theophylline monohydrate

80

The release processes of anomalous (non-Fickian) diffusion characterized the intermediate range between the Fickian diffusion and the zero-order kinetic (Chap. 3.3). The kinetic was affected by swelling, diffusion and erosion. Hence, the diffusion coefficient was also considered (Chap. 3.2.2). The diffusion coefficient is strictly related to the molecular size, which is difficult to determine. Therefore, often the molecular weight is some kind of substitute for the molecular size. The APIs of high molecular weight decrease the diffusion coefficient. Consequently, the drug diffuses slowly out of the matrix, which affects the dissolution rate. Comparing the molecular weight of the APIs spironolactone showed the highest molecule weight (416.6 $g \cdot mol^{-1}$), followed by hydrochlorothiazide (297.7 $g \cdot mol^{-1}$) and last theophylline monohydrate (198.2 $g \cdot mol^{-1}$). Hence, the theoretical order by the molecular weight was similar to the ranking of the solubility. The order of the drug release was confirmed by the dissolution experiments in 0.1 M calcium chloride solution. Furthermore, the ranking of the dissolution profiles was independent of the ratio between API and κ-carrageenan.

5.3.3.4 Summary

The dissolution behavior of micropellets containing hydrochlorothiazide was affected by the presence of gel-promoting ions. Therefore, the drug release was comparable to the dissolution behavior of micropellets based on spironolactone with respect to the dissolution time. The change in ratio between API and κ-carrageenan led to slower drug release in 0.1 M calcium chloride solution. However, independent of the ratio the drug release was completed within 3 h. The dissolution behavior was unchanged in deionized water and therefore completed within 10 min. So far, the dissolution behavior of the micropellets was affected by the ratio between the API and κ-carrageenan. The pellet properties mainly restricted the dissolution behavior of the micropellets. The dissolution profiles varied in the dissolution rate dependent on the solubility and the diffusion of the API. Hence the drug release of micropellets comprising hydrochlorothiazide was located between the dissolution behavior of theophylline monohydrate and spironolactone. Thus, the effects of the ionic interactions between the dissolved ions and κ-carrageenan on the drug release were also obtained for very slightly soluble drugs.

5.3.4 Extrusion/ spheronization of griseofulvin

5.3.4.1 Introduction and objective

In accordance to the specification requirements, griseofulvin was a suitable model substance. For the sake of comparability to the micropellets comprising other APIs, griseofulvin was extruded and spheronized with the standard formulation (Chap. 5.2.4.1). The objective was to confirm the evaluated dissolution behavior of micropellets comprising κ-carrageenan by changing the API, but keeping the solubility classification as spironolactone.

5.3.4.2 Production and characterization

Extrusion took place at constant screw speed of 160 rpm and a powder feed rate of 40 g·min^{-1}. The moisture content of the extrudates varied from batch to batch. The spheronization process was carried out under standard conditions (Chap. 8.2.1.3). The standard formulation was extruded and spheronized successfully.

The batch with the best pellet properties was used for further investigations. It showed an aspect ratio of 1.08 with a pellet size of 524 µm. The yield was 73.2 % and the 10 %-interval was 54.2 %. The mechanical stability was proved by a tensile strength of 11.39 ± 1.5 MPa. Hence, the pellet properties were similar to the standard formulation containing spironolactone (Chap. 5.2.4.1). Due to the same solubility classification of being practically insoluble in water, similar moisture content of the extrudates was expected. The moisture content of the batch with the best pellet properties was 158.1 %. Therefore, the micropellets containing griseofulvin showed slightly higher moisture contents compared to spironolactone.

5.3.4.3 Dissolution behavior

Micropellets comprising the standard formulation were tested in the fast dissolving media (Fig. 44). The drug release of micropellets comprising griseofulvin in deionized water was completed within 90 min, while the drug release in 0.1 M HCl needed about 150 min. The mathematical comparison was calculated up to 150 min (150 time points). The absence of sameness of equivalence was confirmed ($f_2 = 45.5$). Consequently, the dissolution was slower in deionized water and 0.1 M HCl compared to the dissolution behavior of micropellets containing spironolactone.
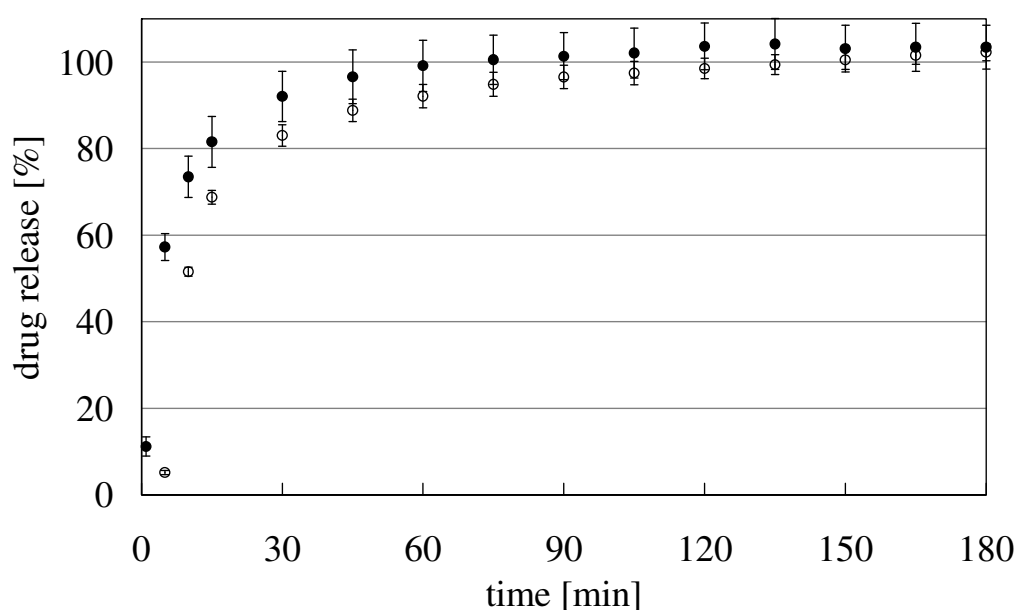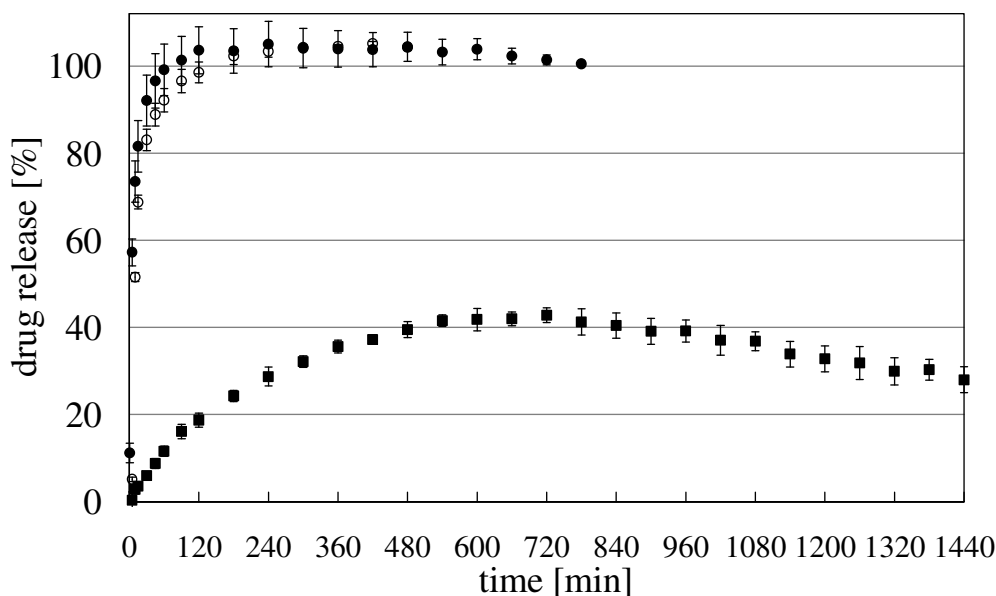

Fig. 44: Release profiles of 10 % GsF in ◆ deionized water, ◇ 0.1 M HCl ($\bar{x}$ ± SD, n = 3)

However, in comparison to the dissolution profile in 0.1 M calcium chloride solution, deionized water and 0.1 M HCl were fast dissolving media for micropellets comprising griseofulvin (Fig. 45). The slightly enhanced values above 100 % were attributed to the turbidity of the media. The complete drug release in 0.1 M calcium chloride solution was not reached at any time. Instead, after approximately 720 min the dissolution profile was decreasing again, which was attributed to the decomposition of griseofulvin.

Fig. 45: **Release profiles of micropellets containing 10 % GsF in ⬧ deionized water, ⬦ 0.1 M HCl, ◼ 0.1 M calcium chloride ($\bar{x} \pm$ SD, n = 3)**

Investigations in biorelevant media were also performed. Likewise to spironolactone, the FeSSIF medium was used (Fig. 46). The dissolution behavior in the FeSSIF medium was carried out twice for at least 120 min. In the first time stirring was continued to evaluate if the dissolution was completed. The last sample was taken out after 360 min. Each sample was analyzed three times in the HPLC (Chap. 8.2.2.7, 8.2.2.8). In the second run, samples were taken out continuously until 360 min. Each sample was analyzed twice in the HPLC. The dissolution profiles were compared to the dissolution profile in 0.1 M sodium chloride solution.

The drug release was completed after approximately 150 min in both types of dissolution media. The dissolution curves were comparable to the dissolution profile in 0.1 M sodium chloride solution. The mathematical comparison was calculated up to 120 min (24 time points). The dissolution profiles of both runs in FeSSIF medium were similar ($f_2 = 63.1$), but not to the 0.1 M sodium chloride solution ($f_{2\ (1st\ run)} = 26.9$, $f_{2\ (2nd\ run)} = 30.0$). However, to verify the observations of the different dissolution behavior, more investigations should be performed. So far, it can be assumed that the dissolution kinetic in both types of media were principally similar. The steady state of the dissolution profile was reached at the same time.

Further, the apparent effect of biliary compounds on κ-carrageenan in the standard formulation could be excluded due to the dissolution comparison of micropellets comprising different amounts of spironolactone (Chap. 5.2.4.2, FeSSIF medium). Therefore, besides the interactions between griseofulvin and the FeSSIF medium, the poor solubility of API might also affect the dissolution behavior of the micropellets.
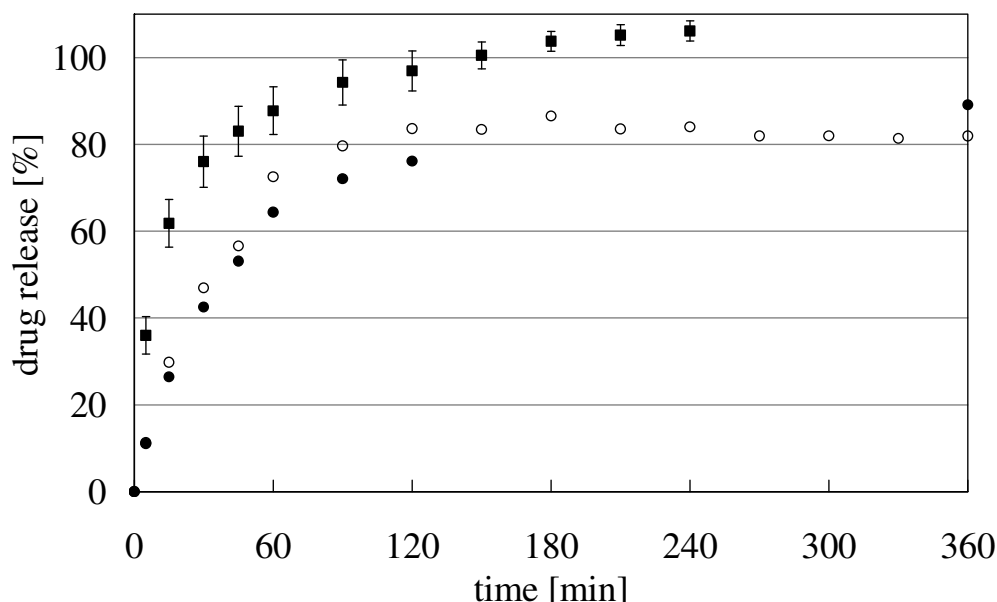
Fig. 46: Release profiles of micropellets containing 10 % GsF in different media: ● 1st run FeSSIF, ○ 2nd run FeSSIF (n = 2), ■ 0.1 M sodium chloride ($\bar{x} \pm SD$, n = 3)

Moreover, the dissolution behavior was investigated in milk. The drug release was compared to 0.1 M calcium chloride solution (Fig. 47). The mathematical comparison based on 190 min (13 time points). The dissolution profiles were similar ($f_{2 \text{ (1st run)}} = 65.6$, $f_{2 \text{ (2nd run)}} = 63.5$).

In comparison to the dissolution profiles of the micropellets containing 10 % spironolactone, micropellets based on griseofulvin showed slower drug release in the milk medium. This was expected due to the poor solubility of the API and the generally slower drug release compared to spironolactone. Nevertheless, the similarity of the dissolution profiles to the one in 0.1 M calcium chloride solution was quite surprising. Consequently, additional interactions were assumed. In fact, Macheras et al. [1990] evaluated the binding and solubility of griseofulvin in milk. The drug binding to milk compounds were independent of drug concentration but strongly affected by the fat content of milk. The solubility of griseofulvin was enhanced in milk, which was attributed to the lipophilicity. In addition, the drug binding to milk compounds correlated with the lipophilicity as well. However, the lipophilicity of griseofulvin was not solely responsible for interactions.
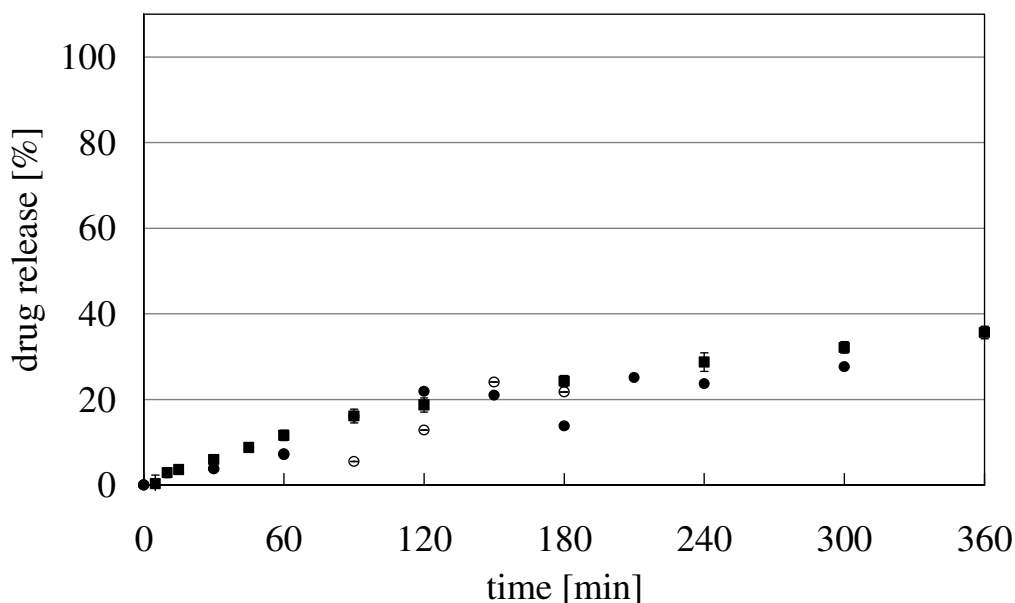
Fig. 47: **Release profiles of micropellets containing 10 % GsF in ◆ 1ˢᵗ run milk, ◇ 2ⁿᵈ run milk, ■ 0.1 M calcium chloride ($\bar{x} \pm$ SD, n = 3)**

In spite of the unsolved discussion concerning the complexity of interactions between griseofulvin and milk as well as κ-carrageenan and the milk compounds, the dissolution profiles of the micropellets emphasized the caution of concomitant application.

5.3.4.4 Summary

The dissolution profiles in fast dissolving media showed drug release within 90 min. The addition of gel-promoting ions to the dissolution media led to prolonged drug release, where the decomposition prevailed after approximately 720 min.

The dissolution profiles in FeSSIF and 0.1 M sodium chloride solution were not similar. Nevertheless, both drug releases were completed within 150 min indicating similar dissolution kinetics. The dissolution profiles in milk were similar to 0.1 M calcium chloride solution. Therefore, with respect to the dissolution profiles of the micropellets containing 10 % spironolactone, additional interactions between griseofulvin and the biorelevant media were assumed. The effects on the bioavailability should be considered.

5.3.5 Extrusion/ spheronization of itraconazole

5.3.5.1 Introduction and objective

The specification requirements were also appropriate for itraconazole. Therefore, the standard formulation was extruded and spheronized (Chap. 5.2.4.1). The objective was to confirm the effects of κ-carrageenan of the ionic interaction on the drug release of practically insoluble APIs.

5.3.5.2 Production and characterization

Extrusion took place at constant screw speed of 160 rpm and a powder feed rate of 40 g·min^{-1}. The moisture content of the extrudates varied from batch to batch. The Schlueter spheronizer was used under standard conditions (Chap. 8.2.1.3). The formulation was extruded and spheronized successfully.

The batch with the best pellet properties was used for further investigations. It had an aspect ratio of 1.10 with a pellet size of 537 µm. The yield was 62.2 % and the 10 %-interval was 56.8 %. The mechanical stability was proven by a tensile strength of 9.19 ± 1.2 MPa. Hence, the pellet properties were similar to the standard formulation containing spironolactone (Chap. 5.2.4.1). However, the yield and the 10 %-interval were rather poor indicating the difficulties of the production. Due to the same solubility classification as spironolactone, similar moisture content of the extrudates was expected. However the moisture content of the extrudates comprising itraconazole was 162.6 % and therefore, slightly increased.

5.3.5.3 Dissolution behavior

To evaluate the effect of κ-carrageenan in the formulation only two different dissolution media were investigated, which represented the fast dissolving and the gel-promoting dissolution media. Therefore, 0.1 M HCl and 0.1 M calcium chloride solution were used (Fig. 48a, b). Dissolution tests were carried out at a wavelength of 254 nm. The dissolution profile in 0.1 M HCl had a marginal drug release at the beginning, which was emphasized by the application of the absorption against the time. The increase in absorption was probably related to fine drug particles on the surface of the micropellets, which dissolved in the acidic medium. In contrast, no drug release was observed in 0.1 M calcium chloride solution. To exclude the possible detection of a marginal drug release at another wavelength, dissolutions were also evaluated at 223 nm with the same result (not shown).

For the micropellets comprising itraconazole, no drug release of therapeutic relevance was observed in both media. Further investigations with higher amounts of API in the formulation were excluded due to the ratio dependent dissolution profiles of spironolactone (Chap. 5.2.4.2). Hence, it was assumed that the presence of κ-carrageenan in the micropellets did not

affect the dissolution behavior at all. The practically insoluble drug was not released from the micropellets and therefore, no conclusions of the ionic interactions derived.
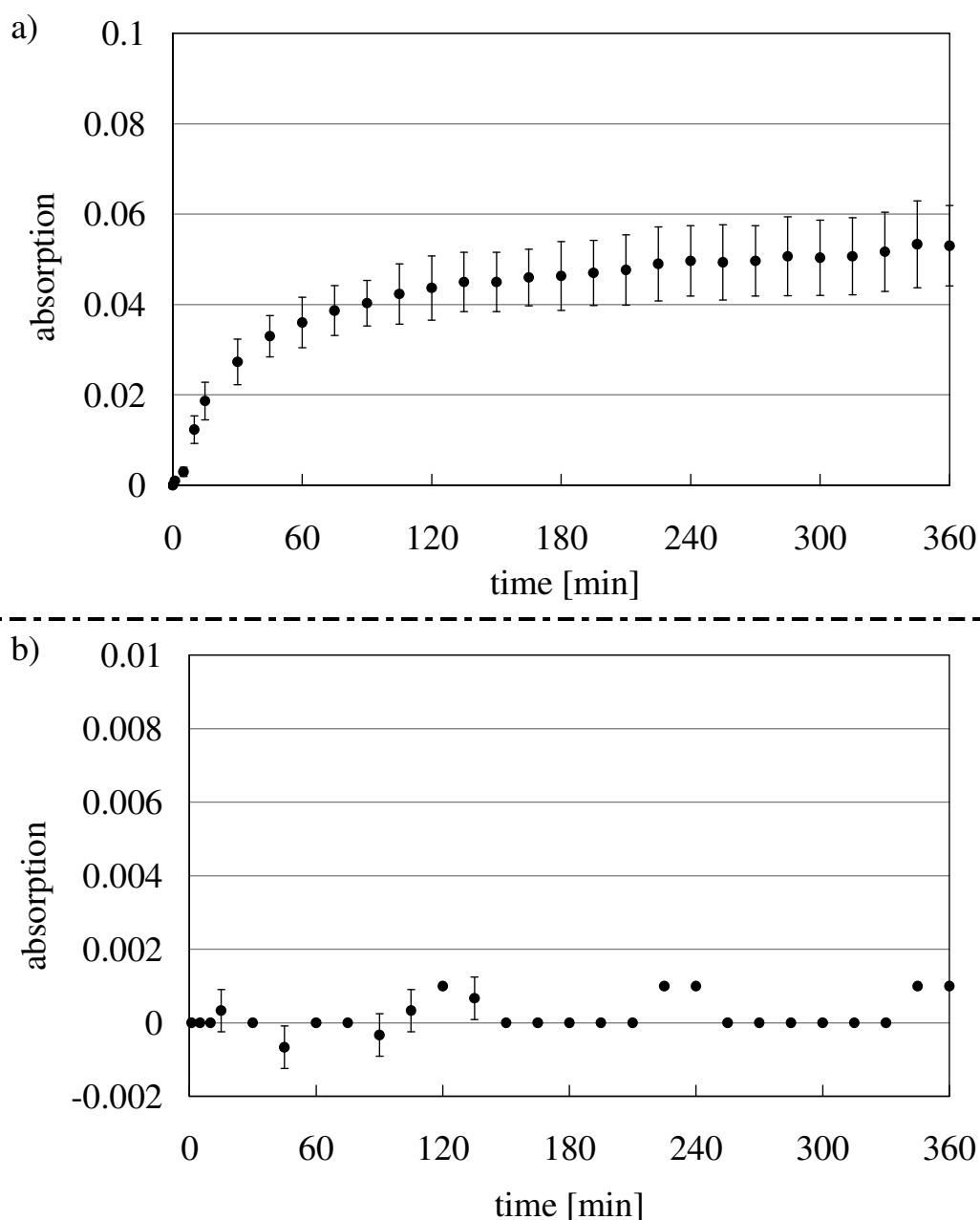
**Fig. 48:** Release profiles of 10 % ICZ in a) 0.1 M HCl, b) 0.1 M calcium chloride ($\bar{x} \pm$ SD, n = 3)

5.3.5.4 Summary

The production of micropellets containing itraconazole as API was successful. However, the presence of κ-carrageenan did not improve the dissolution behavior of micropellets containing the poor soluble itraconazole. Therefore, no drug release of therapeutic relevance was observed in both dissolution media.

5.3.6 Overview of the standard formulations in 0.1 M calcium chloride solution

5.3.6.1 Comparison of the standard formulations containing different fillers

The presence of gel-promoting ions in the dissolution media substantially affected the drug release. In addition, the dissolution rates were dependent on the formulation of the micropellets. The main difference in the dissolution behavior was obtained with high amount of different fillers. Therefore, Fig. 49 summarized the dissolution behavior of the micropellets containing various standard formulations of spironolactone in 0.1 M calcium chloride solution.
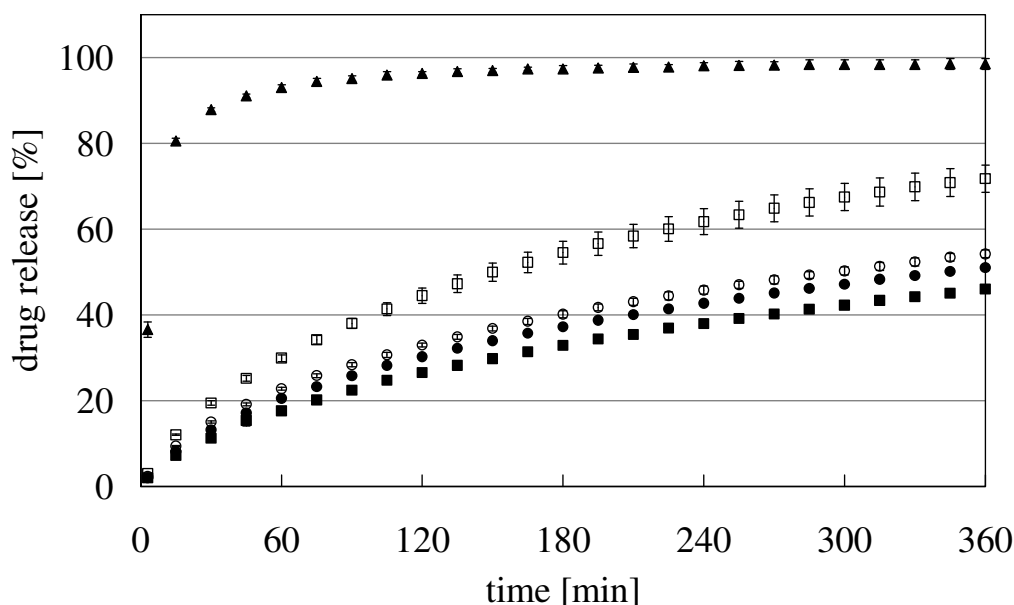
Fig. 49: Release profiles of micropellets based on different standard formulations of 10 % spironolactone in 0.1 M calcium chloride: ◆ 70 % C53-06, ◇ 70 % C13-03, ■ 70 % C92-14, □ 70 % GL200, ▲ 70 % Ca-lactat ($\bar{x} \pm$ SD, n = 3)

The dissolution behavior of the micropellets containing the insoluble fillers (calcium phosphates) showed the slowest drug release. The dissolution profile of the micropellets comprising 70 % C53-06 was used as reference to calculate the similarity factors. The dissolution profiles were similar ($f_{2\ (C13-03)} = 76.2$, $f_{2\ (C92-14)} = 68.8$). The effect of the soluble lactose monohydrate was obtained in the dissolution profile of the micropellets containing 70 % GL200. The drug release was increased and therefore, the sameness of equivalence to the dissolution profile of the micropellets comprising 70 % C53-06 was not confirmed ($f_2 = 10.7$). Although the production of micropellets containing 70 % calcium lactate failed, the dissolution behavior of the cylindrical product was sill investigated. The fast drug release was attributed to the previous interactions between dissolved calcium ions and κ-carrageenan in the extrusion process.

All in all, the comparison of the dissolution profiles in 0.1 M calcium chloride solution showed that the dissolution behavior of micropellets comprising different standard formulations of 10 % spironolactone was mainly affected by the solubility of the filler. Thus,

to assure the therapeutic relevance in the presence of calcium ions, micropellets comprising small amounts of drug load were recommended to be produced with better soluble, but calcium-free fillers. Moreover, the concomitant intake of calcium included drinks is not recommendable.

5.3.6.2 Comparison of the standard formulations containing different APIs

To evaluate the effect of the APIs on drug release, all standard formulations containing C53-06 and κ-carrageenan were tested in 0.1 M calcium chloride solution (Tab. 30). Although the formulation containing hydrochlorothiazide showed 10 % drug load, the amounts of both excipients were switched. However, the dissolution profiles in fast dissolving media were similar independent on the ratio (Chap. 5.3.3.3). In addition, the dissolution profile in 0.1 M calcium chloride solution behaved like an expected standard formulation of 10 % API (Chap. 5.3.3.3). Therefore, the formulation of hydrochlorothiazide comprising 10 % drug load and 70 % κ-carrageenan was used for the comparison. Further, micropellets containing amoxicillin trihydrate (Amoxi) were a gift from Grünenthal GmbH and contained higher drug loads. However, the requirements of the specification on the API were appropriate for the drug and therefore, also added to the comparison. Fig. 50 shows the dissolution profiles in 0.1 M calcium chloride medium for all different APIs.

Tab. 30: Compounds of the standard formulations with different APIs

API [%] Excipient [%]	SpL	ThP	HCT	Amoxi	GsF	ICZ
	10	10	10	64.6	10	10
C53-06	70	70	20	7.3	70	70
κ-Carrageenan	20	20	70	28.1	20	20
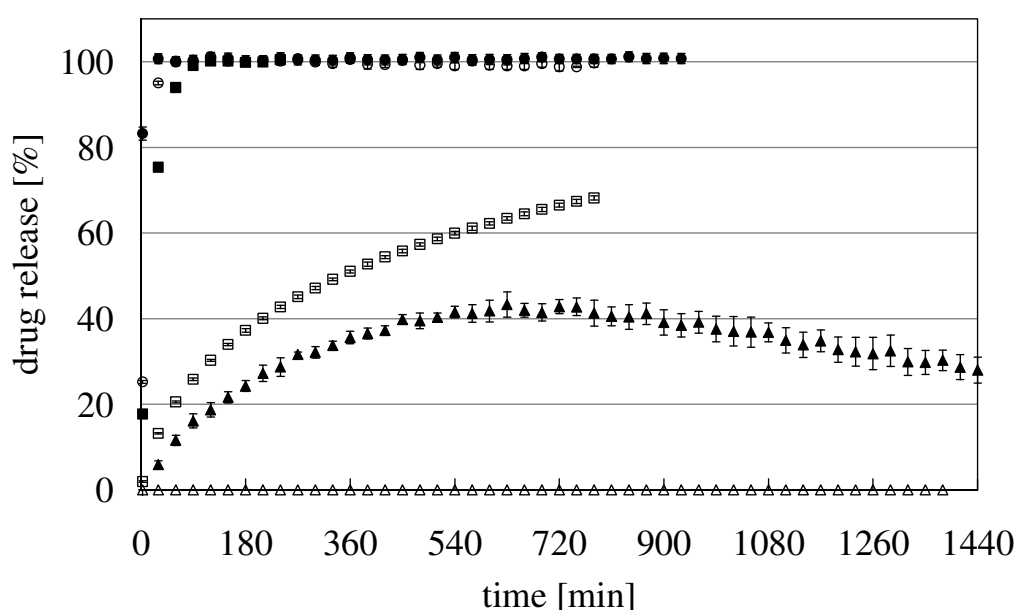
Fig. 50: Release profiles of the standard formulations containing different APIs in 0.1 M calcium chloride: ● ThP, ○ HCT, ■ Amoxi, □ SpL, ▲ GsF, △ ICZ ($\bar{x} \pm$ SD, n = 3)

89

Theophylline monohydrate had the fastest drug release followed by hydrochlorothiazide and amoxicillin trihydrate. The dissolution profile of spironolactone was still adequate, while griseofulvin showed a decrease after 720 min. Itraconazole did not show any drug release at all. The decrease in the dissolution profile of griseofulvin was attributed to the decomposition of the drug, which prevailed after 720 min.

Tab. 31: Overview of the evaluation parameter affecting the dissolution behavior of different APIs

API	Descriptive term	Parts of solvent required for 1 part of solute	M_G [g·mol^{-1}]
Theophylline monohydrate	slightly soluble in water	From 100 to 1000	198.2
Hydrochlorothiazide	very slightly soluble in water	From 1000 to 10 000	297.7
Amoxicillin trihydrate	slightly soluble in water	From 100 to 1000	419.4
Spironolactone	practically insoluble in water	≥ 10 000	416.6
Griseofulvin	practically insoluble in water	≥ 10 000	352.8
Itraconazole	practically insoluble in water	≥ 10 000	706.0

Tab. 31 contains the evaluation parameters, which affected the dissolution behavior of the micropellets comprising different APIs. Basically, the drugs were able to be categorized into better soluble and practically insoluble drugs, indicated by the dotted line in the table. First, the dissolution profiles of the better soluble drugs were evaluated. According to the previous discussion of a theoretical ranking on drug release (Chap. 5.3.5.3), the solubility classifications and the molecular weights of theophylline monohydrate, hydrochlorothiazide and amoxicillin trihydrate were used to evaluate the dissolution behavior (Tab. 31). The dissolution order by the solubility of the APIs would be:

hydrochlorothiazide < theophylline monohydrate ≈ amoxicillin trihydrate

With respect to the diffusion processes in the matrix system, the drug release order differed by the molecular weight:

amoxicillin trihydrate < hydrochlorothiazide < theophylline monohydrate

In both rankings theophylline monohydrate showed the fastest drug release. The dissolution behavior of micropellets comprising theophylline monohydrate in different ratios was not affected by the ionic interactions due to the solubility of the API (Chap. 5.3.2.3). Therefore, it was assumed that the dissolution behavior of micropellets containing amoxicillin trihydrate will be unaffected by the ionic interactions with regard to the same solubility classification (Tab. 31). Hence, the different ratio between amoxicillin trihydrate and κ-carrageenan was considered to be negligible (Tab. 30) and the dissolution order by the solubility classification was expected. However, the exploratory data showed the drug release order by the molecular weight. Theophylline monohydrate was completely released within 10 min, followed by hydrochlorothiazide with 55 min and amoxicillin trihydrate after 105 min. This emphasized

that the molecular weight was relevant to the diffusion process and therefore, affected the dissolution profiles. The mathematical comparison confirmed the absence of sameness of equivalence with theophylline monohydrate as reference ($f_{2\,(HCT)}$ = 39.4, $f_{2\,(Amoxi)}$ = 30.2).

The other three APIs, categorized to be practically insoluble in water, differed in the dissolution profiles as well. With respect to the molecular weight, the slowest drug release was expected from the micropellets based on itraconazole followed by spironolactone. But, spironolactone showed the best dissolution behavior compared to griseofulvin and itraconazole. The results indicated the lack of the coarse classification in the descriptive terms of the Pharmacopoeia (Tab. 31). The undefined range of the solubility term of practically insoluble in water emphasized the solely informational nature. Hence, different factors such as additional interactions and wettability must be considered.

To conclude, the dissolution profiles in the presence of gel-promoting ions were at least dependent on i) the solubility of the drug and; ii) the molecular weight. The dissolution of the micropellets containing slightly soluble drugs, like theophylline monohydrate and amoxicillin trihydrate, was independent of the interactions between dissolved calcium ions and κ-carrageenan. The drug release was fast. The dissolution behavior of micropellets comprising drugs with lower solubility, such as hydrochlorothiazide and spironolactone, were affected by the ionic interactions. The drug release was prolonged and must be considered to the therapeutic availability of the API. The micropellets containing κ-carrageenan were not suitable for some practically insoluble drugs, such as itraconazole.

Hence, the ionic interactions must be considered in the choice of API of the micropellets comprising κ-carrageenan. Especially the hidden ionic concentration as in milk can affect the essential drug release for therapeutic relevance. In addition, the daily intake of dissolved calcium or magnesium ions must be timely adjusted to prevent ionic interactions.

5.3.6.3 Summary

The dissolution profiles of the different standard formulations in 0.1 M calcium chloride solution emphasized the effect of the solubility of the APIs and the different fillers on the drug release of micropellets comprising κ-carrageenan. Additionally, the molecular weight of the API affected the dissolution behavior of better soluble drugs. Independent of the compounds in the formulation of the micropellets, the ionic interaction between calcium ions and κ-carrageenan was always present but not decisive for all drug releases. To ensure the availability of the API, the concomitant intake of drinks containing higher amounts of ions is not recommended.

5.4 Different types of κ-carrageenan

5.4.1 Introduction and objective

Due to its natural source, each type and batch of carrageenan can differ in its type and amount of counter-ions dependent on the process. Therefore, the solubility and gelling properties, differ from one to another. The gelling behavior on ionic interactions was evaluated in numerous investigations [Michel et al., 1997; Piculell et al., 1997; MacArtain et al., 2003]. Moreover, the ionic interactions substantially affected the drug release (Chap. 5.2.4.2).

The objective was to evaluate i) the effects of the observations with regard to the dissolution investigations and; ii) the difference of the κ-carrageenan types on ionic interactions.

5.4.2 Evaluation of different types of κ-carrageenan

5.4.2.1 Concentration of counter-ions

The investigations on the production of micropellets showed that dissolved ions substantially affected the drug release. Moreover, the presence of dissolved calcium ions in the extrusion process evaluated the loss of pelletization ability of κ-carrageenan. Therefore, the question arose if the ability to act as a pelletization aid can be measured on its counter-ion concentration. Different types of carrageenan were investigated to determine the concentration and type of compounds by the inductively coupled plasma optical emission spectrometer (ICP-OES) (Chap. 8.2.3.6). Tab. 32 contained the main counter-ions.

Tab. 32: Concentration of counter-ions in different types of carrageenans

Trade name	Type	Ammonium [%]	Calcium [%]	Potassium [%]	Lithium [mg·kg^{-1}]	Magnesium [%]	Sodium [%]
Gelcarin® GP-911	κ-Carr	< 0.005	2.600	4.000	< 1.000	0.110	0.400
Satiagel® CT-27	κ-Carr	< 0.005	0.088	12.000	< 1.000	0.047	2.900
Satiagel® ME-4	κ-Carr	< 0.005	0.028	12.000	< 1.000	0.036	1.800
Genugel® X930-03	κ-Carr	< 0.005	1.800	4.900	< 0.100	0.040	0.650
Gelcarin® GP-911	κ-Carr	< 0.005	2.600	4.000	< 1.000	0.150	0.450
Gelcarin® GP-911	κ-Carr	< 0.005	2.500	3.800	< 1.000	0.120	0.550
Gelcarin® GP-911	κ-Carr	< 0.005	1.900	5.200	< 1.000	0.100	0.610
Gelcarin® GP-812	κ-Carr	< 0.005	2.400	7.900	< 1.000	0.110	0.560
Gelcarin® GP-379	ι-Carr	0.009	3.400	3.000	< 1.000	0.160	0.960
Viscarin® GP-109	λ-Carr	< 0.005	0.260	1.100	< 1.000	0.300	5.100

In general, the amount of counter-ions varied in the different types of carrageenans. λ-Carrageenan is a non-gelling type of carrageenan [Bubis, 2000]. It contained a major amount of sodium ions, while the other counter-ions were below 1 %. ι-Carrageenan is a gelling type of carrageenan. It contained more sodium ions than the Gelcarin® types of κ-carrageenan. Although the ratio between calcium and potassium ions was almost equal, this type of product is purchased as a moderate calcium salt of iota carrageenan [Bubis, 2000].

The concentrations of counter-ions in the different κ-carrageenans showed substantial differences dependent on the manufacturer. The potassium amount in the Satiagel® types of κ-carrageenan was enhanced, while the amount of calcium ions was below 0.1 %. In fact, the amount of potassium ions was around three times higher compared to Gelcarin® types of κ-carrageenan. In addition, the amounts of sodium ions were the highest of all κ-carrageenans, exceeding 1.5 %.

The Gelcarin® types of κ-carrageenan were classified into moderately low potassium salt (GP-911) and moderately potassium salt of κ-carrageenan (GP-812) [Bubis, 2000]. Therefore, the amount of potassium ions was almost twice in the latter type. The ratio between calcium and potassium ions were around 0.65 in the Gelcarin® types of GP-911 with the exception of one batch (0.36, highlighted in the table). The ratio in the Gelcarin® type of GP-812 was around 0.3. The Genugel® type showed a ratio of 0.36. Hence, independent of the type of κ-carrageenan, the amount of potassium ions was always enhanced than calcium ions.

The ammonium and lithium counter-ions were similar independent of the type of carrageenan. Only ι-carrageenan varied in the amount of ammonium while the Genugel® type of κ-carrageenan contained less lithium. The amount of magnesium ions were below 0.4 % independent of the type of carrageenan.

Thus, in a theoretical recommendation of a κ-carrageenan ranking to produce micropellets, the Satiagels® would be at the end of the ranking due to the amount of gel-promoting counter-ions. However, Thommes and Kleinebudde [2008] found a different sequence with regard to the pellet properties. Thus, additional factors besides the amount of counter-ions affected the extrusion and spheronization of κ-carrageenans.

5.4.2.2 Rheological behavior of different κ-carrageenans

According to the determination of concentration of the counter-ions in the different types of carrageenans rheological investigations were performed (Chap. 8.2.3.6). Despite the fact that the molecular weight was unknown, Fig. 51 contained one out of three measurements of each type of κ-carrageenan.

All carrageenan gels displayed Newtonian behavior.

Due to the enhanced amount of potassium ions in the Satiagel® types of κ-carrageenan and the Gelcarin® GP-812, it was expected that the viscosities were higher compared to Gelcarin® GP-911. However, the opposite was observed. In contrast Genugel® X930-03 showed higher viscosity than Gelcarin® GP-911, which was in common with the enhanced ratio towards potassium. For now, the rheological measurements emphasized that the amount and type of counter-ions in the κ-carrageenans were rather unimportant. However, the determination of the molecular weight and the length of the polymer chains would describe the results in detail.
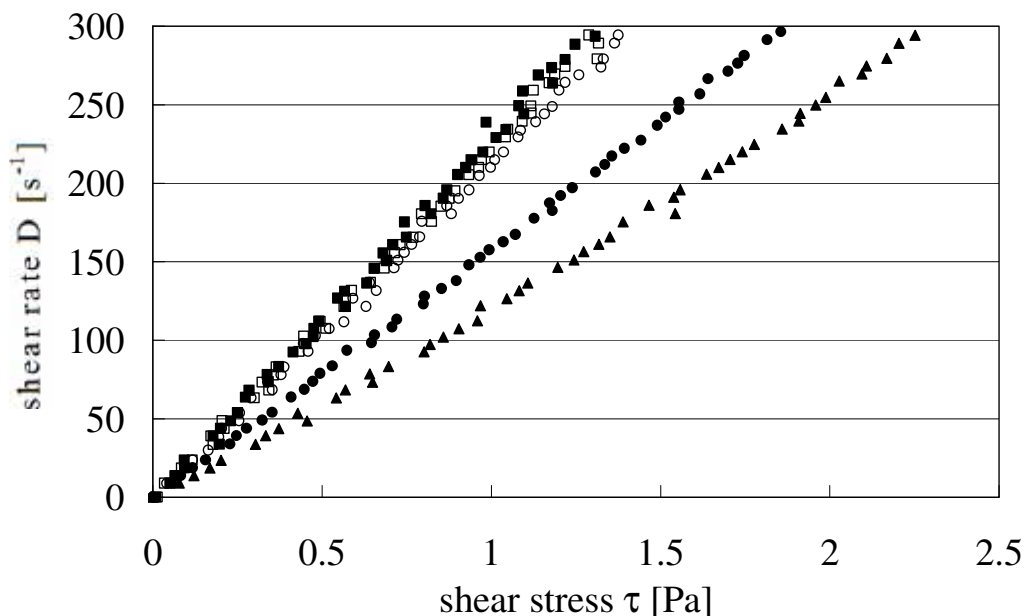
Fig. 51: Rheological measurements of different 0.2 % κ-carrageenans sols in deionized water ◆ GP-911, ◇ GP-812, ■ CT-27, □ ME-4, ▲ X930-03 (n = 1)

Due to the sample preparation, the moisture content of the different κ-carrageenans must be included in the evaluation. Higher moisture content of the raw material meant less κ-carrageenan in the weighted sample, which affected the rheological behavior.

Tab. 33: Moisture content [%] of the different κ-carrageenans ($\bar{x} \pm SD$, n = 3)

Gelcarin[®] GP-911	Satiagel[®]CT-27	Satiagel[®] ME-4	Gelcarin[®] GP-812	Genugel[®] X930-03
9.6 ±0.20	6.7 ±0.03	9.5 ±0.04	11.2 ±0.04	13.7 ±0.02

Tab. 33 indicates that the moisture content did not affect the rheological behavior of the different κ-carrageenans. If the Satigel[®] types of κ-carrageenan had higher moisture contents, the actual amount of κ-carrageenan would have been less than the weighted sample. That would have been a reason for the diminished viscosities. But, the moisture content of the Satiagel[®] types and the Gelcarin[®] GP-911 were similar. Moreover, if the moisture content had a dominant effect on the rheological behavior, the Satiagel[®] CT-27 would have increased the viscosity. Hence, there was no relation between the moisture content and the rheological behavior obtained.

The rheological behavior of κ-carrageenan showed complex interactions between different factors such as length of the polymer chains, the absolute polymer weight, the purity, the moisture content and the amount of counter-ions. Therefore, the rheological behavior could not be predicted by only two factors. However, the rheological behavior is essential for the production and dissolution of micropellets. Therefore, the different types of κ-carrageenan cannot be inoffensively exchanged without further investigations.

5.4.2.3 Rheological behavior of κ-carrageenan in different dissolution media

The different effects of the dissolved ions on micropellets comprising κ-carrageenan were verified by the rheological analysis (Chap. 8.2.3.7). The analysis was performed using the same κ-carrageenan for the micropellets production. Therefore the κ-carrageenan type Gelcarin® GP-911 was used in a concentration, which created a sol to evaluate the gelling effects in the presence of gel-promoting ions. Tab. 34 contains the mean viscosity values of different media at 300 s^{-1}. The ions of the fast dissolving media showed less viscose behavior compared to the pure hydrocolloid solution. In addition, Newtonian behavior was observed (Fig. 52).
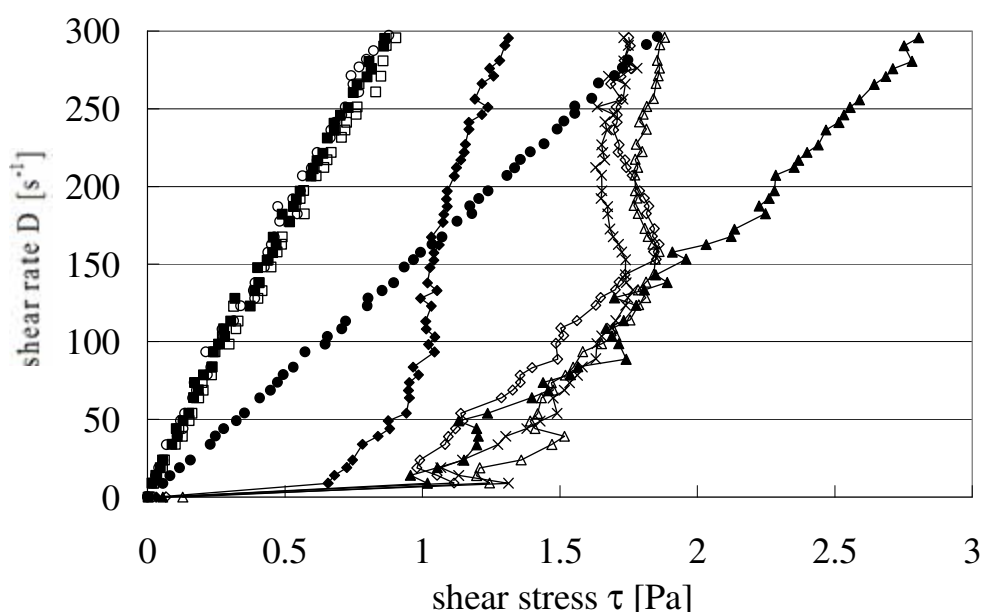
Fig. 52: **Rheological measurements of 0.2 % κ-carrageenan (Gelcarin® GP-911) in different media: ✦ deionized water, ○ 0.1 M sodium chloride, ■ 0.1 M lithium chloride, □ 0.01 M calcium chloride, ▲ 0.05 M calcium chloride, △ 0.1 M calcium chloride, ✦ 0.1 M magnesium chloride, ◇ 2x0.05 M calcium + sodium chloride, ✕ 0.1 M calcium chloride + 0.05 % Brij® 35P (n = 1)**

Solutions containing potassium chlorides were not able to be measured at all. While the dissolution behavior of the micropellets comprising κ-carrageenan seemed to be more affected by the presence of calcium rather than potassium ions, the hydrocolloid solutions were definitely stronger affected by the presence of potassium ions. The strength of the ionic interactions between calcium or potassium ions and κ-carrageenan might be dependent on the present condition of the κ-carrageenan.

The values of the gel-promoting ions were less reproducible due to the gelling of the κ-carrageenan. Moreover, the rheological profiles showed a so-called 'viscoelastic nose', which occurs when the energy is released after the internal structure breaks down [Gehm, 2004].

Tab. 34: Visocosity of 0.2 % κ-carrageenan mingled with different dissolution media ($\bar{x} \pm$ SD, n = 3)

Added dissolution medium	Determined viscosity value at 300 s^{-1} [mPa·s]
Deionized water	6.06 ± 0.2
0.01 M Calcium chloride	2.97 ± 0.2
0.05 M Calcium chloride	9.56 ± 0.2
0.1 M Calcium chloride	5.98 ± 0.3
0.05 M Potassium chloride	-
0.1 M Potassium chloride	-
0.1 M Sodium chloride	2.61 ± 0.3
0.1 M Lithium chloride	2.78 ± 0.3
0.1 M Magnesium chloride	4.31 ± 0.3
2x0.05 M Calcium + potassium chloride	-
0.1 M Calcium chloride + 0.05 % Brij® 35P	5.71 ± 0.2

5.4.3 Summary

The different types of κ-carrageenan varied in the amounts of the different counter-ions, which were related to the production processes (Chap. 1.3.3). The different ratios between the counter-ions did not affect the rheological behavior with respect to the unknown molecular weight and the length of the polymer chains. Also, the moisture content of the κ-carrageenans did not affect the viscosity. Therefore, the potential interchangeability of the different types of κ-carrageenans as a pelletization aid for wet extrusion/ spheronization cannot be simply selected based on the amount of counter-ions.

6   Summary

This is the first report of a systematic investigation on the production of micropellets (500 µm to 700 µm median diameter). In general, κ-carrageenan is a suitable pelletization aid to produce spherical aggregates by wet extrusion/ spheronization. The obtained pellets show fast drug release, which is advantageous for use with slightly soluble drugs.

The mechanism of spheronization for micropellets differed to that for bigger pellets. The conditions for spheronization reported for bigger pellets could not be used to produce micropellets. Adhesion and condensation of water on the spheronizer wall disturbed the twisted-rope movement of the product, which characterizes the spheronization process. The optimization of the process parameters for producing micropellets was performed on two different types of spheronizers. The condensation of water, which had previously been disruptive, could now be exploited in the spheronization process. As a result, the quality of the micropellets was improved.

The dissolution behavior of the micropellets was systematically investigated. First, the effects of ionic interactions on dissolution behavior were investigated in micropellets containing κ-carrageenan and spironolactone. To evaluate the ionic interactions, different chloride salts such as sodium chloride or calcium chloride, among other dissolution media, were added. The different cations used are generally known as 'specific-' and 'non-specific-' binding ions to the κ-carrageenan. A correlation was found between the dissolution behavior of micropellets comprising κ-carrageenan and the classification of the dissolved ions. Consequently, the 'non-specific' sodium or lithium ions in the dissolution medium resulted in fast drug release, while the 'specific' or divalent ions such as potassium and calcium ions showed prolonged drug release.

Second, dissolution investigations were performed on the effects of different APIs (spironolactone, theophylline monohydrate, hydrochlorothiazide, griseofulvin, itraconazole) on the dissolution behavior of micropellets comprising κ-carrageenan. When the ratio between API and κ-carrageenan in the micropellets was varied, a relation between the dissolution rate and the solubility of the API was shown. Micropellets comprising soluble APIs such as theophylline monohydrate showed fast drug release independent of the media. The dissolution rate of soluble drugs was not affected by the ratio. In contrast, the dissolution profiles of micropellets comprising κ-carrageenan and either very slightly soluble or practically insoluble drugs such as hydrochlorothiazide or spironolactone were dependent on the concentration of the ions. For example, drug release from micropellets comprising κ-carrageenan was slower with increasing amounts of calcium ions in the dissolution media. Matrix dissolution of the anomalous (non-Fickian) diffusion type was obtained. The dissolution behavior was affected by ionic interactions. The correlation between the ratio of API and κ-carrageenan only existed when ionic solutions such as calcium chloride were used as the dissolution media and not with deionized water. Further investigations with practically insoluble drugs showed that the API was a key determinant on the dissolution behavior. Thus,

no therapeutic drug release was observed for micropellets comprising κ-carrageenan and itraconazole. By means of a model, the relation between the dissolution behavior of micropellets, the solubility of the API and the ionic interactions with κ-carrageenan was described.

Third, the effects of different fillers (tricalcium phosphates, dicalcium phosphate, lactose monohydrate, calcium lactate) on the dissolution behavior of micropellets containing spironolactone, were investigated. The type and the amount of filler affected the dissolution behavior. The drug release was improved in the presence of water-soluble lactose monohydrate. However, the effect of the solubility of the fillers was negligible on the dissolution behavior when the amount of API was increased and the amount of filler was decreased. The extrudates containing calcium lactate failed to convert into micropellets and additionally the different media did not affect the drug release rate. This was attributed to the ionic interactions between the dissolved calcium ions of the calcium lactate and κ-carrageenan during the extrusion process. The free calcium ions of the undissolved calcium phosphate compounds did not affect the extrusion process.

Fourth, the effects of the ionic interactions of micropellets comprising κ-carrageenan with biorelevant media were investigated in terms of dissolution behavior. The results of the investigations showed that careful attention must be paid to the choice of drinks during and after the administration of micropellets comprising κ-carrageenan and very slightly soluble drugs.

Finally, the effects of counter-ions from the different κ-carrageenan products obtained from various manufacturers were determined. The rheological behavior of the different types of κ-carrageenan was not solely dependent on the counter-ions. Therefore, the type and amounts of counter-ions in κ-carrageenans could be disregarded when choosing the type of κ-carrageenan as a pelletization aid.

Taken together, the solubility of the APIs and fillers, the amount of compounds in the formulation and the ratio between the API and κ-carrageenan, all affected the dissolution behavior. Furthermore, the type and amount of dissolved ions were more likely to impact on the κ-carrageenan than the counter-ions contained in the pelletization aid.

In conclusion, the results of this thesis showed that fast dissolving micropellets were produced by wet extrusion/ spheronization. However, the drug release is strongly dependent on the formulation and the conditions of the dissolution media. Based on the extensive analysis of the ionic interactions on κ-carrageenan it is possible to explain the dissolution behavior of micropellets in the presence of ions, which enables conclusions about food interactions to be drawn. Based on this, measures to improve the availability of the drug can be initiated.

7 Zusammenfassung der Arbeit

κ-Carrageenan ist ein etablierter Hilfsstoff in der Herstellung sphärischer Agglomeratpartikel durch Feuchtextrusion/ Sphäronisation. Die dadurch erhaltenen Pellets besitzen eine schnelle Arzneistofffreisetzung, welches besonders für schwerlösliche Arzneistoffe vorteilhaft ist. In dieser Arbeit wurde erstmalig die Herstellung von Mikropellets (500 µm – 700 µm im Durchmesser) unter Verwendung von κ-Carrageenan systematisch untersucht.

Der Rundungsmechanismus bei Mikropellets unterscheidet sich deutlich von dem der größeren Pellets, wodurch die Anwendung bisheriger Erkenntnisse zu abweichenden Beobachtungen führte. So kommt es durch Adhäsion des Gutes oder durch Kondensation von Wasser an der Sphäroniserwand zur Störung der spiralkranzförmigen Gutbewegung, die ein Charakteristikum des Sphäronisationsprozesses ist. Durch die Optimierung der Prozessparameter erwies sich die bei größeren Pellets störende Kondensation im Gerät für den Rundungsprozess von Mikropellets als vorteilhaft, welche die Mikropelletqualität entscheidend verbesserte. Dazu fanden zwei unterschiedliche Sphäroniser Verwendung.

Freisetzungsuntersuchungen von κ-carrageenanhaltigen Mikropellets mit Spironolacton folgten. Um die ionischen Wechselwirkungen mit dem κ-Carrageenan zu erörtern, wurde das Auflösungsmedium unter anderem mit unterschiedlichen Halogeniden wie beispielsweise Natriumchlorid oder Calciumchlorid versetzt. Die verwendeten Kationen sind bekannt als ‚spezifisch'- und ‚unspezifisch'-bindende Ionen am κ-Carrageenan. Es konnte eine Korrelation des Freisetzungsverhaltens mit der Klassifizierung der Ionen nachgewiesen werden. So führten die ‚unspezifischen' Natrium- oder auch Lithiumionen im Auflösungsmedium zur schnellen Arzneistofffreisetzung, während 'spezifische' oder mehrwertige Kationen wie Calcium- und Kaliumionen die Freisetzung verzögerten. Weitere Freisetzungsuntersuchungen beschäftigten sich mit dem Einfluss unterschiedlicher Arzneistoffe (Spironolacton, Theophyllin monohydrat, Hydrochlorothiazid, Griseofulvin, Itraconazol) auf das Freisetzungsverhalten. Dabei variierte das Verhältnis zwischen Wirkstoff und κ-Carrageenan in den Mikropellets. Ein Zusammenhang zwischen Freisetzungsgeschwindigkeit und Arzneistofflöslichkeit konnte nachgewiesen werden. Mikropellets mit besser wasserlöslichen Wirkstoffen wie Theophyllin monohydrat führten zu schnellen Arzneistofffreisetzungen in allen Medien. Die Freisetzungsgeschwindigkeit blieb von den unterschiedlichen Verhältnissen zwischen Wirkstoff und κ-Carrageenan unberührt. Im Gegensatz dazu standen die Mikropellets mit sehr schwer löslichen bis praktisch unlöslichen Wirkstoffen wie Hydrochlorothiazid oder Spironolacton. Von der Ionenkonzentration abhängig ergaben sich Unterschiede in der Freisetzungsgeschwindigkeit. So ist beispielsweise mit steigender Calciumionenkonzentration die Arzneistofffreisetzung zunehmend verzögert. Es resultierten Matrixfreisetzungen von anomaler (nicht-Fickschen) Diffusion. Zusätzlich beeinflusste das Verhältnis zwischen Arzneistoff und κ-Carrageenan das Freisetzungsverhalten. Diese Korrelation bestand nur bei wässrigen ionischen Lösungen, wie Calciumchlorid, und nicht bei Wasser als Auflösungsmedium. Weitergehende Untersuchungen mit praktisch unlöslichen Arzneistoffen ergaben, dass der Wirkstoff

entscheidend das Freisetzungsverhalten beeinflusste. Beispielsweise führten κ-carrageenanhaltige Mikropellets mit Itraconazol zu keiner relevanten Arzneistofffreisetzung. Anhand eines Modells konnte der Zusammenhang zwischen Freisetzungsverhalten, Arzneistofflöslichkeit sowie der Ioneneinflüsse auf das κ-Carrageenan beschrieben werden.

Mit spironolactonhaltigen Mikropellets wurde der Einfluss von unterschiedlichen Füllstoffen (Tricalciumphosphate, Dicalciumphosphat, Laktosemonohydrat, Calciumlaktat) untersucht. Art und Anteil des Füllstoffes waren ausschlaggebend auf das Freisetzungsverhalten. Die Arzneistofffreisetzung konnte durch das wasserlösliche Laktosemonohydrat in wässrigen ionischen Lösungen verbessert werden. Die Löslichkeit der Füllstoffe wurde mit zunehmendem Anteil an Wirkstoff und daher abnehmendem Anteil an Füllstoff auf die Freisetzungsgeschwindigkeit irrelevant. Die Formulierung mit Calciumlaktat zeigte weder eine Ausrundung der Extrudatstränge noch eine Auswirkung der unterschiedlichen Medien auf die Freisetzung. Dies wurde auf die bereits im Extrusionsprozess stattfindenden ionischen Wechselwirkungen des κ-Carrageenans und den gelösten Calciumionen des Calciumlaktats zurückgeführt. Die geringe Konzentration an freien Calciumionen aus den unlöslichen Calciumphosphatverbindungen war dagegen unbedeutend in der Extrusion.

Aufbauend auf den ionischen Wechselwirkungen der κ-carrageenanhaltigen Mikropellets in der Freisetzung wurden Untersuchungen in biorelevanten Auflösungsmedien durchgeführt, welche auf einen hohen Einfluss der physiologischen Gegebenheiten hindeuten. Der Vergleich zu den biorelevanten Medien betonte die Relevanz der Flüssigkeitswahl bei der Einnahme von κ-carrageenanhaltigen Mikropellets bei sehr schlecht löslichen Arzneistoffen.

Abschließend wurden die Gegenionen in unterschiedlichen κ-Carrageenanprodukten verschiedener Hersteller bestimmt. Das rheologische Verhalten der κ-Carrageenane war nicht allein von den Gegenionen abhängig. Somit konnten Art und Anteile der Gegenionen als Austauschkriterium der κ-Carrageenanprodukte als Pelletierhilfsstoff nivelliert werden.

Insgesamt erwiesen sich die Arzneistofflöslichkeit, die Füllstofflöslichkeit, die Anteile der Bestandteile in der Formulierung und das Verhältnis zwischen Wirkstoff und κ-Carrageenan als ausschlaggebende Faktoren auf die Freisetzungsgeschwindigkeit. Des Weiteren beeinflussten Art und Anteil an gelösten Ionen im Freisetzungsmedium das κ-Carrageenan mehr als seine enthaltenen Gegenionen.

In dieser Arbeit konnte gezeigt werden, dass sich schnell freisetzende Mikropellets mittels Feuchextrusion/ Sphäronisation herstellen lassen. Die Arzneistofffreisetzung ist jedoch stark abhängig von der Formulierung und den Freisetzungsbedingungen. Durch die umfangreiche Analyse der ionischen Wechselwirkungen mit dem κ-Carrageenan ist es gelungen, das Freisetzungsverhalten in Gegenwart von gelösten Ionen zu erörtern, die die Schlussfolgerungen auf Wechselwirkungen mit der Nahrung ermöglichen. Dadurch können Maßnahmen zur Verbesserung der Wirkstoffverfügbarkeit ergriffen werden.

8 Experimental part

8.1 Materials

8.1.1 Carrageenan

The differences in the carrageenans were described in Chap. 1.3.3. Therefore, Tab. 35 contains the different types of κ-carrageenans investigated in this thesis.

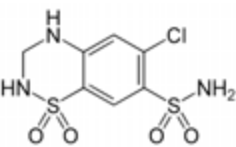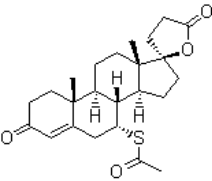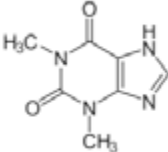**Tab. 35: Overview of the different types of carrageenan**

Trade name	Type	Batch-No.	Manufacturer
Satiagel® CT-27	κ-Carr	20032555	Degussa, Hamburg, Germany
Satiagel® ME-4	κ-Carr	20042823	Degussa, Hamburg, Germany
Genugel® X930-03	κ-Carr	5180004	CPKelco, Lille Skensvec, Denmark
Gelcarin® GP-911 NF	κ-Carr	10802050	FMC, Philadelphia, PA, U.S.A
Gelcarin® GP-911 NF	κ-Carr	20212160	FMC, Philadelphia, PA, U.S.A
Gelcarin® GP-911 NF	κ-Carr	40701120	FMC, Philadelphia, PA, U.S.A
Gelcarin® GP-911 NF	κ-Carr	20719099	FMC, Philadelphia, PA, U.S.A
Gelcarin® GP-812 NF	κ-Carr	10704040	FMC, Philadelphia, PA, U.S.A
Gelcarin® GP-379 NF	ι-Carr	20704040	FMC, Philadelphia, PA, U.S.A
Viscarin® GP-109 NF	λ-Carr	40823000	FMC, Philadelphia, PA, U.S.A

8.1.2 API

The requirements of the specifications are described in Chap. 5.3.1.1.

Experiments were mainly performed with the practically water-insoluble drug spironolactone. Tab. 36 contains the other APIs used for the investigations of the different ratio between API and κ-carrageenan in the formulations. The criterion was the different solubility of the APIs.
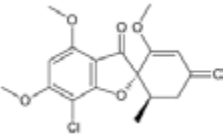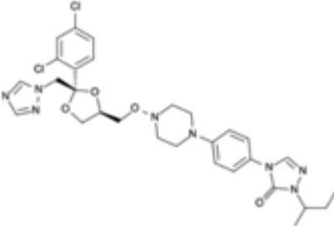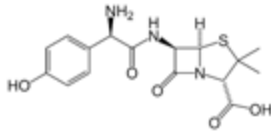
Tab. 36: Overview of the different APIs used for the investigations on the ratio in the formulation

API / Parameter	Hydrochlorothiazide	Spironolactone	Theophylline monohydrate
Chemical structure			
Molecular weight [g·mol^{-1}]	297.7	416.6	198.2
UV wavelength [nm]	271	242	271
Abbreviation	HCT	SpL	ThP
Solubility in water [g·l^{-1}]	0.6	0.028	6
BCS-class	II	II	I
Indication	diuretica	diuretica	bronchodilator
Batch-No.	150709	S0402 + S1119	001M03AX10
Manufacturer	Midas Pharmach., Ingelheim, Germany	Tianjin Jinjin Pharmaceutical, Xiqing District, Tianjin, China	BASF, Ludwigshafen, Germany

Further investigations were performed on practically water-insoluble drugs. Besides the solubility of the APIs, the dissolution behavior of micropellets containing κ-carrageenan was evaluated by the different molecular weights. Tab. 37 shows the API used for further dissolution study.

Tab. 37: Overview of further APIs

Parameter / API	Griseofulvin	Itraconazole	Amoxicillin trihydrate
Chemical structure			
Molecular weight [g·mol^{-1}]	352.8	705.7	365.4
UV wavelength [nm]	294	254	228
Abbreviation	GsF	ICZ	Amoxi
Solubility in water [g·l^{-1}]	0.02	< 0.001	1-10
BCS-class	II	II	III
Indication	antifungal	antifungal	antibiotic
Batch-No.	P060602	F176701	D148710
Manufacturer	Welding GmbH, Hamburg, Germany	Grunenthal GmbH, Aachen, Germany	Grunenthal GmbH, Aachen, Germany

8.1.3 Filler

The main investigations were performed on tricalcium phosphates. Other fillers were used to evaluate the effects of the solubility of the fillers on the dissolution behavior of micropellets containing κ-carrageenan. Lactose monohydrate seemed to be suitable due to the good solubility. Both fillers were described in Chap. 5.2.3. The other calcium phosphate compounds were used to determine a possible difference on the production and the dissolution behavior. Calcium lactate was used to provoke ionic interactions during the extrusion process to analyze the effects of the ions on the production and the following dissolution behavior.

Tab. 38: Overview of the different fillers

	Quality	Solubility [g·l^{-1}]	Batch-No.	Manufacturer
Tricalcium phosphate C53-06	Ph. Eur.	undissolved	A97049A A79483A	cfb, Budenheim, Germany
Tricalcium phosphate C13-03	Food grade	undissolved	A72283A	cfb, Budenheim, Germany
Dicalcium phosphate C92-14	Ph. Eur./USP	undissolved	0036997	cfb, Budenheim, Germany
α-Lactose-monohydrate GL200	Ph. Eur./ USP	200	14058 9452 A4172	Meggle, Wasserburg, Germany
Calcium lactate	Ph.Eur.	(very) soluble	unknown	unknown

8.1.4 Other Substances

Further excipients mainly used in dissolution and analytical methods are listed in Tab. 39.

Tab. 39: Overview of excipients used for dissolution and analytical methods

Substance	Quality	Batch-No.	Manufacturer
Acetone-Chromasolv®	HPLC	8101S	Sigma-Aldrich, Steinheim, Germany
Acetonitrile-Chromanorm®	HPLC	07Z0499	VWR BDH Prolabo, VWR International bvba/sprl, Leuven, Belgium
Ammonium chloride	p.a	9819010011	J.T. Baker, Mallinckrodt Baker B.V., Deventer, Netherlands
Brij® 35P (polyoxyethylene monolauryl ether)		N5003	Uniqema, Everberg, Belgium
Calcium chloride	p.a.	6074A	Riedel-de Haën, Seelze, Germany
Chloroform-LiChroSolv®	HPLC	K37943144742	Merck KGaA, Darmstadt, Germany
Gylceric acid	p.a	07B140509	AnalaR NORMAPUR, VWR International bvba/sprl, Leuven, Belgium
Lipoid E PC S		108036-1/47	Lipoid GmbH, Ludwigshafen, Germany
Lithium chloride	p.a	07G110010	AnalaR NORMAPUR, VWR International bvba/sprl, Leuven, Belgium
Magnesium chloride	p.a	24787572	Carl Roth GmbH, Karlsruhe, Germany
Milfina Milk (long-life, 3.5% fat)		S2.T1.L4 S2.T2. L1 S3.T4.L2	MBP Milchprodukte, Heilbronn, Germany
Potassium chloride	p.a.	A017704901	Across organics, Geel, Belgium
Potassium dihydrogenphosphate	p.a.	4B004110	KMF Laborchemie Handel, Lohmar, Germany
Sodium chloride	p.a	07J020025	AnalaR NORMAPUR, VWR International bvba/sprl, Leuven, Belgium
Sodium edetate-Tritriplex®III	p.a.	OC320344	Merck KGaA, Darmstadt, Germany
Sodium hydroxide	p.a	0511903007	J.T. Baker, Mallinckrodt Baker B.V., Deventer, Netherlands
Sodium taurocholate		2007100274	Prodotti Chimici e Alimentari, Italy
Zinc sulfate-Titrisol®	p.a.	OC321204	Merck KGaA, Darmstadt, Germany

8.2 Methods

8.2.1 Pellet production

8.2.1.1 Blending of raw materials

Before weighing the compounds, the adsorbed moisture content of the raw materials was determined (Chap. 8.2.2.1). In consideration of the moisture content the amount of each compound was calculated.

After weighing the raw materials, the mixture was blended for 15 min at 30 rpm in a laboratory mixer (LM20 or LM40, Bohle, Ennigerloh, Germany).

8.2.1.2 Extrusion

A 'co-rotating' twin-screw extruder (Micro 27GL/28D, Leistritz, Nuremberg, Germany) with an axial screen was used. If nothing else is mentioned, the screen plate had 92 dies and the orifices had a diameter of 0.5 mm and a length of 2.5 mm. The configuration of the screw elements was used according to the manufacturer [Leistritz, 1999]. The extrusion took place at a constant screw speed of 125 rpm. The cylinder temperatures were adjusted to 25 °C. A powder feed rate of 33 g·min^{-1} and an adapted liquid feed rate supplied by a membrane pump (Cerex EP-31, Bran and Luebbe, Norderstedt, Germany) with a flow through metering device were used (Corimass MFC-081/K, Krohne, Duisburg, Germany). Deionized water was used as extrusion liquid.

With the use of a computer, the screw speed, the powder and liquid feed rate, the temperature and the pressure of the die plate and the power consumption were recorded dependent on the process time.

At the beginning, the extrusion was performed with higher moisture content of the extrudates to guarantee a homogeneous wetting of the apparatus. The extrudates for the spheronization were collected in a plastic bowl, when the pressure on the die plate and the power consumption were constant. The extrusion period of each batch depended on the amount of extrusion liquid. For each batch, extrudates in triplicate of about 2 g were separately collected to determine the moisture content (Chap. 8.2.2.1).

8.2.1.3 Spheronization

If nothing else was described, the Schlueter spheronizer was used (RM 300, Schlueter, Neustadt/ Ruebenberge, Germany) with following settings: Batches 400 g of extrudates were dumped into the immobile spheronizer before the process operated for 6 min at 1200 rpm (18.85 m·s^{-1}). The temperature of the spheronizer wall and the inlet air pressure were not adjusted. The friction plate had a diameter of 300 mm. The surface area of the friction plate was cross-hatched. Right after spheronization, the rounded pellets were transferred to the fluid bed apparatus for drying. The friction plate and the spheronizer wall were cleaned after each batch to guarantee the same spheronizer conditions.

8.2.1.4 Drying

The drying step was carried out in a fluid bed apparatus (GPCG 1.1, Glatt, Dresden, Germany) for 2x8 min with an inlet air temperature of 60 °C. The air flow rate was adjusted to the moisture content of the pellets.

8.2.2 Determination of evaluation parameter

8.2.2.1 Moisture content

The moisture content is a parameter to evaluate the process, in which changes during extrusion characterize a bad reproducibility. Hence, a broad pellet size distribution results. The moisture content is defined as the ratio of the mass of water by weight (m_{lqd}) and the mass of the dried material by weight (m_s) (Eq. 12):

$$mc = \frac{m_{lqd}}{m_s} * 100\% = \frac{(m_{undried} - m_s)}{m_s} \qquad \text{Eq. (12)}$$

For determination of the moisture content in the extrudates three samples of extrudates were collected for each batch during the extrusion process and were dried in a vacuum oven (Heraeus VT 6060 M, Kendro, Hanau, Germany) at 60 °C for 336 h. In addition the moisture content of the raw materials was evaluated under the same conditions. The moisture content was calculated based on the dry mass.

8.2.2.2 Yield

Each batch was sieved in order to remove fines and agglomerates (Retsch, Haan, Germany). The sieving was performed with a vibrio (AS200 Control, Haan, Germany) for 3 min at amplitudes of 1.30. The fraction of pellets with diameters between 200 µm and 710 µm was defined as yield. Using a rotary cone sample divider, suitable samples from the yield fraction were obtained (Retschmuehle PT, Retsch, Haan, Germany).

8.2.2.3 Pellet shape, size and distribution

For image analysis, a system was used consisting of a stereo microscope (Leica MZ 75, Cambridge, UK), a ringlight with cold light source (Leica KL 1500, Cambridge, UK), a digital camera (Leica CS 300 F, Cambridge, UK) and image analyzing software (Qwin, Leica, Cambridge, UK). At least 500 pellets from each batch of the yield fraction were analyzed at a suitable magnification (1 pixel = 8.75 µm) and translated into binary images. Contacting pellets were isolated from the data processing using a software algorithm or deleted manually if the automatic function of separation failed. For each pellet, 64 Feret diameters and the projected area were determined. The pellet size and shape were characterized by equivalent diameter and aspect ratio, respectively.

Shape

The aspect ratio is used to describe the micropellet shape. It is defined as the ratio between the maximum (d_{max}) and the Feret-diameter perpendicular to it ($d_{90°}$) (Eq. 13):

$$ar = \frac{d_{max}}{d_{90°}}$$

Eq. (13)

Size and size distribution

The micropellet size is described by the equivalent diameter (d_{eq}), which is calculated on the basis of a projected micropellet surface (A) [Voigt, 2006a] (Eq. 14):

$$d_{eq} = \sqrt{\frac{4A}{\pi}}$$

Eq. (14)

To characterize the similarity of the micropellet size distribution, Kleinebudde [1997] normalized every pellet diameter (d) to the median (d_{50}) of each distribution. The result is a dimensionless diameter (d_d) (Eq. 15):

$$d_d = \frac{d_{eq}}{d_{eq50}}$$

Eq. (15)

where d_d is the dimensionless diameter, d_{eq} the equivalent diameter and d_{eq50} the median of all equivalent diameters [Thommes and Kleinebudde, 2006a].

8.2.2.4 Mechanical stability

The mechanical characteristics of micropellets were investigated using a texture analyzer (TA.XT2i, Stable micro systems, Godalming, UK). The fracture force (F) of 50 pellets per batch at a loading rate of 0.01 mm·s^{-1} was determined as the first peak of a plotted force displacement diagram [Antonyuk et al., 2005]. In addition, the diameter (d) of each micropellet in crushing direction was also determined. To calculate the tensile strength of the micropellets (σ), the introduced correction factor by Shipway and Hutchings [1993] was considered (Eq. 16):

$$\sigma = \frac{1.6F}{\pi * d^2}$$

Eq. (16)

8.2.2.5 Statistical evaluation parameter of the DOE

To verify the reliability of the regression model after pruning, regression analyses are summarized in four parameters: The coefficient of determination (R^2) is a parameter indicating the fraction of variation in the response variable explained by the model whereby 1

indicates a perfect model. Adjusted R^2 (R_{adj}^2) can be used instead of R^2 to adjust for the degrees of freedom (Eq. 17):

$$R_{adj}^2 = 1 - \frac{n-1}{n-p} * \left(1 - R^2\right)$$

Eq. (17)

where n is the sample size, p is the number of parameters in the model, and R^2 is the coefficient of determination.

The goodness of prediction (Q^2) is another parameter to estimate the fraction of variation of the response that can be predicted by the model (Eq. 18):

$$Q^2 = 1 - \frac{\text{PRESS}}{\text{SS}}$$

Eq. (18)

where PRESS is the prediction residual sum of squares and SS is the total sum of squares of Y corrected for the mean.

In general, with $Q^2 > 0.5$ a model should be regarded as good, and with $Q^2 > 0.9$ as excellent. Therefore, values close to 1 for both R_{adj}^2 and Q^2 and not separated by more than 0.2 - 0.3 indicate a very good model with excellent predictive power whereby R_{adj}^2 is an overestimated and Q^2 an underestimated measure of the goodness of fit of the model [Eriksson et al., 2000].

The validity of the model is another diagnostic tool to estimate if the model shows good fit to the data or if the model has a lack of fit meaning a bigger model error as the pure error (reproducibility). A lack of fit is indicated if the value is below 0.25 and the p-value in the analysis of variance (ANOVA) shows values below 0.05, respectively. ANOVA is estimating different types of variability in the response data and comparing these estimates with each other by means of F-tests.

Finally, the reproducibility value is the variation of the response under the same conditions (pure error), often at the center points, compared to the total variation of the responses (Eq. 19):

$$Reproducibility = 1 - \frac{Variance_{PE}}{Variance_{SS}}$$

Eq. (19)

where Variance$_{PE}$ is the mean squares of pure error and Variance$_{SS}$ is the mean squares of total SS corrected.

8.2.2.6 Drug release

The rotating paddle method was used for the dissolution tests (USP apparatus 2) [USP 31 NF26, 2008]. The rotation speed of the paddles was 150 rpm (Sotax AT 6, Sotax AG, Basel, Switzerland). Drug release was conducted in 900 ml of dissolution media at 37 °C ± 0.5 °C under sink conditions. The maximum UV wavelength of each drug in each medium was selected for the spectrophotometrical detection (Tab. 36, Tab. 37). A continuous flow-through system attached to the UV/VIS spectrophotometer was used (Lambda-2, Perkin-Elmer, Ueberlingen, Germany). The dissolution fluid was continuously transported through a filter with a peristaltic pump at maximum pump rate (IPC-8 V1.34, Ismatec, Glattbrugg-Zurich, Switzerland) with modified PVC tubings (Tygon R 3606, Norton, USA). Measurements were performed in triplicate.

To determine the maximum of the wavelength, 10 mg of API was dissolved in 1 l of dissolution medium. The absorption spectra were detected and the wavelength of the peak maximum was used as detection wavelength for the dissolution investigations. To determine the drug release and the concentration of API, each dissolution medium was calibrated by UV-absorption with 12 concentrations, (A = 0.1-0.7). The saturated concentration of spironolactone was measured by weighing 100 mg of API in 100.0 ml dissolution media. The suspension was stirred for 5 days, filtered and diluted before determining the UV-absorption.

Due to the different ratios between API and κ-carrageenan, the weighted sample was calculated on the percentage of the API in the formulations. Therefore, with respect to the sink conditions the weighing varied from ~75 mg to ~10 mg per vessel. All prolonged drug releases were at least detected up to 6 h. To numerically compare the dissolution behavior, the mean dissolution time (MDT) was calculated by the trapezoid method using concentration (c) and time (t) from the dissolution profile [Langguth et al., 2004] (Eq. 20):

$$MDT = \frac{\sum_{i=0}^{\infty}\left[(c_{i+1} - c_i)\left(\frac{t_i + t_{i+1}}{2}\right)\right]}{c_\infty} \qquad \text{Eq. (20)}$$

Further, the pH of each dissolution media was measured to exclude any effects on the dissolution behavior of the micropellets containing different types of tricalcium phosphates (Chap. 8.2.3.12).

8.2.2.7 High performance liquid chromatography

The evaluation of the amount of drug (spironolactone or griseofulvin) per unit time in either FeSSIF or milk medium was conducted by the HPLC analysis method (Hitachi La Chrom Elite, Hitachi Ltd., Tampa, USA). The single units of the HPLC system are given in Tab. 40.

Tab. 40: Equipment of the HPLC (Hitachi La Chrom Elite)

UV-detector	Column oven	Autosampler	Column-thermostat	Pump
L-2400	L-2300	L-2200	L-2130HTA	L-2300 ND

For chromatographic separation, the samples were injected by an autosampler. Different columns were used (Tab. 41). The column oven was tempered at 35 °C independent of the type of column. The mobile phase varied dependent o the type of API and the used column. The compounds of the different mixtures are listed in Chap. 8.2.2.8. The mobile phase was pumped isocratic through the column.

Tab. 41: Columns for the different APIs dependent on the media

API	Medium	Column
SpL	FeSSIF Milk	Nucleodur C18 Gravity, 250x4 mm, 5 µm, Macherey and Nagel, Dueren, Germany Nucleosil 100 C18, 250x4 mm, 5 µm, Macherey and Nagel, Dueren, Germany
GsF	FeSSIF Milk	Nucleosil 100-5 C18 HD, 250x4 mm, Macherey and Nagel, Dueren, Germany

The data were evaluated with the EZChrom Elite software (Chromtech, Idstein, Germany). To this, three different standard solutions of the API were used to calibrate. The standard solutions were diluted either 1:10 or 1:100. The concentration of the API was calculated by the area of the peak.

8.2.2.8 Preparation of biorelevant media

The evaluation of the drug release per unit time in biorelevant media needed sample pretreatment to be detected in the HPLC (Chap. 8.2.2.7). In general, the sample preparation differed dependent on the API, the type of biorelevant media and the HPLC analysis method. Hence numerous procedures of precipitation and extraction were found in the literature. The sample preparations of the APIs were adjusted to the different media.

The dissolution was conducted under the same conditions (Chap. 8.2.2.5).

FeSSIF

The FeSSIF medium was composed from Tab. 42 according to Marques [2004].

The blank FeSSIF was prepared as followed: Sodium hydroxide, glacial acetic acid and sodium chloride were dissolved in distilled water. The pH was adjusted to exactly 5.0 using 1 M NaOH or 1 M HCl solution.

The FeSSIF medium was prepared by dissolving sodium taurocholate in 250 ml of blank FeSSIF. A solution of 29.54 ml was added, which contained 100 mg·ml^{-1} lecithin in methylene chloride. An emulsion was formed. The methylene chloride was eliminated under vacuum at 40 °C using a rotating evaporator at 30 rpm (RV 05, Janke & Kunkel KG, Staufen im Breisgau, Germany). The medium turned clear to slightly hazy, with no perceptible smell of methylene chloride. A good indication of the evaporation was the bubbling of the solution.

The medium was cooled to room temperature before adjusting the volume to 1 l with the blank FeSSIF. For the sake of better comparability the dissolution volume was conducted in 900 ml.

Tab. 42: Composition of the FeSSIF medium

Compounds	Amount
Sodium taurocholate	15 mM
Lecithin	3.75 mM
Sodium Hydroxide (pellets)	4.04 g
Glacial Acetic Acid	8.65 g
Sodium chloride	11.874 g
Distilled water qs.	1000 ml

Medium has a pH of 5.00 and an osmolality of about 670 mOsmol·kg^{-1}.

Tab. 43 lists the parameters of the HPLC for the different APIs. The sample preparations of both APIs (spironolactone, griseofulvin) were the same. Samples of 5 ml were withdrawn at appropriate times. The samples were centrifuged for 15 min at 4200 rpm (Heraeus Multifuge 1L, Thermo electron corporation, Osterode, Germany). Each sample was filtered through 0.45 µm filter (25 mm Syringe filter, Polypropylene membrane, VWR-International, USA) and 1 ml was transferred into the HPLC vial. Each sample was analyzed two to three times. Fig. 53 shows a chromatogram of the drug release of the micropellets based on 10 % griseofulvin.
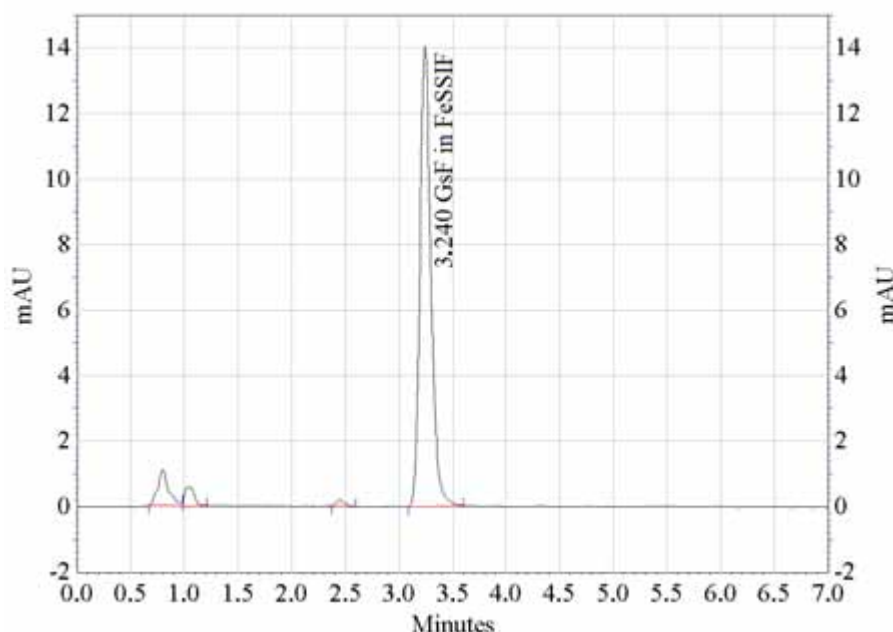
Fig. 53: Chromatogram of the drug release of the micropellets comprising 10 % GsF in FeSSIF medium after 300 min

Tab. 43: Parameters of the HPLC analysis of the different API samples in FeSSIF medium

Parameter / API	Griseofulvin	Spironolactone
Mobile phase (ratio)	0.05 M Sodium dihydrogen phosphate Acetonitrile (30:70)	Distilled water Acetonitrile (50:50)
Injection volume [µl]	5	10
Flow rate [ml·min^{-1}]	1.000	1.250
UV-detection wavelength [nm]	292	242

Milk

To confirm that the API was completely regained after the sample preparation, spiking was performed in the milk medium using spironolactone. To detect reproducible peak areas of the API, reasonable amount of spironolactone was suspended in 200 ml distilled water. The suspension was stirred for 3 h at 37 °C, before the stirring was continued under room conditions for 5 days. The suspension was filtered through 0.45 µm filter (25 mm Syringe filter, Polypropylene membrane, VWR-International, West Chester, PA, USA). 50 g of the solution was weighed in the dissolution vessel and filled with either distilled water or milk to 900 ml. The aqueous medium was used as reference. The media were stirred for 5 h under dissolution conditions (Chap. 8.2.2.5). The sample of milk was prepared as described below. The reference volume of 4 ml was withdrawn and filtered through 0.45 µm filter (25 mm Syringe filter, Polypropylene membrane, VWR-International, West Chester, PA, USA). The filtrate of 1 ml was transferred into the HPLC vial. Each sample was analyzed five times. No substantial differences in the peak areas were obtained between the aqueous sample and the prepared milk sample. Hence, the method of sample preparation described below was used for the evaluation of drug release.

The samples preparation of spironolactone and griseofulvin differed in milk. Tab. 44 contains the main parameters of the HPLC for the different APIs.

Tab. 44: Parameters of the HPLC analysis of the different API samples in milk

Parameter / API	Griseofulvin	Spironolactone
Extraction medium (ratio)	Chloroform (60) Acetone (40)	Chloroform
Mobile Phase (ratio)	0.05 M Sodium dihydrogen phosphate Acetonitrile (30:70)	Distilled water Acetonitrile (30:70)
Injection volume [µl]	5	2
Flow rate [ml·min^{-1}]	0.500	0.750
UV-detection wavelength [nm]	292	242

Samples of 4 ml containing griseofulvin were withdrawn at appropriate times. The same volume of a solution containing chloroform and acetone was added. The samples were centrifuged for 15 min at 4200 rpm (Heraeus Multifuge 1L, Thermo electron corporation, Osterode, Germany). Each sample was filtered through 0.45 µm filter (25 mm Syringe filter,

Polypropylene membrane, VWR-International, USA) and 1 ml was transferred into the HPLC vial. Each sample was analyzed two to three times. Samples of 4 ml containing spironolactone were withdrawn at appropriate times. The same volume of chloroform was added. The extraction took place for 15 min at 175 rpm on a horizontal shaker (SM 25, Edmund Buehler, Tuebingen, Germany) followed by centrifugation for 15 min at 4200 rpm (Heraeus Multifuge 1L, Thermo electron corporation, Osterode, Germany). The chloroform phase was withdrawn and filtered through 0.45 µm filter (25 mm Syringe filter, Polypropylene membrane, VWR-International, USA). The filtrate of 1 ml was pipetted and transferred into the HPLC vial. The chloroform was removed under vacuum and room conditions using a vacuum oven (Heraeus vacutherm, VT 6025, Kendro Laboratory Products, Hanau, Germany). The residue was dissolved in 1 ml of the mobile phase. Each sample was analyzed two to three times. Fig. 54 shows a chromatogram of the drug release of micropellets based on 10 % spironolactone.
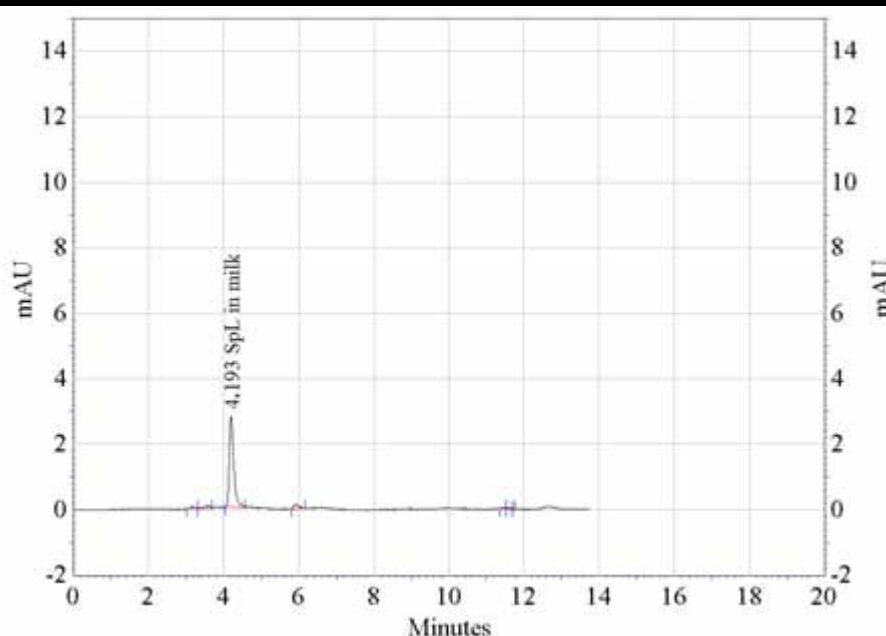

Fig. 54: Chromatogram of drug release of micropellets comprising 10 % SpL in milk after 90 min

8.2.2.9 Similarity of dissolution profiles

The f_2 equation is a logarithmic transformation of the average of the sums of squared vertical distances between the test and reference mean dissolution values [O'Hara et al., 1998].

$$f_2 = 50 \log_{10} \left\{ \left[1 + \frac{1}{n} \sum_{t=1}^{n} w_t (R_t - T_t)^2 \right]^{-0.5} * 100 \right\}$$

Eq. (21)

where n is the number of dissolution time points, R_t and T_t are the cumulative percentage dissolved of the reference and test formulation at the time t, and wt is an optional weight factor. The weight factor was 1.

If nothing else was described, the mathematical comparison was calculated to the following basis: Due to the sensitivity to the number of dissolution time points, for comparison of the prolonged drug releases the maximum time was 360 min (120 time points), while for fast dissolving media the time was 20 min (20 time points). In addition, for the similarity evaluations in deionized water the normalized drug release values at the time t were used to describe R_t and T_t. In the case of 0.1 M gel-promoting ions, the dissolution profile of 0.1 M calcium chloride solution was used as reference. For the comparison of fast dissolving media, deionized water was used as reference. When different ratios in the formulation were compared, the standard formulation was used as reference.

Although the FDA guidance requires at least 12 units of a product to be used [FDA, 1997a], the f_2-values were calculated using only three units of a product.

8.2.3   Analytical methods

8.2.3.1   Scanning electron microscopy

Samples for the scanning electron microscopy were released in different media under the dissolution conditions (Chap. 8.2.2.5) and dried at 60 °C in a drying oven (ET 6130, Heraeus instruments, Kendro Laboratory Products, Hanau, Germany).

Samples were sputtered-coated with gold for 180 s under argon atmosphere using an Agar Manual Sputter Coater (Agar scientific, Stansted, UK). Coated samples were mounted onto specimen stubs with double-sided carbon tape and scanned under high vacuum with a LEO VP 1430 (Carl Zeiss, Jena, Germany). The measurements were operated with a voltage of 10 kV to 20 kV. The morphologies of the micropellets and the micropellets exposed to dissolution were observed. Different magnifications were conducted ranging from 100-fold to 1000-fold.

8.2.3.2   Differential scanning calorimetry

To investigate the ionic interactions between dissolved calcium ions and κ-carrageenan the differential scanning calorimetry (DSC) analysis was performed. The melting and setting of the κ-carrageenan gel was related to the conformational transitions of carrageenan molecules.

Measurements were carried out using a DSC 821e (Mettler-Toledo, Gießen, Germany). Samples of approximately 3 mg were sealed in aluminum pans of 40 µl.

The temperature ranged between 0 °C and 95 °C. The scanning speed was 10 °C·min^{-1}. The samples were cycled twice to remove the effects of moisture and thermal history. An empty pan served as reference. κ-Carrageenan of 2 g was dispersed in 100.0 ml distilled water and left for 24 h under room condition. The first measurement was performed. The so produced gel was transferred into a closed vessel and tempered for 60 min at 85 °C in a drying oven (ET 6130, Heraeus instruments, Kendro Laboratory Products, Hanau, Germany). The sample was left for 24 h under room condition before the measurement was performed. In addition a

portion of the gel was transferred into the 0.1 M calcium chloride solution and left for 1 h before being measured. Each sample was measured in triplicate.

8.2.3.3 Karl-Fischer titration

Moisture content of extrudates or micropellets was determined by Karl-Fischer titration using an automatic Karl-Fischer titrator (Mettler DL 18, Mettler-Toledo GmbH, Gießen, Germany). To determine the moisture content of the micropellets for the dissolution following substances were used to perform Karl-Fischer titration (Tab. 45). The medium was mixed to equivalent parts and used under room conditions.

Tab. 45: Substances used in the Karl-Fischer titration

Parameter	Compounds
Working medium	Hydranal-methanol dry, Lot. 6235A, Riedel-de Haën, Seelze, Germany
	Hydranal-formamid dry, Lot. 6025A, Riedel-de Haën, Seelze, Germany
One-component reagent	Hydranal-Composite 5, Lot. 7022D, Riedel-de Haën, Seelze, Germany
Calibration solution	Hydranal-Water Standard 10.0, Lot. 61640, Riedel-de Haën, Seelze, Germany
	(1 g contains 10.05 mg water)

The intact micropellets or the comminuted product were used. Each sample was around 30 mg. Measurements were performed in triplicate.

8.2.3.4 Laser light diffraction

For the determination of the mean particle size of the raw materials, the powder samples were brought into a laser diffraction system (Helos/ KF-Magic, Sympatec GmbH, Clausthal-Zellerfeld, Germany) through a dry dispersion device with a pressure of 2 bar and a feed rate of 80 % (Vibri, RODOS T4.1, Sympatec GmbH, Clausthal-Zellerfeld, Germany). The detection was conducted using the lens R2 with the range between 0.25 µm and 87.8 µm. The analysis program HELOS was used (Sympatec GmbH, Clausthal-Zellerfeld, Germany). Measurements were performed in triplicate.

To evaluate the dispersive effect of the extrusion process on the particle size of tricalcium phosphate, the wet dispersion method was used. The 50 ml Helos-Cuvette system (Sympatec GbmH) was filled with the tricalcium phosphate dispersion of 2-propanol, which showed an optical concentration of approximately 5 – 10 %. The dispersion was stirred at 1000 rpm for 1 min to assure homogeneous dispersion of the particles. Measurements were performed after 60 min.

8.2.3.5 Imaging of wet micropellets

The same system of image analysis was used to examine the outer appearance of the micropellets in the wetted stage right after the dissolution in 0.1 M calcium chloride solution (Chap. 8.2.2.3). The highest magnification was used (1 pixel = 3.50 µm). After 16 h of dissolution, the micropellets were collected and pipetted on a plane surface. To exclude the drying of the surface area, the micropellets were kept in solution.

8.2.3.6 Inductively coupled plasma optical emission spectrometry

Dissolved ions affected the dissolution behavior and the pelletization ability of κ-carrageenan. To determine the effects of the counter-ions of carrageenan itself, the inductively coupled plasma optical emission spectrometer (ICP-OES) was used to trace the elements (Optima 3300XL, Perkin-Elmer, Norwalk, CT, U.S.A.). ICP-OES is related to the Jablonski term scheme. It is only applicable on cations rather than anions. The main advantage is the multi-element determination. The samples of at least 100 mg were dissolved by several digestion methods such as microwave, high-pressure and acid digestion.

The liquid sample is introduced into argon plasma through a peristaltic pump to a nebulizer system. To ionize the sample, the argon plasma has a temperature of approximately 9000 °C. The elements take up energy from the inductively coupled plasma and the electrons of the elements are excited. By falling back into the original state, the electrons release energy. The spectra emitted are detected and evaluated into the individual wavelengths of the elements by a spectrometer. The metering range was from 130 nm to 800 nm. Calibration was performed with standard solutions. Each raw material was digested twice. The liquid samples were measured three to five times. The means of each counter-ion are given in Tab. 32.

8.2.3.7 Complexometric titration

Due to the fact that only free calcium ions can interact with the κ-carrageenan in the extrusion process, the concentration of dissolved calcium of the suspensions was determined. Therefore the assay of the calcium phosphate in the European Pharmacopoeia [Ph.Eur. 6, 2008] was modified.

Besides deionized water, two solutions with different pH-values (pH = 3; 5) were used. The pH was adjusted with 1 M HCl in deionized water (pH-Meter 766 Calimatic + SE100, pH/Pt 1000 electrode, Knick, Berlin, Germany). Calcium phosphate of 300 mg was suspended in 100 ml of solution. The suspension was stirred at 500 rpm and heated for 5 min at 60 °C. Further stirring was performed for 24 h under room conditions. The supernatant was filtered (Pall, Life Sciences Supor® 800; 0.8 µm, Lot. PE-00563463JG, Pall Corporation, Michigan, U.S.A.) and 25.0 ml was used for complexometric titration. 5.0 ml of 0.1 M sodium edetate was added and diluted with deionized water to 100 ml. The pH was adjusted to about 10 using a concentrated ammonia R solution. 10 ml of ammonium chloride buffer solution pH 10.0 R and a few milligrams of mordant black 11 triturate R were added. The solution was stirred and the excess sodium edentate was titrated with 0.1 M zinc sulfate solution until the color changed from blue to violet. 1 ml of 0.1 M sodium edentate solution is equivalent to 4.008 mg calcium. The measurements were performed in triplicate.

8.2.3.8 Rheological analysis

The rheological analysis was performed by rotation viscosimeter using the couette method (Haake, CV20, Rotovisco RV20, Rotocontroller RC20, Thermo Haake K10, Karlsruhe, Germany). The preset shear stress was 300 s^{-1}.

The time required to reach the shear stress was set to 1 min.

Different types of κ-carrageenans were used in 0.2 % (w/v) solutions. The samples were heated for 30 min at 60 °C. This assured that the polymer chains were freely suspended or at least in the loose coil form of the molecules when being transferred to the beaker. Therefore the arrangement of the κ-carrageenan molecules was less disturbed. The external cell was cooled to 25 °C supporting the gelling of the κ-carrageenan solution. The measurements were performed in triplicate.

To evaluate the sole ionic interactions of the κ-carrageenan in the micropellets on the dissolution, the same type of κ-carrageenan was used. The hydrocolloid solutions were mingled with different types of dissolution media. The samples contained 0.2 % (w/v) κ-carrageenan in different 0.1 M gel-promoting ions. The rheological behavior was compared to 0.2 % (w/v) κ-carrageenan solution in deionized water. The triplicate measurements were performed under the same conditions described above.

8.2.3.9 Ring shear cell tester

The flowability of the different tricalcium phosphates were measured using a computer-controlled ring shear cell tester (RST-01.pc, RST-CONTROL 95, Schulze Schuettgutmesstechnik, Wolfenbuettel, Germany).

The device consists of a bottom ring with a waffled structure base and a lid with baffles. The sample was placed into the bottom ring and presheared with a normal load of 5 kPa until steady state conditions like constant bulk density was reached. Therefore, the working conditions of each sample were the same. Shearing proceeded at four different normal loads beginning with 1 kPa and ending with 4 kPa. The first normal load at 1 kPa was repeated at the end of a measurement cycle to assure that the samples were unaffected by the measurement.

A yield locus is obtained by means of Mohr' circles when the normal loads and determined shear stresses are plotted in σ, τ-diagram. The consolidation stress and unconfined yield strength values are determined.

The flowability of a bulk material is characterized by its unconfined yield strength (σ_c) dependent on the consolidation stress (σ_1). The flowability function, ffc, is the ratio of these two values. It is used to quantify flowability (Eq. 22):

$$\text{ffc} = \frac{\sigma_1}{\sigma_c}$$

Eq. (22)

The flowability improves with increasing ffc-values. The ffc-value is mainly dependent on the consolidation stress; therefore resulting consolidation stress values were around 11 kPa for all measurements to enable a quantitative comparison. The measurements were performed in triplicate.

8.2.3.10 Helium pycnometry

The particle density of the tricalcium phosphate was measured by gas pycnometry with helium as test gas (AccuPyc 1330TC Pycnometer, Micromeritics, Norcross, GA, USA). The insert kit of 10 cm^3 was used. Measurements were performed in triplicate.

8.2.3.11 Bulk density

The bulk density of a powder is the ratio of the mass of an untapped powder sample to its volume. It was measured according to the European Pharmacopoeia [Ph.Eur. 6, 2008]. Into a dry, graduated cylinder, the sample of 50 g was gently introduced. The unsettled apparent volume was determined to the nearest graduated unit. The measurements were performed five times.

8.2.3.12 pH measurements

Saturated concentrations of tricalcium phosphate solutions were used. Approximately 300 mg of tricalcium phosphate was dispersed in 100.0 ml deionized water. The suspension was stirred at 500 rpm and heated for 5 min at 60 °C. Further stirring was performed for 4 days under room conditions. The supernatant was filtered (Pall, Life Sciences Supor® 800; 0.8 µm, Lot. PE-00563463JG, Pall Corporation, Michigan, U.S.A.). The pH was determined in triplicate (pH-Meter 766 Calimatic + SE100, pH/Pt 1000 electrode, Knick, Berlin, Germany).

Furthermore, the pH-values of the different ionic dissolution media were determined before and after the drug release to exclude the effect of the pH on the dissolution behavior of the micropellets containing different tricalcium phosphate compounds. The solutions were filtered (Pall, Life Sciences Supor® 800; 0.8 µm, Lot. PE-00563463JG, Pall Corporation, Michigan, U.S.A.) and the temperature was equilibrated to room conditions. The pH was determined in triplicate (pH-Meter 766 Calimatic + SE100, pH/Pt 1000 electrode, Knick, Berlin, Germany).

8.2.3.13 X-ray diffraction

To evaluate the crystalline structures of the different tricalcium phosphates, the Miniflex apparatus (Rigaku, Tokyo, Japan) with CuKα radiation was used. Sample preparations into the aluminum frames were performed by mounting the front of the frames on smooth Teflon® plate. A suitable amount of the sample was filled into the window. To prevent a preferential orientation of the particles, the samples were compressed with a slide.

Diffraction patterns were obtained at a voltage of 20 kV and a current of 10 mA. Scanning was performed in the two-Theta-Scale range from 5° to 70°. The scanning speed was 2 °·min^{-1} at an intensity of 1000 cps.

9 References

Akiyama, Y., Yoshioka, M., Horibe, H., Hirai, S., Kitamori, N. and Toguchi, H., 1993. Novel oral controlled-release microspheres using polyglycerol esters of fatty-acids. *J Control Release*, 26, 1-10.

Amidon, G.L., Lennernas, H., Shah, V.P. and Crison, J.R., 1995. A theoretical basis for a biopharmaceutic drug classification - The correlation of In-Vitro drug product dissolution and In-Vivo bioavailability. *Pharm Res*, 12, 413-420.

Amimi, A., Mouradi, A., Givernaud, T., Chiadmi, N. and Lahaye, M., 2001. Structural analysis of Gigartina pistillata carrageenans (Gigartinaceae, Rhodophyta). *Carbohyd Res*, 333, 271-279.

Antonyuk, S., Tomas, E., Heinrich, S. and Morl, L., 2005. Breakage behaviour of spherical granulates by compression. *Chem Eng Sci*, 60, 4031-4044.

Baert, L., Fanara, D., Debaets, P. and Remon, J.P., 1991. Instrumentation of a gravity feed extruder and the influence of the composition of binary and ternary mixtures on the extrusion forces. *J Pharm Pharmacol*, 43, 745-749.

Baert, L., Fanara, D., Remon, J.P. and Massart, D., 1992. Correlation of extrusion forces, raw-materials and sphere characteristics. *J Pharm Pharmacol*, 44, 676-678.

Baert, L., Remon, J.P., Elbers, J.A.C. and Vanbommel, E.M.G., 1993a. Comparison between a gravity feed extruder and a twin-screw extruder. *Int J Pharm*, 99, 7-12.

Baert, L., Vermeersch, H., Remon, J.P., Smeyersverbeke, J. and Massart, D.L., 1993b. Study of parameters important in the spheronization process. *Int J Pharm*, 96, 225-229.

Bains, D., Boutell, S.L. and Newton, J.M., 1991. The influence of moisture-content on the preparation of spherical granules of barium-sulfate and microcrystalline cellulose. *Int J Pharm*, 69, 233-237.

Bechgaard, H. and Nielsen, G.H., 1978. Controlled-release multiple-units and single-unit doses - Literature review. *Drug Dev Ind Pharm*, 4, 53-67.

Berchane, N.S., Carson, K.H., Rice-Ficht, A.C. and Andrews, M.J., 2007. Effect of mean diameter and polydispersity of PLG microspheres on drug release: Experiment and theory. *Int J Pharm*, 337, 118-126.

Bornhoft, M., Thommes, M. and Kleinebudde, P., 2005. Preliminary assessment of carrageenan as excipient for extrusion/spheronisation. *Eur J Pharm Biopharm*, 59, 127-131.

Boutell, S., Newton, J.M., Bloor, J.R. and Hayes, G., 2002. The influence of liquid binder on the liquid mobility and preparation of spherical granules by the process of extrusion/spheronization. *Int J Pharm*, 238, 61-76.

Bouwman, A.M., Henstra, M.J., Westerman, D., Chung, J.T., Zhang, Z., Ingram, A., Seville, J.P.K. and Frijlink, H.W., 2005. The effect of the amount of binder liquid on the granulation mechanisms and structure of microcrystalline cellulose granules prepared by high shear granulation. *Int J Pharm*, 290, 129-136.

Breitkreutz, J. and Boos, J., 2007. Paediatric and geriatric drug delivery. *Expert Opin Drug Deliv*, 4, 37-45.

Bubis, W.A., 2000. Carrageenan. FMC Corporation Food Ingredients Division Philadelphia, PA, 1-34.

Bundesministerium für Gesundheit, 2006. Anlage 4. Verordnung über die Zulassung von Zusatzstoffen zu Lebensmitteln zu technologischen Zwecken (ZZulV).

Carrigan, P.J., Brinker, D.R., Cavanaugh, J.H., Lamm, J.E. and Cloyd, J.C., 1990. Absorption characteristics of a new valproate formulation - Divalproex sodium-coated particles in capsules (Depakote Sprinkle*). J Clin Pharmacol*, 30, 743-747.

cfb Budenheim, 2008. Technical data of different raw materials. Budenheim, Germany.

Chapman, S.R., Rowe, R.C. and Newton, J.M., 1988. Characterization of the sphericity of particles by the one plane critical stability. *J Pharm Pharmacol*, 40, 503-505.

Charoenthai, N., Kleinebudde, P. and Puttipipatkhachorn, S., 2007. Use of chitosan-alginate as alternative pelletization aid to microcrystal line cellulose in extrusion/spheronization. *J Pharm Sci*, 96, 2469-2484

CIAA, 2007. GDA: Nutrition values. Confederation of the Food and Drink Industries in the EU, Brussels, Belgium.

Collins, K.D., 1997. Charge density-dependent strength of hydration and biological structure. *Biophys J*, 72, 65-76.

Conine, J.W. and Hadley, H.R., 1970. Preparation of small solid pharmaceutical spheres. *Drug Cosmet Ind*, 106, 38-41.

DAB-10 Kommentar, 1994. Calciumlactat. Wissenschaftliche Verlagsgesellschaft mbH Stuttgart, Bd. 2, 432-434.

Davis, S.S., Stockwell, A.F., Taylor, M.J., Hardy, J.G., Whalley, D.R., Wilson, C.G., Bechgaard, H. and Christensen, F.N., 1986. The effect of density on the gastric-emptying of single-unit and multiple-unit dosage forms. *Pharm Res*, 3, 208-213.

Dawes, C.J., Stanley, N.F. and Stancioff, D.J., 1977. Seasonal and reproductive aspects of plant chemistry, and iota-carrageenan from Floridian-Eucheuma (Rhodophyta, Gigartinales). *Bot Mar*, 20, 137-147.

Dressman, J.B. and Reppas, C., 2000. In vitro-in vivo correlations for lipophilic, poorly water-soluble drugs. *Eur J Pharm Sci*, 11, 73-80.

Dupont, G., Flament, M.P., Leterme, P., Farah, N. and Gayot, A., 2002. Developing a study method for producing 400 mu m spheroids. *Int J Pharm*, 247, 159-165.

Eldem, T., Speiser, P. and Hincal, A., 1991. Optimization of spray-dried and spray-congealed lipid micropellets and characterization of their surface-morphology by scanning electron-microscopy. *Pharm Res*, 8, 47-54.

Eriksson, L., Johansson, E., Kettaneh-Wold, N., Wikström, C. and Wold, S., 2000. Design of Experiments - Principle and applications. Umetrics Academy.

Erkoboni, D.F., 2003. Extrusion/spheronization, ed. Ghebre-Sellassie, I. and Marin, C., *Pharmaceutical extrusion technology*. Marcel Dekker New York, 133, 277-322.

FDA, 1997a. Guidance for Industry: Dissolution testing of immediate release solid oral dosage forms. Rockville, MD, USA.

FDA, 1997b. Guidance for industry: Modified release solid oral dosage forms: Scale-up and post-approval changes (SUPAC-MR): Chemistry, manufacturing and controls, In Vitro dissoltuion testing, and In Vivo bioequivalence documentation. Rockville, MD, USA.

Fiedler, 1996. Lexikon der Hilfsstoffe für Pharmazie und Kosmetik. EVC-Editio-Cantor-Verlag Aulendorf, 312-314.

Fielden, K.E., Newton, J.M. and Rowe, R.C., 1992. The influence of lactose particle-size on spheronization of extrudate processed by a ram extruder. *Int J Pharm*, 81, 205-224.

FMC, 1993. Product information brochure: Marine colloids: Carrageenan - General technology. Corporation Food Ingredients Division, Philadelphia, PA, USA, 1-8.

Galia, E., Nicolaides, E., Horter, D., Lobenberg, R., Reppas, C. and Dressman, J.B., 1998. Evaluation of various dissolution media for predicting in vivo performance of class I and II drugs. *Pharm Res*, 15, 698-705.

Garcia, J. and Ghaly, E.S., 2001. Evaluation of bioadhesive glipizide spheres and compacts from spheres prepared by extruder/marumerizer technique. *Pharm Dev Technol*, 6, 407-417.

Gazzaniga, A., Sangalli, M.E., Bruni, G., Zema, L., Vecchio, C. and Giordano, F., 1998. The use of beta-cyclodextrin as a pelletization agent in the extrusion/spheronization process. *Drug Dev Ind Pharm*, 24, 869-873.

Gehm, L., 2004. Seminar: Grundlagen der Rheologie. Behr Labor Technik, ProRheo.

Ghebre-Sellassie, I., 1989a. Pellets - A general overview, ed. Ghebre-Sellassie, I., *Pharmaceutical pelletization technology*. Marcel Dekker New York, 1-14.

Ghebre-Sellassie, I., 1989b. Mechanism of pellet formation and growth, ed. Ghebre-Sellassie, I., *Pharmaceutical pelletization technology*. Marcel Dekker New York, 123-144.

Giunchedi, P. and Conte, U., 1995. Spray-drying as a preparation method of microparticulate drug-delivery systems - An overview. *STP Pharma Sci*, 5, 276-290.

Goodhart, F.W. and Jan, S., 1989. Dry powder layering, ed. Ghebre-Sellassie, I., *Pharmaceutical pelletization technology*. Marcel Dekker New York, 165-185.

Grasdalen, H. and Smidsrod, O., 1981. Cs-133 NMR in the sol-gel states of aqueous carrageenan - Selective site binding of cesium and potassium-ions in kappa-carrageenan gels. *Macromolecules*, 14, 229-231.

Gupta, V.K., Hariharan, M., Wheatley, T.A. and Price, J.C., 2001. Controlled-release tablets from carrageenans: effect of formulation, storage and dissolution factors. *Eur J Pharm Biopharm*, 51, 241-248.

Hänsel, R., Stricher, O. and Steinegger, E., 1999. Pharmakognosie - Phytopharmazie. Springer Verlag Berlin, Heidelberg, New York, 378-396.

Harrison, P.J., Newton, J.M. and Rowe, R.C., 1985. Flow defects in wet powder mass extrusion. *J Pharm Pharmacol*, 37, 81-83.

Hassan, E.E., Eshra, A.G. and Nada, A.H., 1995. Formulation of prolonged release lipid micropellets by emulsion congealing - Optimization of ketoprofen entrapment and release. *Int J Pharm*, 121, 149-155.

Hellen, L. and Yliruusi, J., 1993. Process variables of instant granulator and spheroniser: 3. Shape and shape distributions of pellets. *Int J Pharm*, 96, 217-223.

Hellen, L. and Yliruusi, J., Kristoffersson,E., 1993a. Process variables of instant granulator and spheroniser: 2. Size and size distributions of pellets. *Int J Pharm*, 96, 205-216.

Hellen, L., Yliruusi, J., Merkku, P. and Kristoffersson, E., 1993b. Process variables of instant granulator and spheroniser: 1. Physical-properties of granules, extrudate and pellets. *Int J Pharm*, 96, 197-204.

Hennink, W.E. and van Nostrum, C.F., 2002. Novel crosslinking methods to design hydrogels. *Adv Drug Deliver Rev*, 54, 13-36.

Hicks, D.C. and Freese, H.L., 1989. Extrusion and spheronizing equipment, ed. Ghebre-Sellassie, I., *Pharmaceutical pelletization technology*. Marcel Dekker New York, 71-100.

Higuchi, T., 1961. Rate of release of medicaments from ointment bases containing drugs in suspension. *J Pharm Sci,* 50, 874-875.

Higuchi, T., 1963. Mechanism of sustained-Action medication - Theoretical analysis of rate of release of solid drugs dispersed in solid matrices. *J Pharm Sci*, 52, 1145-1149.

Hoffman, A.S., 2002. Hydrogels for biomedical applications. *Adv Drug Deliver Rev*, 54, 3-12.

Hossain, K.S., Miyanaga, K., Maeda, H. and Nemoto, N., 2001. Sol-gel transition behavior of pure i-carrageenan in both salt-free and added salt states. *Biomacromolecules*, 2, 442-449.

Hugerth, A.M., 2001. Micropolarity and microviscosity of amitriptyline and dextran sulfate/carrageenan-amitriptyline systems: The nature of polyelectrolyte-drug complexes. *J Pharm Sci*, 90, 1665-1677.

Jantratid, E., Janssen, N., Reppas, C. and Dressman, J.B., 2008. Dissolution media simulating conditions in the proximal human gastrointestinal tract: An update. *Pharm Res*, 25, 1663-1676.

Johnson&Johnson, 2004. Technical data of itraconazole. Beerse, Belgium.

Jones, D.M., 1989. Solution and suspension layering, ed. Ghebre-Sellassie, I., *Pharmaceutical pelletization technology*. Marcel Dekker New York, 145-164.

Kanbe, H., Hayashi, T., Onuki, Y. and Sonobe, T., 2007. Manufacture of fine spherical granules by an extrusion/spheronization method. *Int J Pharm*, 337, 56-62.

Kearns, G.L., Abdel-Rahman, S.M., Alander, S.W., Blowey, D.L., Leeder, J.S. and Kauffman, R.E., 2003. Developmental pharmacology - Drug disposition, action, and therapy in infants and children. *New Engl J Med*, 349, 1157-1167.

Kim, C.K., Kim, M.J. and Oh, K.H., 1994. Preparation and evaluation of sustained-release microspheres of terbutaline sulfate. *Int J Pharm*, 106, 213-219.

Kjellman, N.I.M., Croner, S., Leijon, I., Friberg, K. and Thuresson, S.O., 1988. Theophylline pharmacokinetics in children, comparing sustained-release spheres (Theo-Dur Sprinkle) with elixir. *Eur J Pediatr*, 148, 278-280.

Klein, S., Butler, J., Hempenstall, J.M., Reppas, C. and Dressman, J.B., 2004. Media to simulate the postprandial stomach I. Matching the physicochemical characteristics of standard breakfasts. *J Pharm Pharmacol*, 56, 605-610.

Kleinebudde, P., 1994. Shrinking and swelling properties of pellets containing microcrystalline cellulose and low substituted hydroxypropylcellulose: 1. Shrinking properties. *Int J Pharm*, 109, 209-219.

Kleinebudde, P., 1995. Use of a power-consumption-controlled extruder in the development of pellet formulations. *J Pharm Sci*, 84, 1259-1264.

Kleinebudde, P., 1997. Pharmazeutische Pellets durch Extrudieren/ Sphäronisieren. *Habilitation Christian-Albrechts University in Kiel, Germany*.

Kleinebudde, P., Solvberg, A.J. and Lindner, H., 1994. The power-consumption-controlled extruder - A tool for pellet production. *J Pharm Pharmacol*, 46, 542-546.

Knop, K., 1991. Pellets, ed. Nürnberg, E. and Surmann, P., *Hagers Handbuch der pharmazeutischen Praxis*. Springer Verlag Berlin, 2, 827-832.

Korsmeyer, R.W. and Peppas, N.A., 1981. Effect of the morphology of hydrophilic polymeric matrices on the diffusion and release of water-soluble drugs. *J Membrane Sci*, 9, 211-227.

Korsmeyer, R.W., Gurny, R., Doelker, E., Buri, P. and Peppas, N.A., 1983. Mechanisms of solute release from porous hydrophilic polymers. *Int J Pharm*, 15, 25-35.

Krause, J. and Breitkreutz, J., 2008. Improving drug delivery in paediatric medicine. *PharmMed*, 22, 41-50.

Kristensen, J., Schaefer, T. and Kleinebudde, P., 2000. Direct pelletization in a rotary processor controlled by torque measurements. I. Influence of process variables. *Pharm Dev Technol*, 5, 247-256.

Kunz, W., Henle, J. and Ninham, B.W., 2004. 'Zur Lehre von der Wirkung der Salze' (about the science of the effect of salts): Franz Hofmeister's historical papers. *Curr Opin Colloid In*, 9, 19-37.

Langendorff, V., Cuvelier, G., Michon, C., Launay, B., Parker, A. and De kruif, C.G., 2000. Effects of carrageenan type on the behaviour of carrageenan/milk mixtures. *Food Hydrocolloids*, 14, 273-280.

Langguth, P., Fricker, G. and Wunderli-Allenspach, H., 2004. Biopharmazie. WILEY-VCH Verlag, Weinheim, 278.

Leistritz, 1999. Operating instructions - Micro 27GL/28D. Leistritz AG Nuremberg.

Leuenberger, H., 2001. Physikalische Pharmazie. Wissenschaftliche Verlagsgesellschaft mbH Stuttgart.

Liew, C.V., Gu, L., Soh, J.L.P. and Heng, P.W.S., 2005. Functionality of cross-linked polyvinylpyrrolidone as a spheronization aid: A promising alternative to microcrystalline cellulose. *Pharm Res*, 22, 1387-1398.

Lovgren, K. and Lundberg, P.J., 1989. Determination of sphericity of pellets prepared by extrusion spheronization and the impact of some process parameters. *Drug Dev Ind Pharm*, 15, 2375-2392.

MacArtain, P., Jacquier, J.C. and Dawson, K.A., 2003. Physical characteristics of calcium induced kappa- carrageenan networks. *Carbohyd Polym*, 53, 395-400.

Macheras, P., Koupparis, M. and Apostolelli, E., 1987. Dissolution of 4 controlled-release theophylline formulations in milk. *Int J Pharm*, 36, 73-79.

Macheras, P.E., Koupparis, M.A. and Antimisiaris, S.G., 1988. Effect of temperature and fat-content on the binding of hydrochlorothiazide and chlorothiazide to milk. *J Pharm Sci*, 77, 334-336.

Macheras, P.E., Koupparis, M.A. and Antimisiaris, S.G., 1989. Effect of temperature and fat-content on the solubility of hydrochlorothiazide and chlorothiazide in milk. *J Pharm Sci*, 78, 933-936.

Macheras, P.E., Koupparis, M.A. and Antimisiaris, S.G., 1990. Drug-binding and solubility in milk. *Pharm Res*, 7, 537-541.

Mammarella, E.J. and Rubiolo, A.C., 2003. Crosslinking kinetics of cation-hydrocolloid gels. *Chem Eng J*, 94, 73-77.

Mancinelli, R., Botti, A., Bruni, F., Ricci, M.A. and Soper, A.K., 2007. Hydration of sodium, potassium, and chloride ions in solution and the concept of structure maker/breaker. *J Phys Chem B*, 111, 13570-13577.

Mancini, M., Moresi, M. and Rancini, R., 1999. Mechanical properties of alginate gels: Empirical characterisation. *J Food Eng*, 39, 369-378.

Mangione, M.R., Giacomazza, D., Cavallaro, G., Bulone, D., Martorana, V. and Biagio, P.L.S., 2007. Relation between structural and release properties in a polysaccharide gel system. *Biophys Chem*, 129, 18-22.

Marques, M., 2004. Dissolution media simulating fasted and fed states. *Dissolution Technologies*.

Maschke, A., Becker, C., Eyrich, D., Kiermaier, J., Blunk, T. and Gopferich, A., 2007. Development of a spray congealing process for the preparation of insulin-loaded lipid microparticles and characterization thereof. *Eur J Pharm Biopharm*, 65, 175-187.

Merck Index, 1989. Different monographs in The Merck Index - an encyclopaedia of chemicals, drugs and biologicals. Merck & Co Rahway, NJ, USA.

Mesiha, M.S. and Valles, J., 1993. A screening study of lubricants in wet powder masses suitable for extrusion-spheronization. *Drug Dev Ind Pharm*, 19, 943-959.

Michel, A.S., Mestdagh, M.M. and Axelos, M.A.V., 1997. Physico-chemical properties of carrageenan gels in presence of various cations. *Int J Biol Macromol*, 21, 195-200.

Millili, G.P. and Schwartz, J.B., 1990. The strength of microcrystalline cellulose pellets - the effect of granulating with water/ethanol mixtures. *Drug Dev Ind Pharm*, 16, 1411-1426.

Miyazaki, S., Ishii, K. and Nadai, T., 1981. The use of chitin and chitosan as drug carriers. *Chem Pharm Bull*, 29, 3067-3069.

Mollan, M., 2003. Historical overview, ed. Ghebre-Sellassie, I. and Martin, C., *Pharmaceutical extrusion technology*. Marcel Dekker New York, 133, 1-18.

Montero, P. and Perez-Mateos, M., 2002. Effects of Na^+, K^+ and Ca^{2+} on gels formed from fish mince containing a carrageenan or alginate. *Food Hydrocolloids*, 16, 375-385.

Moore, J.W. and Flanner, H.H., 1996. Mathematical comparison of dissolution profiles. *Pharmaceutical Technology,* 6, 64-74.

Morris, E.R., Rees, D.A. and Robinson, G., 1980. Cation-specific aggregation of carrageenan helices - Domain model of polymer gel structure. *J Mol Biol*, 138, 349-362.

Naim, S., Samuel, B., Chauhan, B. and Paradkar, A., 2004. Effect of potassium chloride and cationic drug on swelling, erosion and release from kappa-carrageenan matrices. *AAPS PharmSciTech*, 5, Article 25.

Nilsson, S. and Piculell, L., 1991. Helix-coil transitions of ionic polysaccharides analyzed within the Poisson-Boltzmann cell model .4. Effects of site-specific counterion binding. *Macromolecules*, 24, 3804-3811.

Norton, I.T., Morris, E.R. and Rees, D.A., 1984. Lyotropic effects of simple anions on the conformation and interactions of kappa-carrageenan. *Carbohyd Res*, 134, 89-101.

O'Connor, R.E. and Schwartz, J.B., 1989. Extrusion and spheronization technology, ed. Ghebre-Sellassie, I., *Pharmaceutical pelletization technology*. Marcel Dekker New York, 187-216.

O'Connor, R.E. and Schwartz, J.B., 1993. Drug release mechanism from a microcrystalline cellulose pellet system. *Pharm Res*, 10, 356-361.

O'Hara, T., Dunne, A., Butler, J. and Devane, J., 1998. A review of methods used to compare dissolution profile data. *Pharm Sci Technol To*, 1, 214-223.

Park, S.Y., Lee, B.I., Jung, S.T. and Park, H.J., 2001. Biopolymer composite films based on kappa-carrageenan and chitosan. *Mater Res Bull*, 36, 511-519.

Payens, T.A.J. and Snoeren, T., 1972. Effect of simple electrolytes on sol-gel transition of kappa-carrageenan. *J Electroanal Chem*, 37, 291-296.

Pedersen, S. and Mollerpetersen, J., 1984. Erratic absorption of a slow-release theophylline sprinkle product. *Pediatrics*, 74, 534-538.

Ph.Eur. 4.06 Kommentar, 2005. Hydrochlorothiazid. Wissenschaftliche Verlagsgesellschaft mbH Stuttgart.

Ph.Eur. 5 Kommentar, 2006. Theophylline. Wissenschaftliche Verlagsgesellschaft mbH Stuttgart.

Ph.Eur. 6, 2008. Various monographies in Pharmacopoeia Europaea. Deutscher Apotheker Verlag Stuttgart.

Picker, K.M., 1999. Matrix tablets of carrageenans. I. A compaction study. *Drug Dev Ind Pharm*, 25, 329-337.

Piculell, L., Nilsson, S. and Strom, P., 1989. On the specificity of the binding of cations to carrageenans - counterion NMR-spectroscopy in mixed carrageenan systems. *Carbohyd Res*, 188, 121-135.

Piculell, L., Borgstrom, J., Chronakis, I.S., Quist, P.O. and Viebke, C., 1997. Organisation and association of kappa-carrageenan helices under different salt conditions. *Int J Biol Macromol*, 21, 141-153.

Ragnarsson, G., Sandberg, A., Johansson, M.O., Lindstedt, B. and Sjogren, J., 1992. Invitro release characteristics of a membrane-coated pellet formulation - Influence of drug solubility and particle-size. *Int J Pharm*, 79, 223-232.

Rang, H.P., Dale, M.M. and Ritter, J.M., 1999. Pharmacology (4th edition). Churchill Livingstone.

Reynolds, A.D., 1970. A new technique for production of spherical particles. *Manuf Chemist*, 41, 40-43.

Ridout, M.J., Garza, S., Brownsey, G.J. and Morris, V.J., 1996. Mixed iota-kappa carrageenan gels. *Int J Biol Macromol*, 18, 5-8.

Ritger, P.L. and Peppas, N.A., 1987a. A simple equation for description of solute release I. Fickian and non-Fickian release from non-swellable devices in the form of slabs, spheres, cylinders or discs. *J Control Release*, 5, 23-36.

Ritger, P.L. and Peppas, N.A., 1987b. A simple equation for description of solute release II. Fickian and anomalous release from swellable devices. *J Control Release*, 5, 37-42.

Rochas, C. and Heyraud, A., 1981. Acid and enzymic-hydrolysis of kappa-carrageenan. *Polym Bull*, 5, 81-86.

Rochas, C. and Rinaudo, M., 1980. Activity-coefficients of counterions and conformation in kappa-carrageenan systems. *Biopolymers*, 19, 1675-1687.

Rochas, C. and Rinaudo, M., 1984. Mechanism of gel formation in kappa-carrageenan. *Biopolymers*, 23, 735-745.

Rochas, C., Rinaudo, M. and Landry, S., 1989. Relation between the molecular-structure and mechanical-properties of carrageenan gels. *Carbohyd Polym*, 10, 115-127.

Rosario, N.L. and Ghaly, E.S., 2002. Matrices of water-soluble drug using natural polymer and direct compression method. *Drug Dev Ind Pharm*, 28, 975-988.

Roth, H.J. and Fenner, H., 2000. Arzneistoffe (3rd edition). Deutscher Apotheker Verlag Stuttgart.

Rowe, R.C., York, P., Colbourn, E.A. and Roskilly, S.J., 2005. The influence of pellet shape, size and distribution on capsule filling - A preliminary evaluation of three-dimensional computer simulation using a Monte-Carlo technique. *Int J Pharm*, 300, 32-37.

Santos, H., Veiga, F., Pina, M., Podczeck, F. and Sousa, J., 2002. Physical properties of chitosan pellets produced by extrusion-spheronisation: influence of formulation variables. *Int J Pharm*, 246, 153-169.

Scherer RP, 2003. Vegicaps Soft – Technical brochure. Eberbach, Germany.

Schirm, E., Tobi, H., de Vries, T.W., Choonara, I. and De Jong-van den Berg, LTW., 2003. Lack of appropriate formulations of medicines for children in the community. *Acta Paediatr*, 92, 1486-1489.

Schmidt, C. and Kleinebudde, P., 1998. Comparison between a twin-screw extruder and a rotary ring die press. Part II: Influence of process variables. *Eur J Pharm Biopharm*, 45, 173-179.

Schmidt, C. and Kleinebudde, P., 1999. Influence of the granulation step on pellets prepared by extrusion/spheronization. *Chem Pharm Bull*, 47, 405-412.

Schmidt, C., Lindner, H. and Kleinebudde, P., 1997. Comparison between a twin-screw extruder and a rotary ring die press. Part I: Influence of formulation variables. *Eur J Pharm Biopharm*, 44, 169-176.

Schroder, M. and Kleinebudde, P., 1995. Structure of disintegrating pellets with regard to fractal geometry. *Pharm Res*, 12, 1694-1700.

Sergio, A.P., Isabel, D.F.D.C., Jose, B.M. and Otero-Espinar, F.J., 2007. Fast and controlled release of triamcinolone acetonide from extrusion-spheronization pellets based on mixtures of native starch with dextrin or waxy maize starch. *Drug Dev Ind Pharm*, 33, 945-951.

Shah, V.P., Tsong, Y., Sathe, P. and Liu, J.P., 1998. In vitro dissolution profile comparison - Statistics and analysis of the similarity factor, f(2). *Pharm Res*, 15, 889-896.

Shipway, P.H. and Hutchings, I.M., 1993. Fracture of brittle spheres under compression and impact loading. 1. Elastic stress distributions. *Philos Mag A*, 67, 1389-1404.

Sipahigil, O. and Dortunc, B., 2001. Preparation and in vitro evaluation of verapamil HCl and ibuprofen containing carrageenan beads *Int J Pharm*, 228, 119-128.

Soh, J.L.P., Liew, C.V. and Heng, P.W.S., 2006. Torque rheological parameters to predict pellet quality in extrusion-spheronization. *Int J Pharm*, 315, 99-109.

Souci, S.W., Fachmann, W. and Kraut, H., 1986. Food composition and nutrition tables 1986/87. Wissenschaftliche Verlagsgesellschaft mbH Stuttgart.

Souto, C., Rodriguez, A., Parajes, S. and Martinez-Pacheco, R., 2005. A comparative study of the utility of two superdisintegrants in microcrystalline cellulose pellets prepared by extrusion-spheronization. *Eur J Pharm Biopharm*, 61, 94-99.

Sriamornsak, P. and Kennedy, R.A., 2007. Effect of drug solubility on release behavior of calcium polysaccharide gel-coated pellets. *Eur J Pharm Sci*, 32, 231-239.

Standing, J.F. and Tuleu, C., 2005. Paediatric formulations - Getting to the heart of the problem. *Int J Pharm*, 300, 56-66.

Stortz, C.A. and Cerezo, A.S., 2003. MM3 potential energy surfaces of trisaccharides. II. Carrageenan models containing 3,6-anhydro-D-galactose. *Biopolymers*, 70, 227-239.

Sutter, J.L. and Lau, E.P.K., 1975. Spironolactone, ed. Brittain, H. G. and Florey, K., *Analytical profiles of drug substances and excipients*. Academic Press, New York, 4, 431-451.

Tako, M. and Nakamura, S., 1986. Indicative evidence for a conformational transition in kappa-carrageenan from studies of viscosity-shear rate dependence. *Carbohyd Res*, 155, 200-205.

Tako, M., Nakamura, S. and Kohda, Y., 1987. Indicative evidence for a conformational transition in iota-carrageenan. *Carbohyd Res*, 161, 247-255.

Tayade, P.T. and Kale, R.D., 2004. Encapsulation of water-insoluble drug by a cross-linking technique: Effect of process and formulation variables on encapsulation efficiency, particle size, and in vitro dissolution rate. *AAPS PharmSci*, 6, Article 12.

te Nijenhuis, K., 1997. Carrageenans in *Advances in polymer science: Thermoreversible networks-Viscoelastic properties and structure of gels*. Springer Verlag Berlin Heidelberg, 130, 203-218.

Thommes, M., 2006. Systematische Untersuchungen zu Eignung von kappa-Carrageenan als Pelletierhilfsstoff in der Feuchtextrusion/ Sphäronisation. *Dissertation Heinrich-Heine University in Duesseldorf.*

Thommes, M. and Kleinebudde, P., 2006a. Use of kappa-carrageenan as alternative pelletisation aid to microcrystalline cellulose in extrusion/spheronisation. I. Influence of type and fraction of filler. *Eur J Pharm Biopharm*, 63, 59-67.

Thommes, M. and Kleinebudde, P., 2006b. Use of kappa-carrageenan as alternative pelletisation aid to microcrystalline cellulose in extrusion/spheronisation. II. Influence of drug and filler type. *Eur J Pharm Biopharm*, 63, 68-75.

Thommes, M. and Kleinebudde, P., 2008. The behavior of different carrageenans in pelletization by extrusion/spheronization. *Pharm Dev Technol*, 13, 27-35.

Thommes, M., Blaschek, W. and Kleinebudde, P., 2007. Effect of drying on extruded pellets based on kappa-carrageenan. *Eur J Pharm Sci*, 31, 112-118.

Tuleu, C., 2005. An overview of paediatric drug delivery. *Drug Delivery Report*, Autumn/Winter 2005, 19-21.

Tuleu, C., Khela, M.K., Evans, D.F., Jones, B.E., Nagata, S. and Basit, A.W., 2007. A scintigraphic investigation of the disintegration behaviour of capsules in fasting subjects: A comparison of hypromellose capsules containing carrageenan as a gelling agent and standard gelatin capsules. *Eur J Pharm Sci*, 30, 251-255.

USP 31 NF26, 2008. Various monography in United States Pharmacopoeia. *United States Pharmacopoeia Convention Inc*. Rockville, MD, USA.

Vervaet, C., Baert, L. and Remon, J.P., 1994. Enhancement of in vitro drug-release by using polyethylene glycol 400 and PEG-40 hydrogenated castor oil in pellets made by extrusion/spheronisation. *Int J Pharm*, 108, 207-212.

Vervaet, C., Baert, L. and Remon, J.P., 1995. Extrusion-spheronisation: A literature review. *Int J Pharm*, 116, 131-146.

Voigt, R., 2006a. Pharmazeutische Technologie. Deutscher Apotheker Verlag Stuttgart, 39.

Voigt, R., 2006b. Pharmazeutische Technologie. Deutscher Apotheker Verlag Stuttgart, 332.

Voragen, A.C.J., 2001. Polysaccharides - Carrageenan. *Ullmanns Encyclopedia of Industrial Chemistry* - Electronic Release.

Wade, A. and Weller, P.J., 1994. Handbook of pharmaceutical excipients 2nd edition. The Pharmaceutical Press.

Wagner, H., 1999. Polysaccharide aus Meeresalgen: Carrageenan in *Pharmazeutische Biologie*. Wissenschaftliche Verlagsgesellschaft mbH Stuttgart, 2, 360-361.

Wan, L.S.C. and Jeyabalan, T., 1985. Operating-conditions for the formation of pellets. *Chem Pharm Bull*, 33, 5449-5457.

Wan, L.S.C., Heng, P.W.S. and Liew, C.V., 1993. Spheronization conditions on spheroid shape and size. *Int J Pharm*, 96, 59-65.

Wassvik, C.M., Holmén, A.G., Bergström, C.A.S., Zamora, I. and Artursson, P., 2006. Contribution of solid-state properties to the aqueous solubility of drugs. *Eur J Pharm Sci*, 29, 294-305.

Wu, C.Y. and Benet, L.Z., 2005. Prediction drug disposition via application of BCS: Transport/absorption/elimination interplay and development of a biopharmaceutics drug disposition classification system. *Pharm Res*, 22:1, 11-23.

Woodruff, C.W., Nuessle, N.O., 1972. Effect of processing variables on particles obtained by extrusion-spheronization processing. *J Pharm Sci*, 61, 787-790.

Yamada, K., Kamada, N., Odomi, M., Okada, N., Nabe, T., Fujita, T., Kohno, S. and Yamamoto, A., 2005. Carrageenans can regulate the pulmonary absorption of antiasthmatic drugs and their retention in the rat lung tissues without any membrane damage. *Int J Pharm*, 293, 63-72.

Zimm, K.R., Schwartz, J.B. and O'Connor, R.E., 1995. Drug release from a multiparticulate pellet system. *Pharm Dev Technol*, 1, 37-42.

10 Acknowledgement